

**COASTAL OCEANOGRAPHY OF THE NORTHEASTERN GULF OF ALASKA**

**by**

**Robin D. Muench, Paul R. Temple,  
John T. Gunn, and Lon E. Hachmeister**

**Science Applications. Inc.**

**Final Report  
Outer Continental Shelf Environmental Assessment Program  
Research Unit 600**

**January 1982**

## TABLE OF CONTENTS

List of Figures . . . . .	689
List of Tables . . . . .	692
1. INTRODUCTION . . . . .	693
1.1 Statement of Purpose . . . . .	693
1.2 Geographical Setting . . . . .	695
1.3 Meteorological Conditions . . . . .	697
1.4 Regional Oceanographic Conditions . . . . .	698
2. OBSERVATIONAL PROGRAM . . . . .	703
2.1 Program Rationale . . . . .	703
2.2 Current Observation Program . . . . .	704
2.2.1 Moored Current Meters . . . . .	704
2.2.2 Lagrangian Current Observations . . . . .	709
2.2.3 Littoral Current Observations . . . . .	711
2.3 Temperature and Salinity Observations . . . . .	714
2.3.1 CTD Observations . . . . .	714
2.3.2 Temperature and Conductivity Time Series . . . . .	717
2.4 Wind Observations . . . . .	718
3. THE AUTUMN EXPERIMENT . . . . .	720
3.1 Autumn Distributions of Temperature and Salinity . . . . .	720
3.2 Observed Autumn Near-shore Circulation . . . . .	731
3.2.1 Autumn Moored Current Observations . . . . .	731
3.2.2 Autumn <b>Drogued Buoy Observations</b> . . . . .	<b>742</b>
<b>3.2.3 Autumn Littoral Currents</b> . . . . .	<b>750</b>
3.2.4 Autumn Wind Observations . . . . .	756
3.3 Discussion of the Autumn Experiment . . . . .	756
3.3.1 Temperature-Salinity Analyses . . . . .	758
3.3.2 Circulation Analyses . . . . .	762
3.3.3 Littoral Currents . . . . .	765
3.3.4 Summary . . . . .	765

4.	THE SPRING EXPERIMENT . . . . .	767
	4.1 Spring Distributions of Temperature and Salinity . . . . .	767
	4.2 Observed Spring Near-shore Circulation . . . . .	781
	4.2.1 Spring Moored Current Observations . . . . .	781
	4.2.2 Spring <b>Drogued</b> Buoy Observations . . . . .	789
	4.2.3 Spring Littoral Currents . . . . .	796
	4.2.4 Spring Wind Observations . . . . .	798
	4.3 Discussion of the Spring Experiment . . . . .	802,
	4.3.1 Temperature-Salinity Analyses . . . . .	802
	4.3.2 Circulation Analyses . . . . .	806
	4.3.3 Littoral Currents . . . . .	808
	4.3.4 Summary . . . . .	808
5.	OVER-WINTER WINDS AND CURRENTS . . . . .	810
	5.1 Over-Winter Currents at Mooring 6 . . . . .	810
	5.2 Over-Winter Local Winds . . . . .	812
	5.3 Summary . . . . .	818
6.	SUMMARY AND DISCUSSION . . . . .	819
7.	REFERENCES . . . . .	827

## LIST OF FIGURES

1. Geographical setting of the study area in the northeast **Gulf of Alaska**
2. Locations of moored current meter deployments in the northeast **Gulf of Alaska**
3. Configurations of current meter moorings using vector-averaging current meters (a) and Aanderaa current meters (b)
4. Configuration of radar-tracked drogued drifter used for **Lagrangian** drift studies
5. Launch site and schematic sea bed drifter paths from study of littoral currents in October-November 1980 and March-April 1981
6. Locations of CTD stations occupied in October-November 1980
7. Locations of **CTD** stations occupied in March-April 1981
8. Horizontal distributions of temperature (**a**) and salinity (**b**) at 5-m depth for 23 October-4 November 1980
9. Horizontal distributions of temperature (a) and salinity (b) at 100-m depth for 23 October-4 November 1980
10. Vertical distributions of temperature (a) and salinity (b) along a transect normal to the coastline on 2 November 1980
11. Vertical distributions of temperature along four transects normal to the coast and having closely-spaced stations
12. Vertical profiles of temperature, salinity, and density at Station **1a** in Yakutat Bay
13. Vertical profiles of temperature, salinity, and density at Station **B1** just off Ocean Cape
14. Vertical profiles of temperature, salinity, and density of Station **D5** on mid-shelf
15. Vertical profiles of temperature, **salinity**, and density **at** Station 13 near the shelfbreak
16. One-hour **lowpass-filtered** time **series** of currents from autumn Mooring **1**
17. One-hour **lowpass-filtered** time series **of** currents from autumn Mooring **4**
18. Direction histogram illustrating the **bimodal** flow direction at autumn Mooring **1**

19. One-hour **lowpass-filtered** time series of currents from the 40-m deep meter at autumn Mooring 2
20. One-hour lowpass-filtered time series of currents from the 129-m deep meter at autumn Mooring 2
21. Histogram illustrating the flow direction tendencies at the shallow meter on autumn Mooring 2
22. One-hour lowpass-filtered time series of currents from the 17-m deep meter at autumn Mooring 5
23. One-hour lowpass-filtered time series of currents from the 29-m deep meter at autumn Mooring 6
24. One-hour lowpass-filtered time series of currents from the 102-m deep meter at autumn Mooring 6
25. Composite picture showing all drogued drifter tracks observed in autumn 1980
26. Individual **drogue** tracks (a), (b), (c) followed by Drifters 1, 2, 3 respectively in the first autumn 1980 **drogue** experiment
27. Individual **drogue** tracks (a), (b), (c) followed by Drifters 1, 2, 3 respectively for the second autumn 1980 **drogue** experiment
28. Plot of separation between **drogues** as a function of **time** for the autumn 1980 drifter experiment
29. Plot of **drogue** speeds as a function of time and vector wind observed at Dry Bay
30. Histograms of **longshore** speed for Group 1 (a), Group 2 (b), and Group 3 (c) fall 1980 seabed drifter studies
31. One-hour **lowpass-filtered** time series plots of wind speed, **along-shore** and cross-shelf components at the Dry Bay (a) and Ocean Cape (b) meteorological stations **during** the autumn field program
32. Composite temperature-salinity diagram for autumn 1980, showing the relationships between near-shore, shelf and deep ocean water masses
- 33a. Horizontal distribution of temperature ( $^{\circ}\text{C}$ ) at 5-m depth, 20 March-3 April 1981
- 33b. Horizontal distribution of salinity ( $^{\circ}/\text{oo}$ ) at 5-m depth, 20 March-3 April 1981
- 34a. Horizontal distribution of temperature ( $^{\circ}\text{C}$ ) at **100-m** depth, 20 March-3 April 1981
- 34b. Horizontal distribution of salinity ( $^{\circ}/\text{oo}$ ) at 100-m depth, 20 March-3 April 1981

- 35a. Vertical distribution of temperature ( $^{\circ}\text{C}$ ) along a cross-shelf transect 30 March 1981
- 35b. Vertical distribution of salinity ( $^{\circ}/\text{oo}$ ) along a cross-shelf transect 30 March 1981
36. Vertical distribution of temperature ( $^{\circ}\text{C}$ ) at four transects normal to the coastline 20-24 March 1981
37. Vertical profiles of temperature, salinity and density at Station 18 in Yakutat Bay
38. Vertical profiles of temperature, salinity and density at Station 43 near the coast
39. Vertical profiles of temperature, salinity and density at Station 6 at mid-shelf
40. Vertical profiles of temperature, salinity and density at Station 40 seaward of the **shelfbreak**
41. Time-series plots of one-hour filtered current velocity, alongshore and cross-shore speed and temperature at 17 m, Mooring 1
42. Time-series plots of one-hour filtered current velocity, **alongshore** and cross-shore speed and temperature at 34 m, Mooring 4
43. Time-series plots of one-hour filtered current velocity, alongshore and cross-shore speed and density at 52 m, Mooring 5
44. Time-series plots of one-hour filtered current velocity, alongshore and cross-shore speed and density at 37 m, Mooring 3
45. Time-series plots for one-hour filtered current velocity, alongshore and cross-shore speed and density at 120 m, Mooring 3
46. Time-series plots for one-hour filtered current velocity, **alongshore** and cross-shore speed and density at 102 m, Mooring 6
47. Plot of separation **between drogues** 5 and 6 as a function of time
48. Drift tracks for **drogues** 5 (a) and 6 (b) during the first spring **drogue** experiment
49. Drift tracks for **drogues** 4 (a), 5 (b) and 6 (c) during the second spring drogue experiment
50. Plots of wind velocity as a function of time and **drogue** velocity derived from trajectories as a function of time
51. Histogram of **alongshore** speed for seabed drifters from groups 1 (a), 2 (b), and 3 (c)
52. Time-series plots of one-hour filtered wind velocity, alongshore and cross-shelf speed at Ocean Cape (a) and Dry Bay (b)

53. Composite temperature-salinity plot for the northeast Gulf of Alaska in spring 1981
54. One-hour filtered currents at Mooring 6 for the 102-M **deep current meter** plotted as a function of time
55. Thirty-hour filtered winds as observed at **Yakutat** airport and as computed **geostrophic** winds plotted as a function of time **for September 1980-April 1981**
56. Thirty-hour filtered east and north wind speed components from Yakutat airport and as computed **geostrophic winds plotted as a function** of time for September-December **1980**
57. Thirty-hour filtered east and north wind speed components from Yakutat airport and as computed **geostrophic** winds plotted as a function of time for January-April 1981
58. Normalized spectral estimate for computed geostrophic wind speeds **during** November 1980, computed using a Maximum Entropy Method routine
59. Surface current vectors constructed by application of a diagnostic model to March 1979 density data, assuming presence of a moderate south-easterly wind stress
60. Vector-averaged currents from current meters deployed in March-April **1981** and **for the October 1980-April 1981 record obtained at Mooring 6**
61. Vector-averaged currents from current meters deployed in October-November 1980

#### LIST OF TABLES

1. Summary of Information Concerning Deployment of, and Information Obtained From, Current Meter Moorings Utilized **in the Autumn 1980** Field Program in the Northeast Gulf of Alaska
2. **Summary** of Information Concerning Deployment of, and Information **Obtained** From, Current Meter Moorings Utilized in the Spring **1981** **Field** Program in the Northeast Gulf of Alaska
3. Autumn **Drogued** Buoy Speed Statistics
4. Autumn Surface Current Velocity Estimated From Wave Parameters
5. Spring Survey **Drogued** Buoy Speed Statistics
6. Spring Surface Current Velocity Estimated From Wave Parameters

## 1. INTRODUCTION

### 1.1 Statement of Purpose

The primary objective of the Alaska Outer Continental Shelf (OCS) Environmental Studies Program is to develop an information base permitting prediction of the spatial and temporal distribution of petroleum-related contaminants following their hypothetical release in coastal waters. Such information, taken in conjunction with seasonal and spatial descriptions of potentially vulnerable marine resources, **provides a critical input to the Bureau of Land Management (BLM) environmental assessment program. BLM's program requires background information for management decisions which may be necessary** to protect the OCS marine environment from possible damage during oil and gas exploration and development. To enable performance of this protective duty (a direct outgrowth of the National Environmental Policy Act of 1969), pertinent data must be available in readily **useable** form so that informed management decisions can be made before serious environmental damage occurs.

In assessing the potential impact of OCS development upon the marine environment, information on transport and transformation of petroleum-related contaminants is of key importance. **When** introduced into the environment, such contaminants can be transported in the atmosphere, in the water, or by sea ice. During transport these contaminants undergo continual physical and chemical changes brought about by processes such as evaporation, flocculation, emulsification, weathering, biodegradation, and chemical decomposition.

The study discussed **in this** report addresses problems relating to transport **of** contaminants. The OCS Environmental Studies Program transport studies have been designed specifically to provide data that **will** enable BLM and other agencies to:

- Plan stages and siting of offshore petroleum development so as to minimize potential risk to environmentally sensitive areas;
- Provide trajectory, coastal landfall and impact predictions required for cleanup operations in the event of an oil **spill** or the introduction of other contaminants;
- Assist in planning the locations of long-term environmental monitoring stations in the study area.

Several inter-disciplinary studies have resulted from this program; the coastal oceanography and meteorology element directly addresses the problem of contaminants movement in continental shelf waters.

The primary objective of OCSEAP oceanography and meteorology studies in the northeast Gulf of Alaska coastal region has been to provide, through interactive field programs and analytical techniques, a capability for predicting movement and distribution of OCS contaminants in the northeast Gulf of **Alaska** coastal environment. Specific program elements have required methodology development and implementation of studies to supply information on:

- Temporal and spatial variability of coastal oceanic circulation in the northeast Gulf of Alaska;
- Local wind fields and their influence on coastal circulation;
- Influence of regional **climatological** factors, especially coastal runoff, upon coastal circulation and water mass structure;
- o Influence of bottom topography upon circulation and mixing;
- Methods of applying data to the prediction of potential pollutant pathways and impact sites in order to aid in assessing the vulnerability of biotic resources and in design of effective cleanup strategies.

These information requirements have **been addressed through an integrated program combining field and analytical research.** Circulation has been addressed by comparing currents inferred from the temperature and salinity distributions with those observed directly using taut-wire moorings and **drogues**; inferred and observed currents have also been compared qualitatively with local freshwater input. Littoral currents have **been estimated from the incident wavefield and from seabed drifter studies.** Local wind effects have been estimated by comparing locally observed and computed regional **geostrophic** winds with the observed currents. The remainder of this report addresses the results of these analyses. The topographical, oceanographic and meteorological setting and the scientific background are **covered in the remainder of Section 1; the observational program is detailed in Section 2; observational results are presented and discussed in Sections 3 - 5, and Section 5 integrates these results and summarizes them within the context of OCSEAP program needs.**

## 1.2 Geographical Setting

In addressing physical oceanographic processes **in the northeast Gulf of Alaska**, the focus is **upon coastal and continental shelf** regimes. Physical factors which are **known to exert primary control over circulation and mixing processes in such regions include bottom slope and depth, continental shelf width, and orientation of the coastline relative to the earth's rotational axis**. On a smaller scale, **coastline and bottom topographic irregularities can** exert significant influence over local circulation patterns. Since a range of temporal and spatial scales of oceanographic processes are addressed, those geographical and bottom features which are expected a priori to significantly affect oceanographic conditions **must be discussed** in some detail.

The northern Gulf of Alaska coastline forms **an arcuate east-west trending bight which comprises the extreme northern portion of the northeastern Pacific Ocean (Figure 1)**. The study reported here **has focused upon the northeast Gulf of Alaska continental shelf portion of this region**. The study area extended seaward from the coastline to the continental **shelfbreak** (defined approximately by the 200-m **isobath**) and extended alongshore from about Point Manby, marking the westernmost entry to Yakutat Bay, to Cape Spencer on the northern coast of Cross Sound. Although temperature and salinity data were obtained throughout this continental shelf area, the program's major emphasis was upon the coastal region within about 10 km **of shore**.

The continental shelf region encompassed by the study area has complex bottom topography. While the overall shelf width is about 100 km, the presence of transverse troughs effectively decreases the width in some places (Figure 1). Off Yakutat Bay, the **shelf is transected by Yakutat Canyon, with depths of about 200 m, which extends to the northwest across the mouth of the Bay and then seaward**. To the southeast, off Dry Bay, the shelf is again transected by a major trough -- **Aisek Canyon -- which also has depths of about 200 m**. Both Yakutat and Aisek canyons are about 20-km wide. The Fairweather Ground, an extensive bank with depths of less than about 100 m, lies southeast of Aisek Canyon and near the **shelfbreak**.

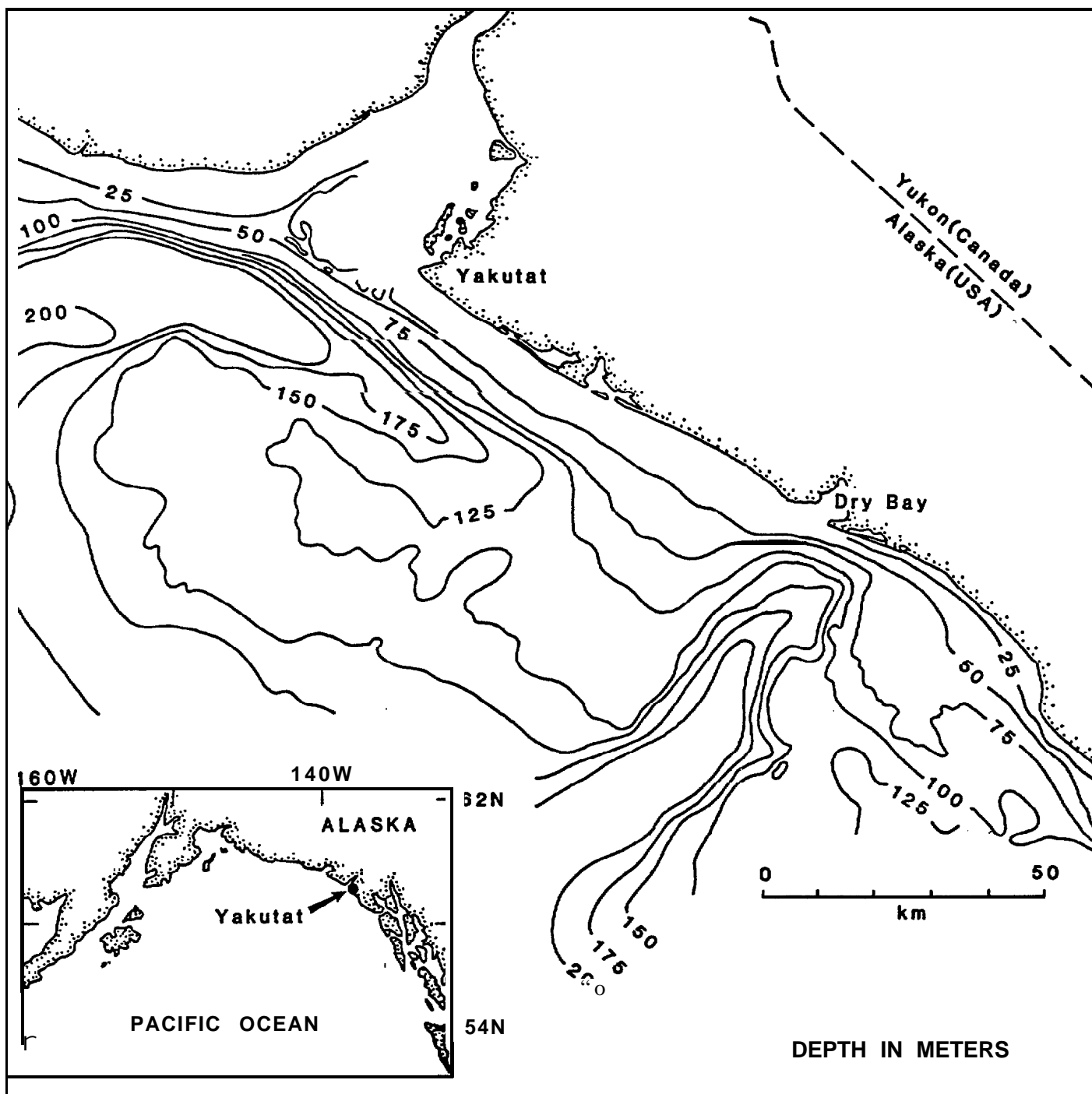


Figure 1. **Geographical** setting of the study area in the northeast Gulf of Alaska.

The coastline within the study region is nearly linear between Yakutat Bay and Cross Sound, showing little of the curvature which characterizes the northern Gulf of Alaska coast on a larger scale. Major gaps in the coast are formed **only** by Yakutat **Bay and Cross Sound at the northwestern and southeastern boundaries, respectively, of the study area.** The coastline itself is composed of nearly continuous mountains with elevations in excess of **1000 m, including isolated peaks** as high as about 4000 m. Breaks in these mountains, in **the** form of transverse valleys which lead through the mountain ranges, occur at Yakutat and Dry bays and at the mouth of the Dangerous River.

### 1.3 Meteorological Conditions

Meteorological conditions in the northeast Gulf of Alaska coastal region are dominated by seasonal variability. Atmospheric circulation over the northern Gulf of Alaska is dominated during winter by a low-pressure trough, the Aleutian Low, which defines a mean trajectory for severe **cyclonic** storms which originate to the west along the Aleutian Islands, then migrate to the northeast and intensify. Migration speed of these lows is typically 10-12 m/sec off Kodiak Island, but they tend to slow and intensify over the northeast Gulf. Wind speeds during these storms can be high; speeds higher than 48 kt occurred **for 1 percent of the samples obtained during November-February over a 15-year period in the coastal region** off Yakutat (Brewer et al., 1977). Though the statistics **have not been rigorously analyzed**, time scales for these storms appear to be 4-6 days. During winter the coastal waters are therefore subjected to a series of wind events which, averaged over an entire season, yield a mean southeasterly wind.

During summer the Aleutian Low weakens and is displaced by an atmospheric high pressure system, the North Pacific High. The eastward-migrating **low-pressure** systems are much weaker than in winter, and the resulting winds are light and variable although there is still a net easterly component in **summer.** **As in winter**, the wind field is event-dominated.

The presence of topographically-complex high mountain ranges along the coastline probably has a strong influence on the local near-coastal wind field. While these problems have not been specifically addressed in this study, physical reasoning suggests that winds would be constrained by the coastal

mountains to parallel the coastline within a certain distance offshore. In addition, **katabatic** or drainage winds commonly blow **from valleys breaching the coastal mountains throughout southeast Alaska as relatively** dense and cold air from the interior drains through the valleys to sea level. These winds can extend for an indefinite distance seaward and are characterized by high **speeds and low air temperatures**. Informal sources in southeast Alaska have reported winter wind speeds in excess of 50 m/sec and air temperatures well below freezing.

**Finally, mean monthly winter air temperatures** in the near-coastal region off **Yakutat** vary from a minimum of about -10 °C to a maximum of about +8 °C (Brewer et al., 1977).

The above combination of **climatological** factors leads to an annual freshwater discharge in the coastal band with a maximum approximately in October -- the normal time for onset of the winter storm season prior to the period when most precipitation (due to depressed temperatures) occurs as snow. Freshwater discharge is minimal in February-March, when most near-coastal precipitation **occurs as snow. There is a small secondary freshwater discharge maximum in about May**, when the onset of above-freezing temperatures leads to melting of the coastal accumulation of snow.\* Examination of coastal geography in the northeast Gulf suggests that freshwater discharge will likely come primarily from three sources within the study area: **Yakutat** Bay, with **sources at the glacial streams entering the head** of the Bay; Dry Bay, via the Alsek **River whose watershed extends through the coastal mountains; and Cross Sound**, which has extensive freshwater **sources in the southeast Alaska Archipelago to the south.**

#### 1.4 Regional Oceanographic Conditions

Circulation in a continental **shelf** region is expected a priori to be controlled by a number of environmental variables. These variables include

---

\* An up-to-date discussion of coastal freshwater discharge in the northeast Pacific, complete with statistical **summaries** of discharge data, is presented in Royer (1979).

the current along the shelfbreak seaward of the shelf, which can introduce momentum onto the shelf through **lateral** transfer either as eddies or mean flow; local winds which drive Ekman current systems; freshwater input as it affects the **baroclinic** field; **and, incident** surface waves which generate littoral currents. The resulting circulation is strongly influenced by the local bottom topography. This section first summarizes recent oceanographic exploration and results in the northeast Gulf of Alaska shelf region. Next, the large-scale oceanic **circulation which controls flow along the shelfbreak is briefly discussed. Finally, those physical processes expected to be of major importance in the coastal region are summarized.**

Research in the northern Gulf of Alaska has been hampered in the past by a lack of field data. The earliest reported study was that of McEwen, Thompson and Van **Cleve** (1930) who used temperature and salinity data obtained along sections normal to the coastline, including one off **Yakutat** Bay, to describe and discuss regional **hydrographic** structure and currents over the shelf and shelfbreak. Little fieldwork was carried out in the northeast Gulf of Alaska between the work of McEwen et al. and the onset of the **BLM-sponsored** Alaska **OCS** Program in 1974. This lack of information was pointed out by Favorite, **Dodimead** and Nasu (1976) who provided a thorough oceanographic summary of the subarctic Pacific covering research through 1972, but found insufficient data to address detailed oceanographic features in the northeast Gulf of Alaska.

A vigorous program of oceanographic data acquisition from the northeast Gulf of Alaska continental shelf region commenced in 1974. This resulted first in a characterization of **seasonal** variations in the water column in the northern Gulf by Royer (1975). Later, Royer and **Muench** (1977) discussed some large-scale surface temperature features which were related to the regional circulation and **to vertical mixing processes on the shelf. Hayes and Schumacher (1976), Hayes (1978), and Holbrook and Halpern (1977) discussed variations in winds, currents and bottom pressures on the shelf west of Yakutat Bay over February-May 1975. Current observations obtained from the shelf west of Yakutat Bay over 1974 through 1978 were analyzed by Lagerloef, Muench and Schumacher (1981). An assessment of the effect of freshwater input on coastal circulation in the northeast Gulf of Alaska was provided by Schumacher and Reed (1981) and by Royer (1981b). A summary of overall oceanographic conditions in the northeast**

Gulf was prepared by **Muench** and Schumacher (1979). Results of these studies were all consistent with the concept of a general northwesterly mean alongshore flow, with wind-driven events occurring nearer **the coastline** and current events farther offshore **being more closely related to oceanic flow processes at the shelfbreak.**

**Shelfbreak circulation is controlled by the cyclonic(anticlockwise) mean circulation in the North Pacific subarctic gyre, driven by the large-scale atmospheric flow and leading to northwesterly alongshore flow along the shelf-break. The subarctic gyre has been indirectly discussed by various researchers (cf. Munk, 1950; Carrier and Robinson, 1962; and numerous others). These largely theoretical studies hypothesized that the gyre was driven by regional wind stress. Only recently, the presence of an actual closed gyral circulation in the Gulf of Alaska was proven using satellite-tracked drogued buoys by Reed (1980). Water for this circulation originates in the North Pacific Drift, which flows eastward from the vicinity of Japan and bifurcates west of Vancouver Island so that the north-flowing branch follows the coastline and eventually becomes the northwest-flowing Alaska Current off Yakutat. The lower-latitude origin of this water gives rise to its characteristic temperature and salinity features, which are then locally modified by severe cooling, wind mixing, and freshwater addition on the northern Gulf of Alaska shelf as discussed by Royer (1975), Royer and Muench (1977), and Royer (1981b and c).**

**Current speeds and volume transports along the shelfbreak in the northeast Gulf of Alaska remain uncertain, although there is most certainly appreciable seasonal variability in both. Computations of volume transport carried out for the Gulf of Alaska gyre using wind stress curl by Ingraham, Bakun, and Favorite (1976) suggested summer transports of near zero, while winter transports were as great as about  $25 \times 10^6 \text{ m}^3/\text{sec}$  (in 1969), and also indicated a large year-to-year variability. Their conclusions were borne out by Reid and Mantyla (1976), who used sealevel data to estimate alongshore flow along the northern Gulf of Alaska coastline. Reed et al. (1980) found, however, that baroclinic transports in the Alaska Current off Kodiak Island show no detectable annual variation. Most recently Royer (1981a) has used all available baroclinic transport data to detect a weak annual signal. These varying results must all be extrapolated to the northeast Gulf shelfbreak with caution, because intensification of the**

gyre **into a concentrated shelfbreak boundary** flow occurs only far to the west off Kodiak **Island** (Thomson, 1972; Reed et al., 1980).

Shelfbreak flow in the northeast Gulf of **Alaska** is important to the present study results only inasmuch as energy from this flow is transferred onto the continental **shelf**. One mechanism for such a transfer is an alongshore **sealevel** slope, due to the **shelfbreak** flow, which can in turn drive near-shore currents as has been discussed for the Gulf of Maine by **Csanady** (1974). Another mechanism is lateral frictional transfer of **mean** flow energy onto the shelf, e.g., in the form of eddy-like features splitting off from the **shelfbreak** currents and migrating shoreward as has been observed along the Florida Current (Lee, 1975). This **process, discussed** in detail by **Csanady** (1975), can result in transfer of kinetic energy onto the shelf from the shelf edge currents. Such features have been observed on the shelf west of Yakutat Bay by both Hayes (1978) and Royer et al. (1979).

Local winds are of major importance in generating currents on continental shelves. This is expected to be particularly true in the northeast Gulf because of the high intensity of the storm-driven winds during winter. Based upon current data, Hayes (1978) concluded that local winds generated a significant 'local current response near shore west of Yakutat Bay, but had insignificant effects upon circulation near the shelfbreak. Locally wind-driven circulation on the continental shelves can be classified either as free and forced waves (**continental shelf waves**) which propagate **along** the coastline, or as transient responses (storm surges); some knowledge of the behavior of these waves is necessary for understanding and anticipating locally wind-driven shelf circulation features. A vast quantity of research has been carried out on these processes, as reflected in the large amount of pertinent literature; an excellent up-to-date summary has been prepared by Mysak (1980).

In **summary**, circulation in the northeast Gulf of Alaska region addressed in this study is expected to exhibit a broad spectrum of phenomena which have become commonly accepted as typifying continental **shelf behavior**. The driving forces for the shelf circulation are a shelfbreak current, an internal **baroclinic** field due to local coastal freshwater input, and extremely vigorous local winds.

Once established, this integrated circulation is subject to control by a complex bottom topography. Seasonal variations, **due to variability both in** coastal freshwater input and in intensity of local **winds, are** also expected to be appreciable. In the remainder of this **report, field** data obtained **in the region in** 1980 through 1981 will be analyzed with the intention of clarifying which of these processes are significant in the near-shore area **and** relating them to the fate of **OCS-related** contaminants.

## 2. OBSERVATIONAL PROGRAM

### 2.1 Program Rationale

Given a relatively simple physical situation, the oceanic velocity field could ideally be recreated from first principles using a computer model. As noted above in Section 1, however, the northeast Gulf of **Alaska** shelf region poses an extremely complex set of physical problems which combine to make **a priori modeling impractical**. The approach which has been used in this study is, rather, application of relatively simple (i.e. when compared to a computer model) analytic theories to carefully chosen observational results in such a way as to extend the results and allow prediction of what might occur under a given set of conditions.

The experimental program discussed below was designed and implemented with the above philosophy in mind. However, the size of the Alaskan continental shelf defies adequate measurement when considered within the context of pollutant transport processes. Therefore, the program was designed to establish statistics of the velocity field at a few selected locations and to supplement these with process-oriented studies addressing both specific dynamical problems and site-specific problems. The dynamical studies relate the observed velocity fields to wind forcing, bathymetry, and freshwater input. The site-specific studies address such problems as flow patterns at the heads of the two major regional cross-shelf troughs and within the surf zone.

The field experiments were planned in such a way as to encompass the extreme seasonal variability due to **variations** in the forcing parameters such as winds and freshwater input (see Section 1). These experiments were conducted on two separate cruises, each about 12 days in length. The first cruise was in October-November 1980 when maximum annual accumulation of freshwater was assumed to be present in the marine system, prior to the onset of winter storm activity with attendant high local wind speeds. The second cruise took place in March-April 1981 when accumulated freshwater in the system was minimal, following the period of most vigorous winter wind activity. In order to establish a statistical basis for regional wind and current activity, during the October 1980 through April 1981 period, time series of winds were obtained both from Yakutat Airport

and as computed **geostrophic winds**, and **current observations were obtained from a single mid-shelf mooring**.

The autumn and spring field **experiments were identical to each other** in planning, execution, and goals. The intention was to observe the near-shore (inside about 10 km) circulation and to relate these observations to the local winds, coastal freshwater input, circulation farther offshore, and bathymetry. Current observations were made using taut-wire moorings and radar-tracked drogued buoys. **Winds** were observed using recording instruments deployed on the coastline, from the vessel, and at Yakutat Airport, and were also computed for the entire region as **geostrophic** winds. Temperature and salinity observations were carried out from shipboard **using a CTD** and were recorded as time series by the recording current meters on the moorings. Finally, littoral currents were determined using seabed drifters deployed and recovered from a light aircraft. These observational programs are discussed below in detail.

## 2.2 Current Observation Program

The current observation program in the northeast **Gulf of Alaska** utilized **both current meter moorings and drogued** buoys. The moorings provided **time - series** records at fixed locations and allowed estimation of regional circulation patterns, current variability, and time scales for significant current events. The **drogues** provided estimates of the trajectories for near-surface water, and thus the pathways likely to be followed by spilled petroleum. The **drogue** tracks also provided supplementary data on the regional circulation. Finally, seabed drifters were used to estimate littoral currents within a few hundred meters of the beach.

### 2.2.1 Moored Current Meters

Current meters were deployed on taut-wire moorings in such a manner as to record currents from about 4 km offshore to near the shelfbreak, with emphasis on the region within about 10 km of shore (Figure 2). Six moorings were deployed at the beginning of the autumn 1980 field program. Moorings 1-5 were recovered at the end of the autumn field program, and Mooring 6 was left in throughout the winter and was recovered at the end of the spring 1981 field program. In the

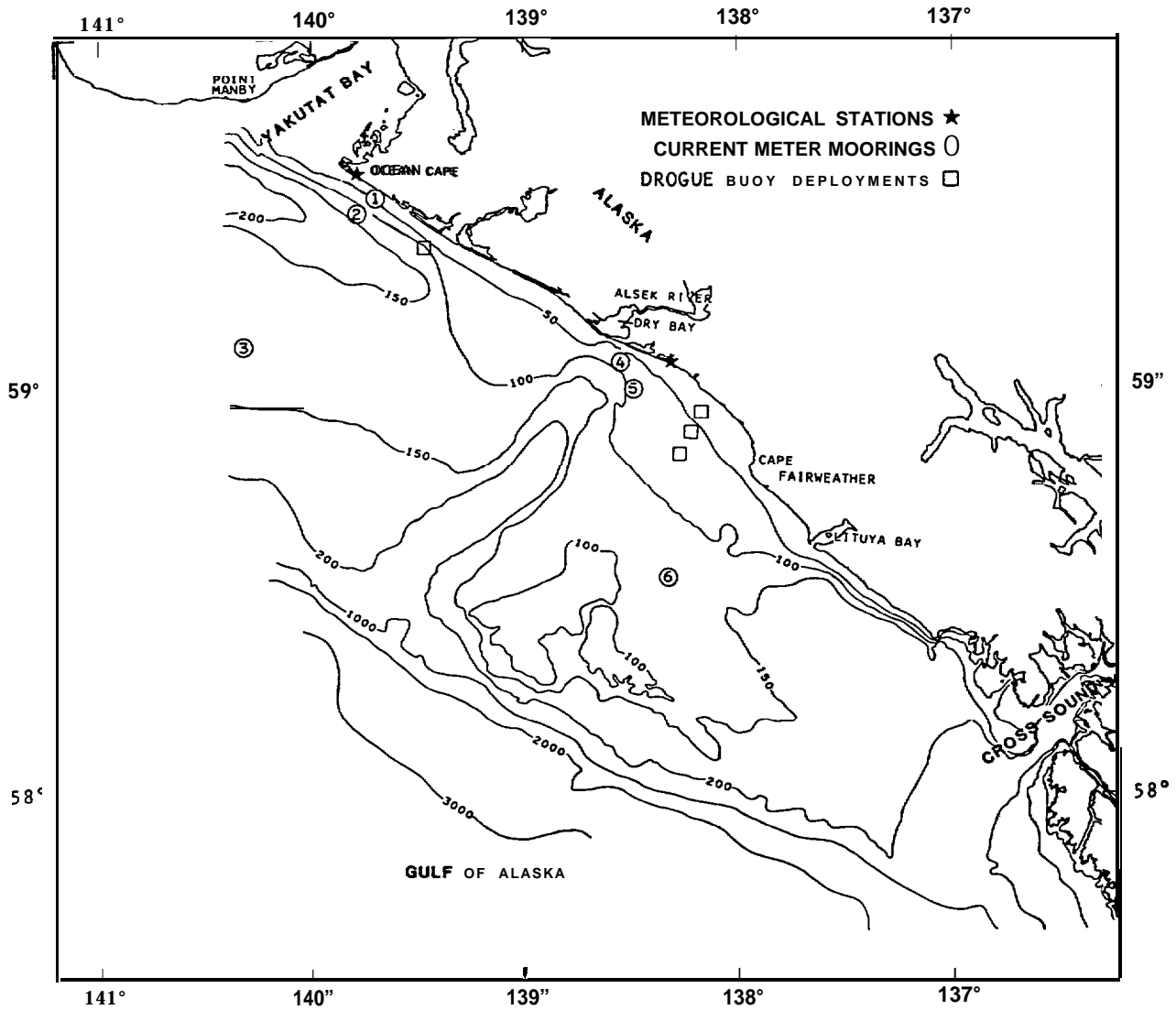


Figure 2. Locations of moored current meter deployments in the northeast Gulf of Alaska. Moorings 1-5 were deployed twice, from October-November 1980 and again from March-April 1981. Mooring 6 was deployed during the entire October 1980-April 1981 period. Drogue deployments are indicated by squares and meteorological stations are indicated by stars.

spring, five moorings **were deployed** at the same locations as the fall moorings (1-5) and were recovered at the termination of the spring field program along with Mooring 6. Particulars for these moorings are given in Tables 1 and 2.

Moorings configurations were basically similar **to those used for previous OCSEAP moorings** in the region (documented in **Muench** and Schumacher, 1979). Each mooring consisted of one or two current meters suspended in a taut-wire **configuration using a 41-inch spherical float** for primary buoyancy, a 2100-pound anchor constructed from three railroad **wheels, and an acoustic release (Figure 3). To aid in mooring** recovery in the event of failure of the primary spherical floats, secondary flotation was designed into each mooring in the form of 12-inch vinyl floats. This configuration provided enough tension for the mooring **line** (about 1000 **pound gross** positive buoyancy) to minimize chances of mooring noise introducing contamination into the current records.

Two different types of current meters, each having distinctly different modes for recording data, were used. The two near-shore moorings (1 and 4) each utilized a single AMF SeaLink Model 610 vector-averaging current meter to minimize wave contamination of the current records due to interaction of incoming **swell** with a shoaling bottom. The vector-averaging meters sense speed using a **Savonius** rotor (east-west and north-south velocity components are sampled eight times per rotor revolution) and sense direction using a vane and compass. **For the present study these values were vector-averaged at 7.5-minute intervals and recorded along with temperature; the effect of the averaging is to remove wave- and mooring-induced** noise from the recorded data. The remaining moorings each used two Aanderaa Model **RCM-4** recording current meters provided by **OCSEAP** through the Coastal Physics Group, Pacific Marine Environmental Laboratory. These current meters record an average speed, along with an instantaneous direction, at the end of each recording interval. The recording interval for Moorings 2, 3 and 5 was 5 minutes, while the interval at Mooring 6 was 30 minutes to allow acquisition of the considerably longer record from that mooring. The vector-averaging meters had respective minimum threshold speed and accuracy of 3 **cm/sec** and 2 **cm/sec**. Corresponding values for the Aanderaa current meters were 1 **cm/sec** for both parameters.

**Table 1**

SUMMARY OF INFORMATION CONCERNING DEPLOYMENT OF, AND INFORMATION OBTAINED FROM, CURRENT METER MOORINGS UTILIZED IN THE AUTUMN 1980 FIELD PROGRAM IN THE NORTHEAST GULF OF ALASKA

MOORING ID	LATITUDE N	LONGITUDE W	DEPLOYMENT DATE/HR	RECORD LENGTH (days)	BOTTOM DEPTH (m)	METER DEPTH (m)
1	59° 27. 2'	139° 44. 1'	10-23-80/1909	10	57	26
2	59° 24. 1'	139° 46. 4'	10-23-80/2033	10	<b>139</b>	40
2	59° 24. 1'	139° 46. 4'	10-23-80/2033	10	139	125
3	59° 06. 8'	140° 20. 3'	10-24-80/0030	10	132	37
4	59° 04. 5'	138° 31. 1'	10-22-80/1048	<b>11</b>	75	38
5	59° 00. 0'	138° 28. 5'	10-22-80/1159	11	65	15
6	58° 31. 5'	138° 19. 5'	10-22-80/1500	31	118	29*

\* correct speed and direction only for first 31 days

**Table 2**

SUMMARY OF INFORMATION CONCERNING DEPLOYMENT OF, AND INFORMATION OBTAINED FROM, CURRENT METER MOORINGS UTILIZED IN THE SPRING 1981 FIELD PROGRAM IN THE NORTHEAST GULF OF ALASKA

MOORING ID	LATITUDE N	LONGITUDE W	DEPLOYMENT DATE/HR	RECORD LENGTH (days)	BOTTOM DEPTH (m)	METER DEPTH (m)
<b>1</b>	59° 26. 8'	139° 43. 1'	3-20-81/2355	13	46	17
2	59° 24. 6'	139° 46. 2'	3-20-81/2322	2	128 115	27
3	59° 06. 4'	140° 21. 2'	3-21-81/0242	13i	132	~ 37 ~ 20
4	59° 04. 5'	138° 31. 8'	3-20-81/1923	13	~ <b>71</b>	~ 34
5	58° 59. 9'	138° 28. 6'	3-20-81/1824	12+	~ 64	16
6	58° 31. 5'	138° 19. 5'	10-22-80/1520	162	118	102

† has 6½-day data gap in middle of record

‡ only temperature, conductivity, and pressure

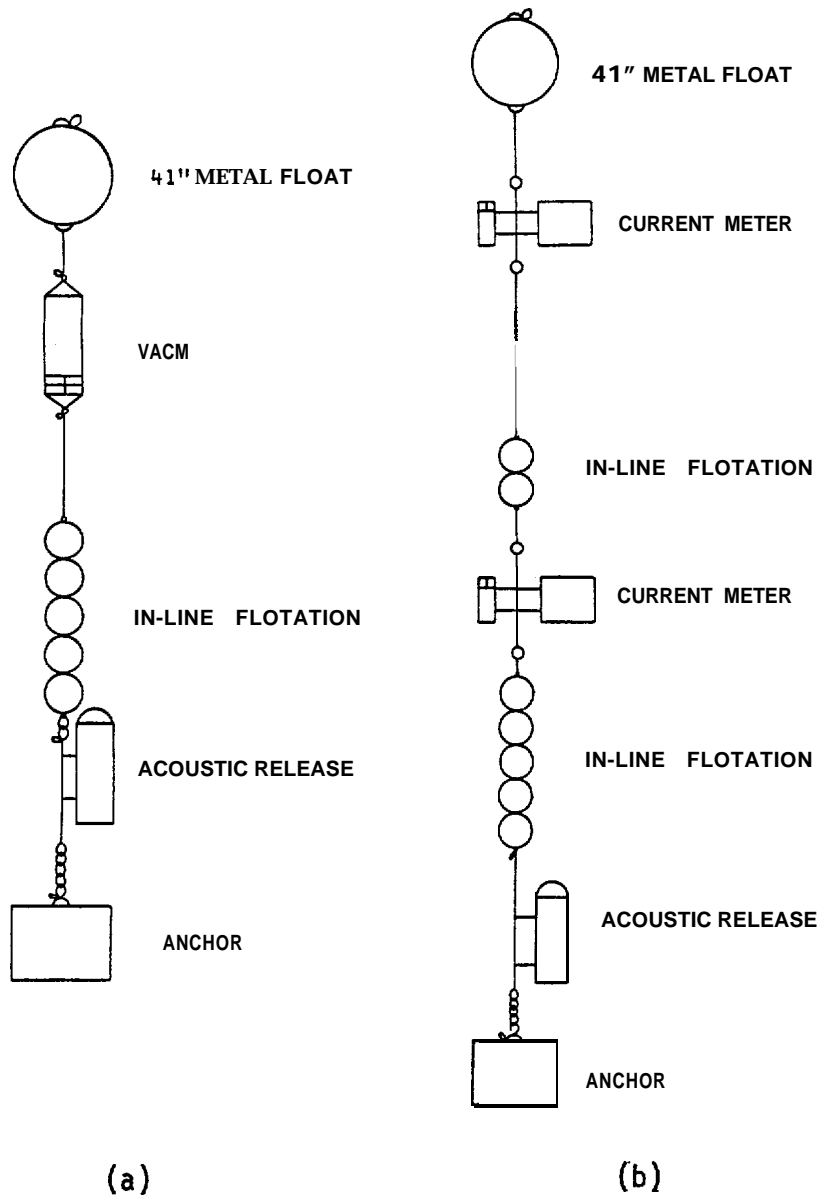


Figure 3. Configurations of current meter moorings using vector-averaging current meters (a) and Aanderaa current meters (b).

Calibration (prior to and following each deployment) and data tape translation were carried out for the vector-averaging current meters by the Technical Services Group at the Graduate School of Oceanography, University of Rhode Island. Data tape translation for the Aanderaa current meters was performed by Marine Data Services of **Corvallis**, Oregon. After being transcribed onto nine-track tape, all data were processed at **SAI/Northwest** on a **PDP-11/60** computer system.

In evaluating the results of the current meter moorings, the effects upon the resulting records from the two meter types' different recording modes must be kept in mind. As noted above, the vector-averaging meters minimize wave- and mooring-induced noise. On the other hand, the Aanderaa meters are subject to contamination of records by wave and mooring noise. The meters deployed in the northeast Gulf of Alaska were 15 m below the surface or, except for autumn Mooring 5, deeper. Pearson et al. (1981) concluded that, in the case of meters where the surface float was more than 18 m below the water surface, contamination of the records was insignificant insofar as effects upon tidal and lower frequency currents. Based upon this, it is possible that the uppermost meter at autumn Mooring 5 suffered some contamination but that the remaining records are relatively uncontaminated. Detailed **intercomparisons** between data sets recorded using these different instruments have been reported upon by **Halpern** and Pillsbury (1976a; **1976b**) and Beardsley et al. (1977). Additional commentary on the validity of records from Aanderaa current meters has been provided by Mayer et al. (1979) and Pearson et al. (1981).

### 2.2.2 Lagrangian Current Observations

**Lagrangian** current observations were made in the near-shore region of the northeast Gulf of Alaska using window-shade **drogues** attached to surface buoys. **Drogue** depths were set so as to follow water motion at about 15 m. The buoys were equipped with radar transponders to allow tracking using the research vessel's radar. Configuration of the drifters is illustrated diagrammatically in Figure 4.

There were two separate and distinct Lagrangian drifter experiments during each of the two field programs. In the first of each pair of experiments, the **drogues** were deployed about 0.5 km apart and their subsequent separation distances

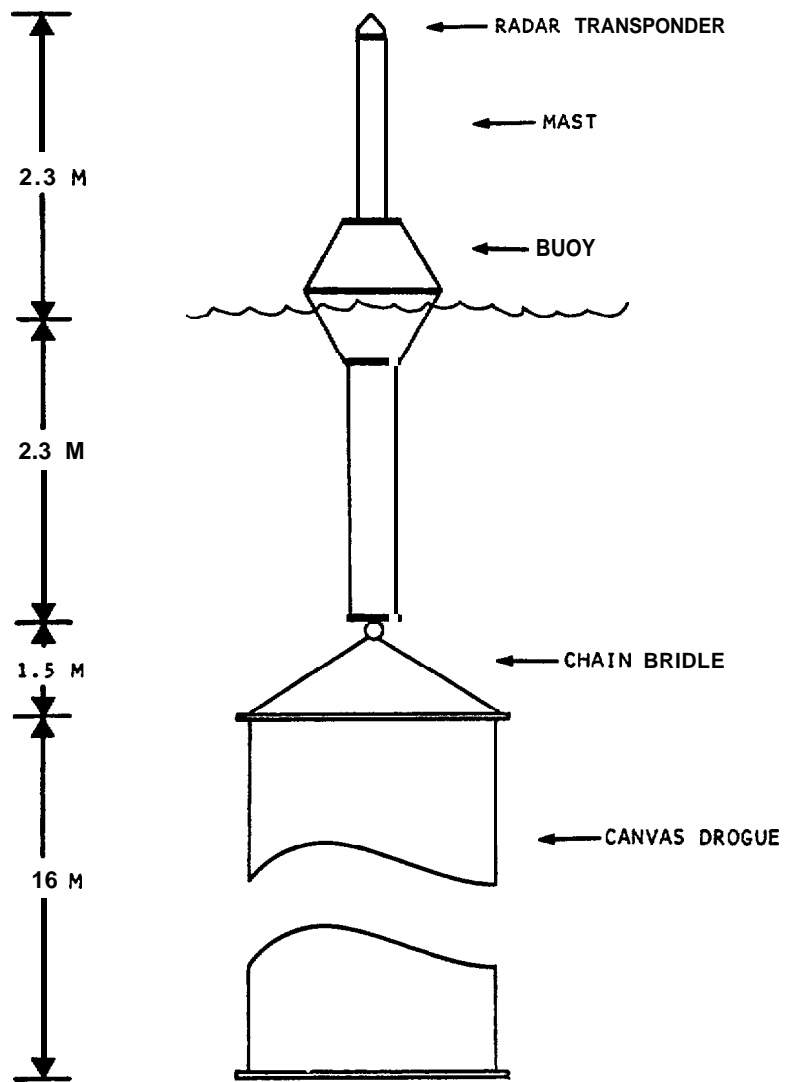


Figure 4. Configuration of radar-tracked drogued drifter used for **Lagrangian** drift studies.

during the experiment were recorded in an attempt to estimate dispersion. The second experiment of each pair consisted of buoy deployments along a line normal to the **longshore** current and subsequent tracking to better define the flow field. Deployment locations coincided as closely as possible with current meter mooring sites, to enable later comparison between drifter and current meter results. The approximate areas covered by the autumn and spring drifter experiments are indicated on Figure 2.

**Drogued** buoy positions were recorded at half-hour intervals during the experiments. Positioning was accomplished by recording the ship's location, determined using Loran C, along with a radar range and bearing to the buoy. In cases where the locations suggested that a **drogue** was in danger either of running aground or of exceeding the range of the ship's radar, the **drogue** was recovered and redeployed. The resulting buoy positions were edited for "wild points" which may have been due either to questionable Loran positions or error in recording radar fixes. Such points were generally quite obvious, and were discarded and replaced with interpolated values. The final data set was run through a 5-point 2.5-hour "boxcar" filter to remove high frequencies and facilitate **intercomparison** with other data.

### 2.2.3 Littoral Current Observations

Longshore water transports and bottom currents in the region in and just offshore from the surf zone (< 400 m from shore) were addressed using two different methods. First, bottom currents were estimated directly using **deployment-recovery** results for seabed drifters. Second, **longshore** wave-induced currents were computed using estimated wave characteristics in conjunction with known empirical formulae.

• Seabed drifters were deployed on 18-30 October 1980 and 21-24 March 1981 at the approximate sites shown on Figure 5. These drifters consisted of an 18-cm diameter hemispherical head attached to a weighted tail-like shaft 50 cm long. They were grouped into bundles of 50 each, held together for deployment by a salt block that would dissolve to release them about three hours following deployment. These bundles were launched from a light aircraft just following high tide, in the surf zone along lines normal to the coastline. Three bundles

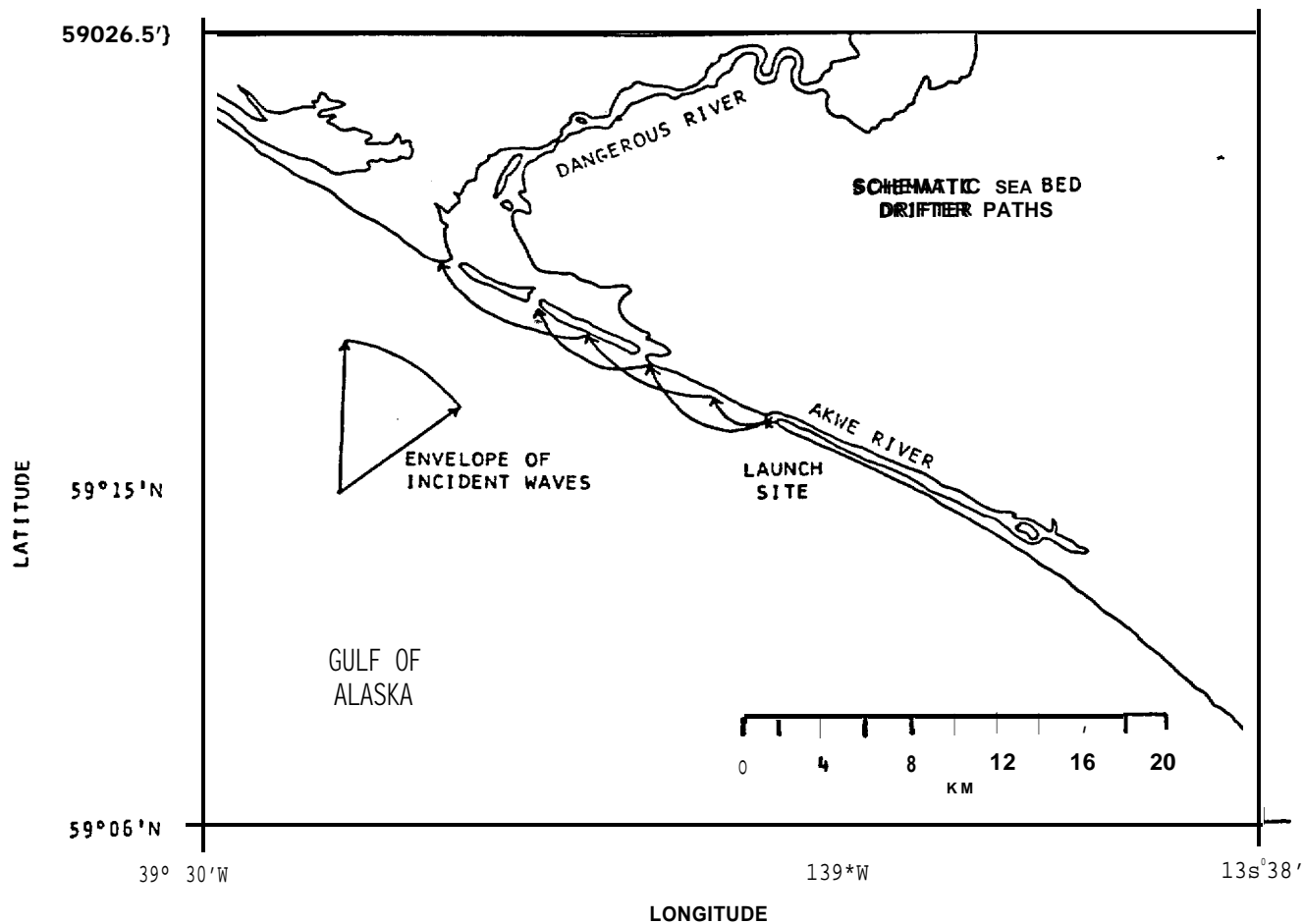


Figure 5. Launch site and schematic sea bed drifter paths from study of littoral currents in October-November 1980 and March-April 1981 (see appropriate sections for actual speeds and directions).

of drifters were released at each deployment. The innermost was deployed **shore-**ward of the breakers, the next group directly in them, and the outermost group about 150 m seaward of the breakers. For three days following each set of launches the beach was searched for drifters during the daylight low tide period using a light aircraft. The relatively uniform and sandy aspect of the beach made spotting of beached drifters easy, suggesting that most of the drifters which **actually** went ashore were recovered.

Several factors contribute to the uncertainties in **longshore** speed computed from the drifter recovery and release points. **First, time of beaching is not known precisely but is** assumed to have been at or near high tide because most of the recovered drifters were found at or near the high tide mark. Because recoveries were limited to the daylight **low** tide, beaching may have occurred at either of the two **high tides between** the second- and third-day recoveries. Second, the release time for some drifters is uncertain because, at the time of launching, the airstream generated by the aircraft broke 5-10 drifters loose from the bundle at any given launch. In addition, wave action might have accelerated dissolution of **some of the salt blocks more than others**. **Third, the drifters may somewhat rectify a time-varying current and may therefore show an apparent component** due to wave-induced pumping. The magnitude of this effect is uncertain, but it is not felt to be significant here relative to the actual longshore currents. A final consideration stems from the fact that the drifters passed through various regions (depending upon the tidal cycle) en route from their launch site to the beach and that their residence times in each of these regions are unknown. Presumably a pollutant passing through the surf zone would be subject to the same effects, **however, so this is not viewed as a critical problem**.

In order to provide an independent estimate of longshore currents, in the form of a surface speed rather than the near-bottom velocity resulting from the seabed drifter observations, computations were carried out using empirical equations **in conjunction with estimated wave parameters**. **Estimates of the longshore surface currents produced by breaking waves were calculated using**

the equation

$$v = 1.19(gH_b)^{\frac{1}{2}} \sin\alpha \cos\alpha \quad (\text{Komar et al.}, 1976)$$

where  $\alpha$  = angle of breaking wave relative to the coast,

$H_b$  = height of breaking wave, and

$g$  = acceleration of gravity.

The wave height was estimated visually during deployment and recovery of the seabed drifters, and concurrent photographs were taken from a light plane for later determination of the wave angle. Because of the complexity of the surf zone, the wave height and angle measurements were primarily of the dominant wave train. Irregular bottom slope and the contributions from different wave directions make the situation complex, but it is felt that these observations can provide a reasonable order-of-magnitude estimate of longshore currents. Results are presented in Sections 3 and 4.

### 2.3 Temperature and Salinity Observations

Temperature and salinity observations necessary for determination of water mass interactions such as mixing, for determination of the origins of water types, and to aid in interpretation of current data were obtained from shipboard and as time series from the current moorings. The shipboard sampling pattern encompassed both large-scale shelf-wide spatial scales and small-scale near-shore features through close-spaced sections.

#### 2.3.1 CTD Observations

Temperature and salinity were observed at selected locations as a function of depth using a shipboard conductivity/temperature/depth recording system (CTD). These CTD operations were carried out coincident with the current studies described above. Individual CTD casts were made both on a predetermined grid (Figures 6 and 7) designed to define the regional fields of temperature and salinity, along closely spaced near-coastal sections to define the temperature-salinity structure of the near-coastal currents, and following the radar-tracked drogues described above. Data (such as locations and times) pertinent to these CTD stations are given in Appendix 1.

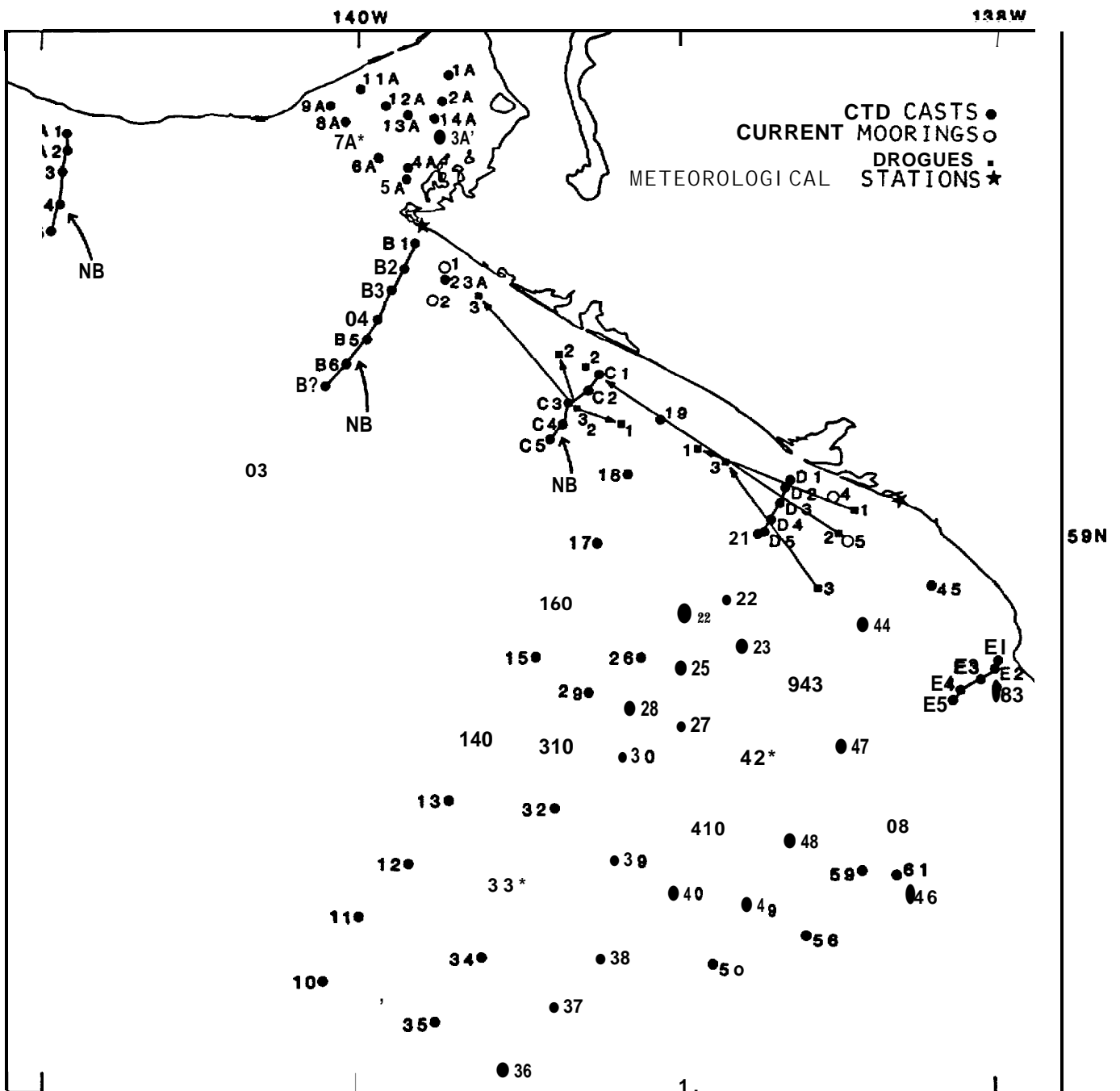


Figure 6. Locations of CTD stations occupied in October-November 1980.

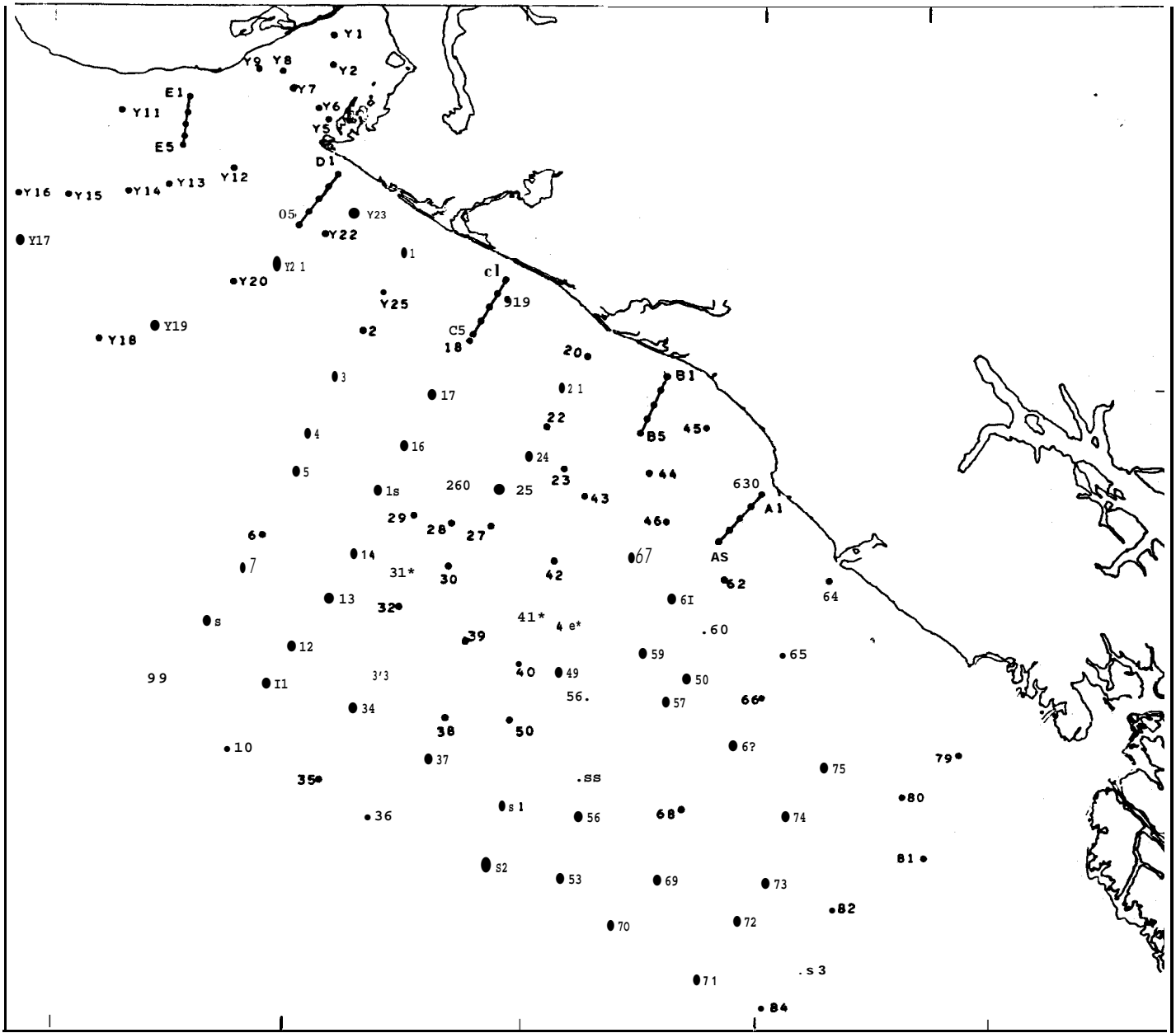


Figure 7. Locations of CTD stations occupied in March-April 1981.

Occupation of the CTD stations followed the general guidelines used in the past for OCSEAP work (cf, for example, Muench and Schumacher, 1979). Data were recorded only on the downcast, and the CTD lowering rate was held to 0.5 m/sec or less to minimize spiking induced by sharp vertical temperature gradients. Sampling was stopped at about 5m above the bottom in shallow water and at about 10 m in deep water to avoid damage to the sensors. A water sample was obtained for calibration purposes on every third cast. Sample interval during the down-cast was 0.1 sec.

Calibrations for the CTD used for both autumn and spring cruises, furnished by the Northwest Regional Calibration Center, provide an estimate of the standard deviation for expected error in the measurements. For the CTD used on the autumn cruise, accuracies for conductivity, temperature and pressure were respectively 0.009 mmho/cm, 0.013 °C and 1 psi. Corresponding values for the CTD used on the spring cruise were 0.011 mmho/cm, 0.009 °C and 1 psi.

Both of the cruises used Plessey Model 9040 CTD systems. For the autumn cruise, data were digitally recorded on a Grundy Model 8400 deck unit and seven-track Kennedy tape recorder. For the spring cruise, data were recorded through a Grundy Model 8700 deck unit and a PDP-11/34 computer onto a DEC Model TS03 nine-track tape recorder. Final processing of the CTD data was carried out on a PDP-11/60 computer located at SAI/Northwest. Processing routines were standard procedures such as utilized for previous OCSEAP work and-described in previous documents, and will not be described here.

### 2.3.2 Temperature and Conductivity Time Series

As described above, each of the Aanderaa recording current meters deployed was equipped with sensors for measuring temperature and conductivity. Throughout the records, these parameters were recorded at the same intervals as the current information, and locations for these time series are the same as for the current records (Figure 2). In contrast, the vector-averaging current meters did not have provision for recording conductivity. They did, however, record temperature throughout the mooring periods.

The accuracy for the temperature and conductivity values recorded on the moorings is approximately **0.1 °C** and **0.1 mmho/cm**, respectively, which is considerably lower than that obtained from the CTD **units**. Preliminary comparison between the recorded values and values obtained from adjacent coincident (**in** time) stations using the CTD suggest that these estimated accuracies are reasonable. Despite the relatively low accuracy, the time series records are capable of detecting variations **which can then be compared with coincident events in the current field, making the time series records useful in interpreting the overall data set.**

#### 2.4 Wind Observations

During the autumn and **spring field experiments**, the **local** wind field was measured through recording of wind speed and direction at two locations along the coastline, at Yakutat Airport and aboard the research vessel, and was computed as **geostrophic** winds by **FNWC in Monterey, California.**

Coastal winds were recorded during the field programs at locations along the beach at Dry Bay and Ocean Cape (Figure 2) using **Aanderaa** automatic recording weather stations. These stations were deployed prior to the beginning of the oceanographic field program for both the autumn and spring cruises and were recovered after the end of the oceanographic program, so that wind data were acquired over the entire period. Station sites were chosen so as to be on flat topography away from significant surface **features**, hills or forested areas. Locations on the shore just inland from the beach proved particularly satisfactory from this viewpoint because of the flat topography. The weather stations were equipped with 10-meter masts and were set to record at 10-minute intervals. The recording mode was the same as for the Aanderaa current meters, with speed accumulated through the recording interval and wind direction recorded instantaneously once per interval. Minimum threshold wind speed for these instruments is 30-50 cm/see, with an accuracy of **±2** percent, with directional accuracy to better than **±5** degrees.

Data from the Aanderaa weather stations were supplemented with the data recorded by the National Weather Service at Yakutat Airport, which were supplied on **a** magnetic tape. The airport wind observations were recorded at 3-hour

intervals. Additional supplementary data were available in the form of the computed **geostrophic** winds, available at six-hour intervals, provided by the Fleet Numerical Weather Central **by Mr. A. Bakun** and computed according to Bakun (1975). Finally, winds were observed at hourly intervals from the oceanographic vessel during the field programs.

Long-term wind data were obtained in the form of the winds recorded at three-hour intervals at **Yakutat** Airport, and in the form of six-hourly computed **geostrophic winds**. These long time-series records coincided with the current record obtained from Mooring 6 during October 1980 to April 1981.

### 3. THE AUTUMN EXPERIMENT

#### 3.1 Autumn Distributions of Temperature and Salinity

The **temperature and salinity distributions** for the northeast Gulf of Alaska continental shelf region were determined using a shipborne CTD system and recording current meters equipped with temperature and conductivity sensors (see **Section 2**). **The spatial distributions of temperature and salinity are presented in this section.**

The **regional temperature and salinity fields** are presented here as plan views at depths of 5 m (Figure 8) and 100 m (Figure 9) and as vertical distributions along a transect across the **shelf from the coastline to seaward of the shelfbreak (Figure 10)**. **The most prominent feature of the distribution was the narrow ( $\sim 6$  km) near-surface coastal band of low temperature ( $< 8.5$  °C) and low salinity ( $< 31.0$  ‰) water.** There was some tendency for the band to widen by about a factor of two into a "bulge" southwest of Dry Bay (Figure 9a) and to be somewhat narrower to the northwest than to the southeast of this widening. On the vertical sections (Figure 10) the band is evidenced as a surface wedge of water which had temperatures below about 8.5 °C and salinities below about 31.0 ‰. The band was not evident at 100 m depth (Figure 9), being constrained generally to depths **above  $\sim 20$  m.**

Farther offshore, the horizontal distributions of temperature and salinity were irregular (Figure 10). At 5 m the temperature and salinity well offshore south of Dry Bay appeared similar to that in the coastal band but were separated from it by a region of warmer and more saline water. The depressed **isohalines** at this location were also evident at 100 m depth. Prominent temperature elevations ( $> 9.5$  °C) were evident at 100 m depth overlying **Alsek** Canyon south of Dry Bay. The general tendency at 5 m was for both temperature and salinity to increase in the offshore direction. At 100 m, salinity increased offshore as temperature decreased.

Because the near-shore band was the dominant feature in the temperature and salinity distributions, it **will** be investigated in somewhat greater detail. Four close-spaced ( $\sim 5$  km between stations) CTD transects occupied in autumn 1980 are

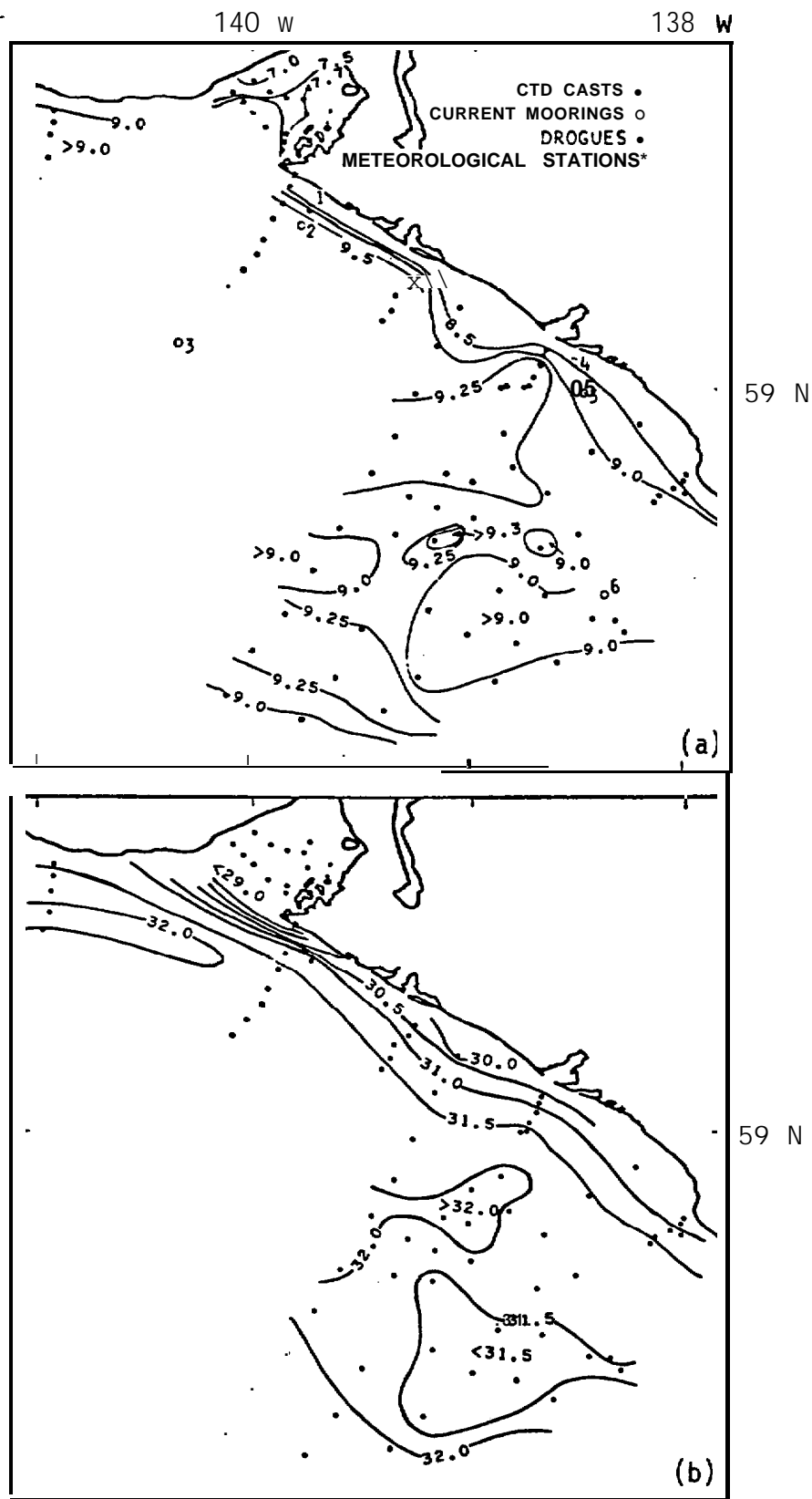


Figure 8. Horizontal distributions of temperature (a) and salinity (b) at 5 m depth for 23 October-4 November 1980. Salinity distribution within Yakutat Bay is not shown, because the contours there are too closely packed for adequate horizontal resolution on this scale.

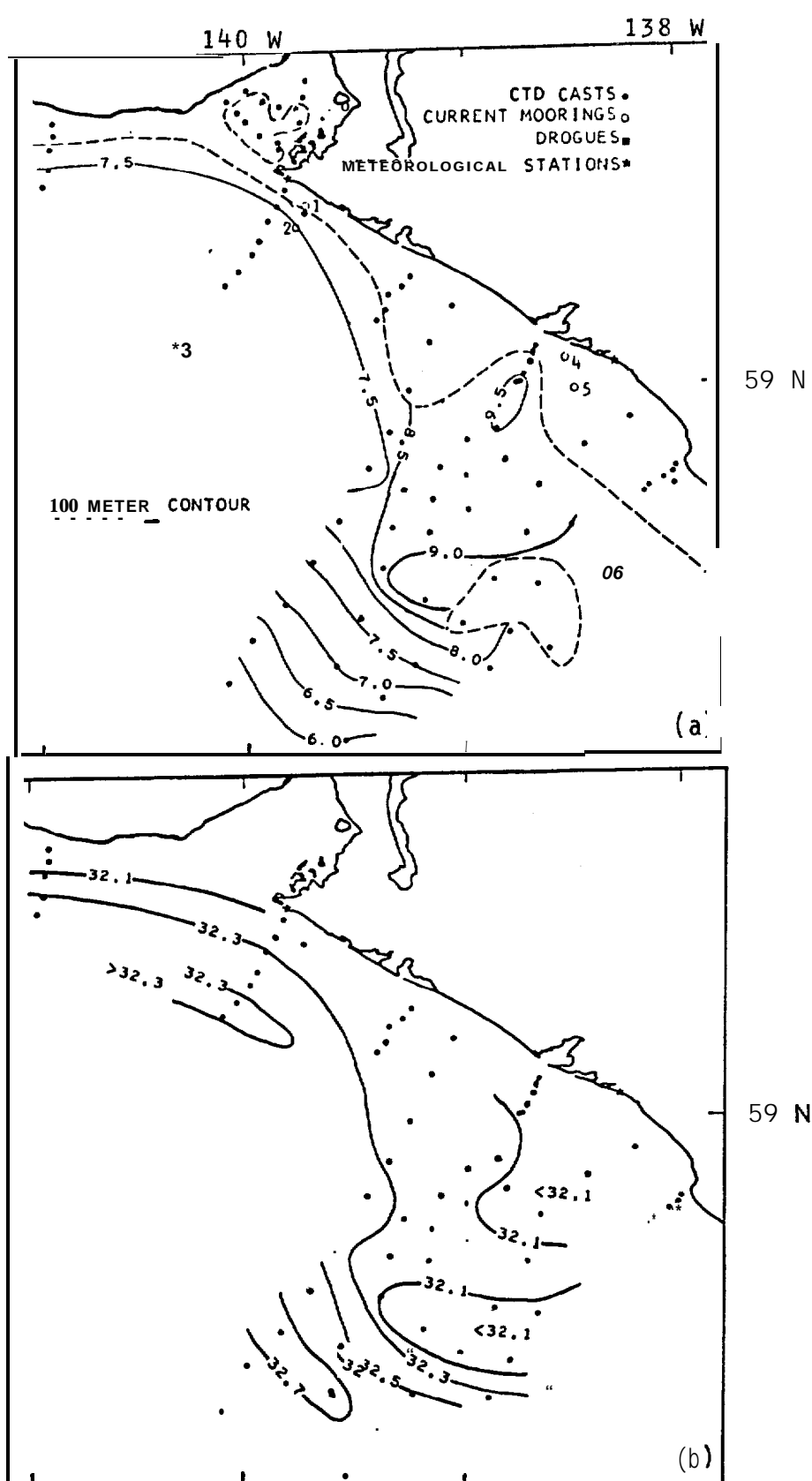


Figure 9. Horizontal distributions of temperature (a) and salinity (b) at 100 m depth for 23 October - 4 November 1980.

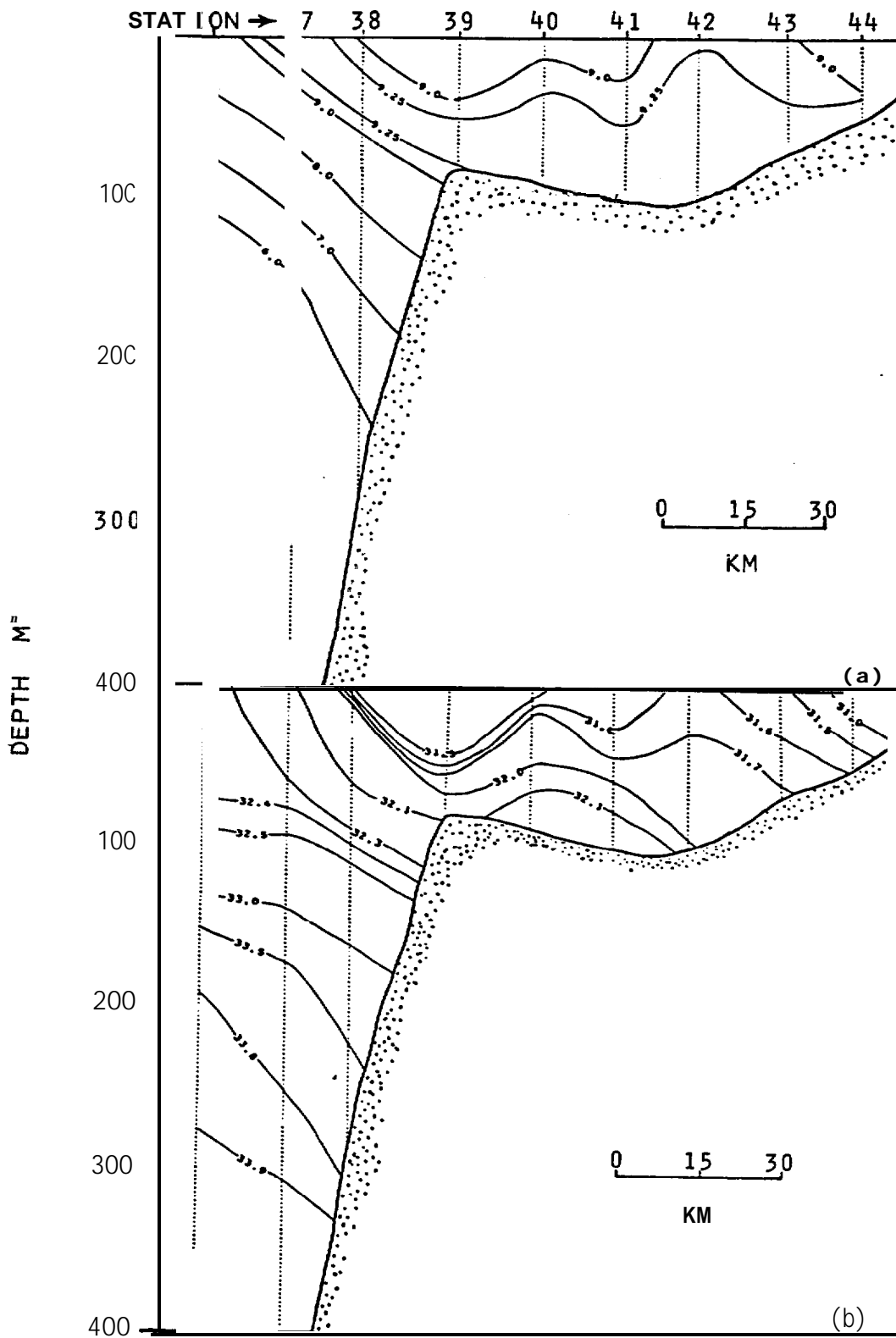


Figure 10. Vertical distributions of temperature (a) and salinity (b) along a transect normal to the coastline on 2 November 1980. See Figure 6 for location of transect.

especially suitable for documenting this feature. **The vertical distributions of temperature along these transects** are shown on Figure 11. Temperature, rather than salinity, is used as a tracer because it effectively shows the same features and was, in several cases, a better indicator of water mass distribution (cf. for example Figure 10). These CTD transects clearly indicate the relatively constant (5-6 km) offshore extent and spatial continuity of the band in the along-shore direction and its lack of penetration below about 20 m depth. **Near-surface temperatures in the band were somewhat lower (typically 8.5 to 9.0 °C) than at depth, although it is probable that observations along Sections C and D (Figures 11b and c) did not extend close enough to the coastline to have detected the lowest temperatures present.** Section B (Figure 11a) shows particularly well a **thermocline** which was present throughout the deeper portions of the study region at about 100 m where the bottom was sufficiently deep.

Features observed in the vertical distributions of temperature, salinity, and density can be better seen in selected vertical profiles (Figures 12-15). The strongest vertical gradients observed occurred in **Yakutat Bay**, where particularly cold ( $< 8$  °C) and less saline ( $< 27$  ‰) water was underlain by warmer ( $\sim 10$  °C) and more saline ( $> 31$  ‰) water (Figure 12). Outside Yakutat Bay in the coastal band just off Ocean Cape, a similar vertical structure was observed with the upper layer having slightly higher salinities than in Yakutat Bay (Figure 13). The deep **layer**, following the pattern of these two stations, was typified throughout the study region by temperatures of  $\sim 10$  °C and salinities of  $\sim 31.5$  ‰. Farther offshore outside the coastal band, the upper layer of the water column tended toward vertical homogeneity and was underlain by a persistent gradient region at 75 to 125 m depth (Figure 14). Temperature decreased sharply as salinity increased throughout this vertical gradient region. The final profile illustrates the vertical distributions of temperature and salinity near the shelfbreak (Figure 15). At the location of this station, near-surface values were affected by a particularly cold and less saline **lens** of water which was not present throughout the region as indicated by the patchy upper-level temperature distribution (Figure 8).

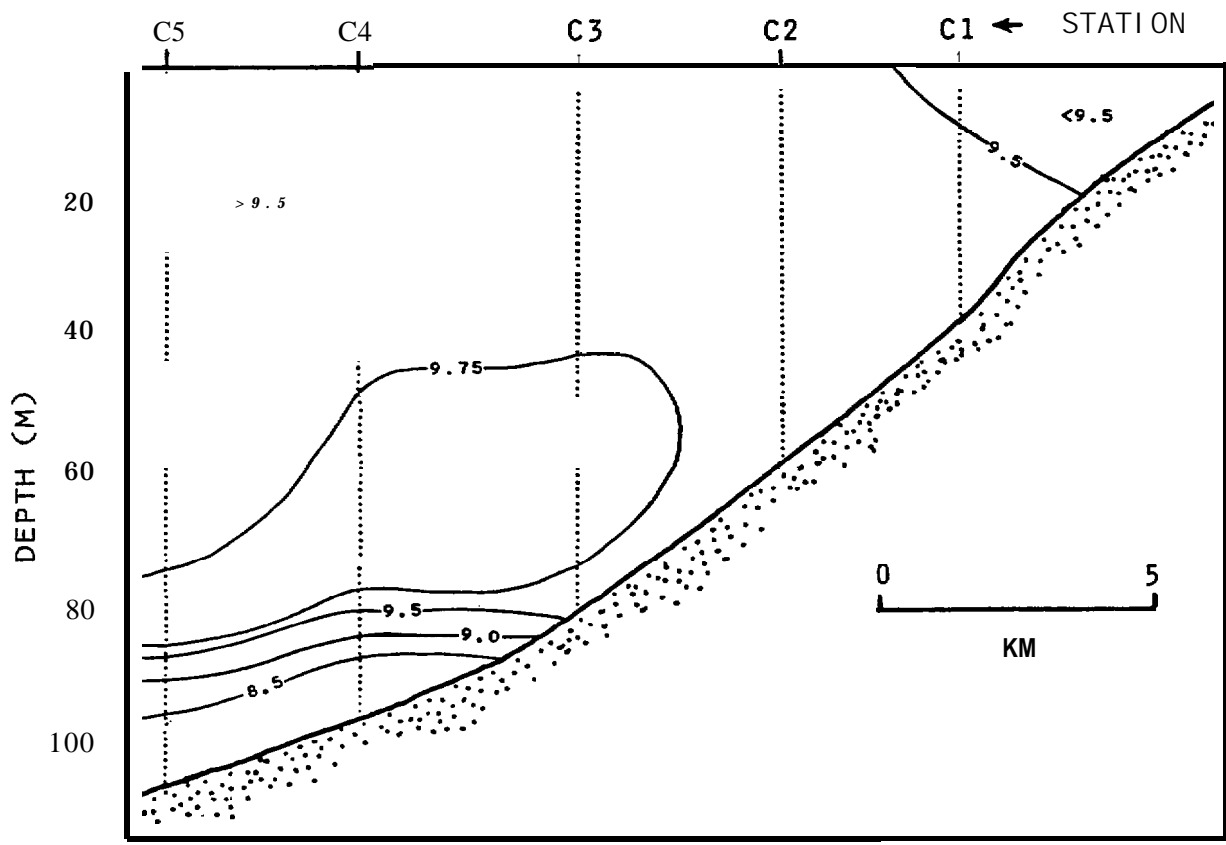
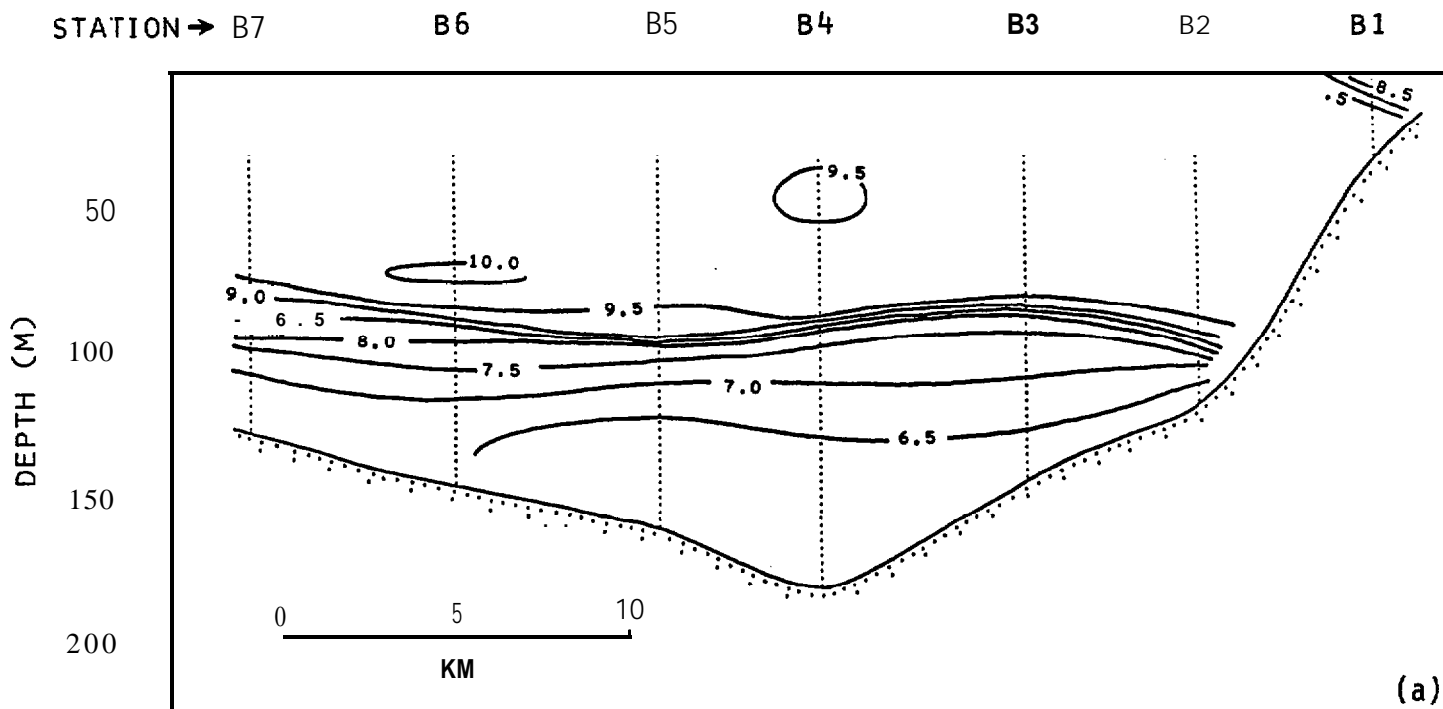


Figure 11. Vertical distributions of temperature along four transects normal to the coast and having closely-spaced stations. See Figure 6 for transect locations.

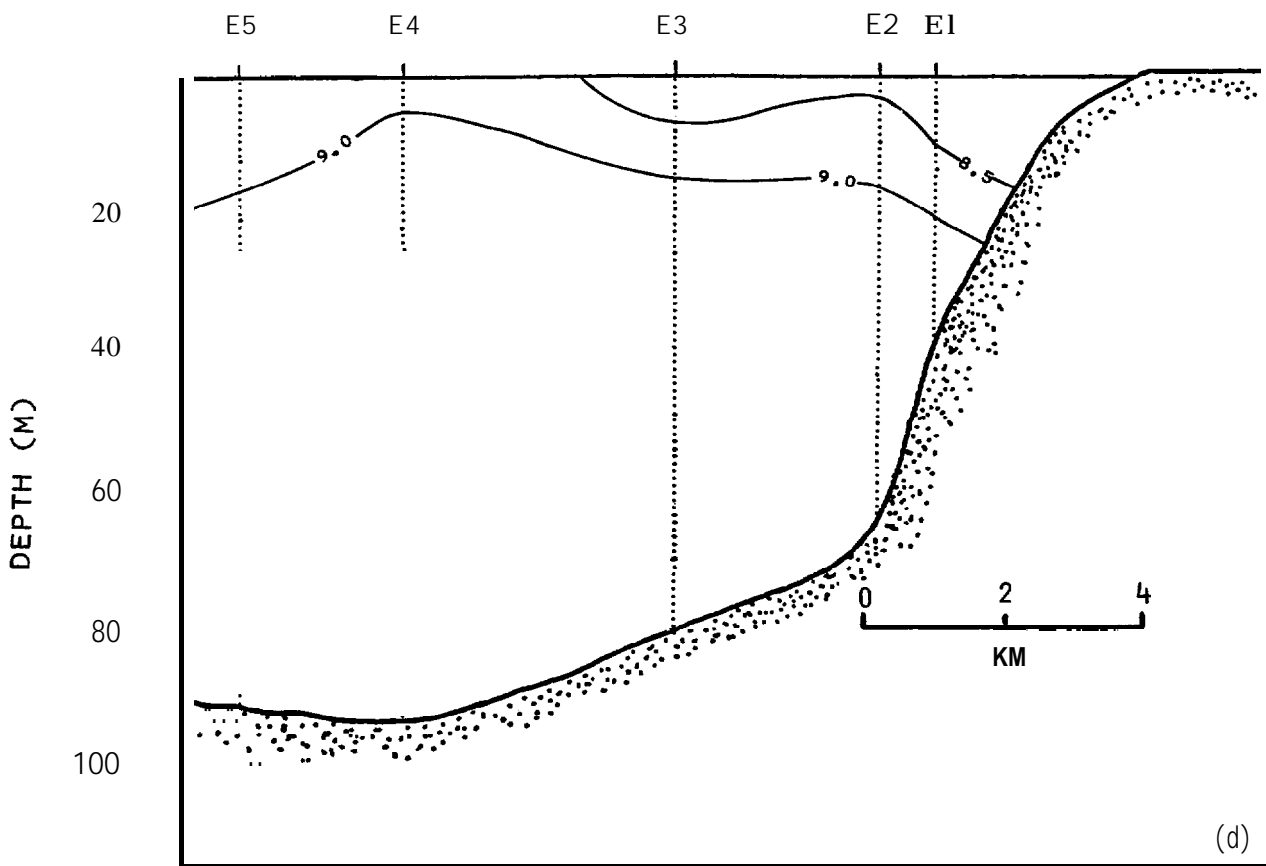
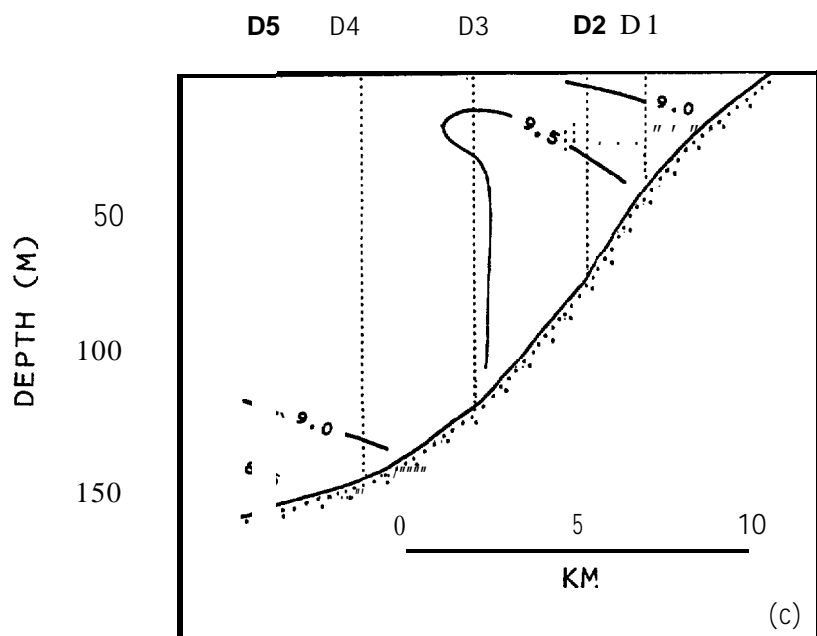


Figure 11 (continued)

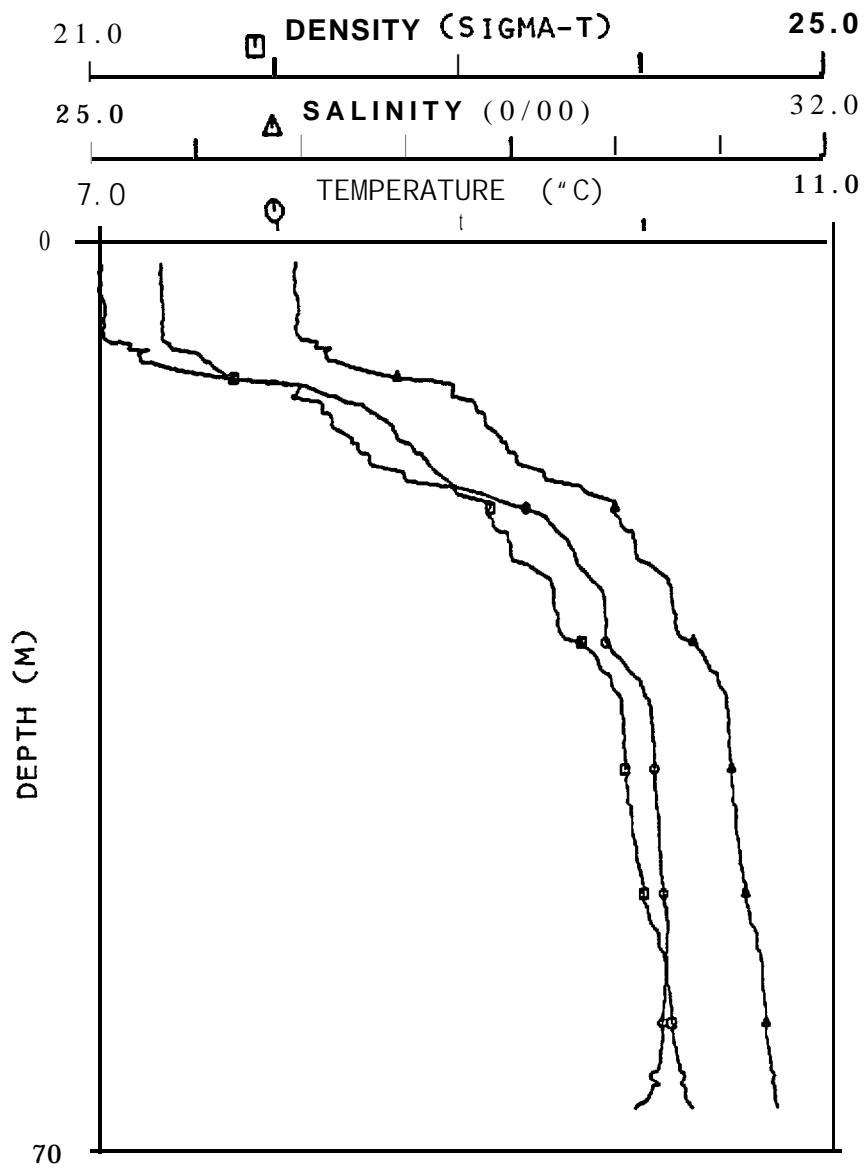


Figure 12. Vertical profiles of temperature, salinity, and density at Station 1a in Yakutat Bay. Station location is shown on Figure 6.

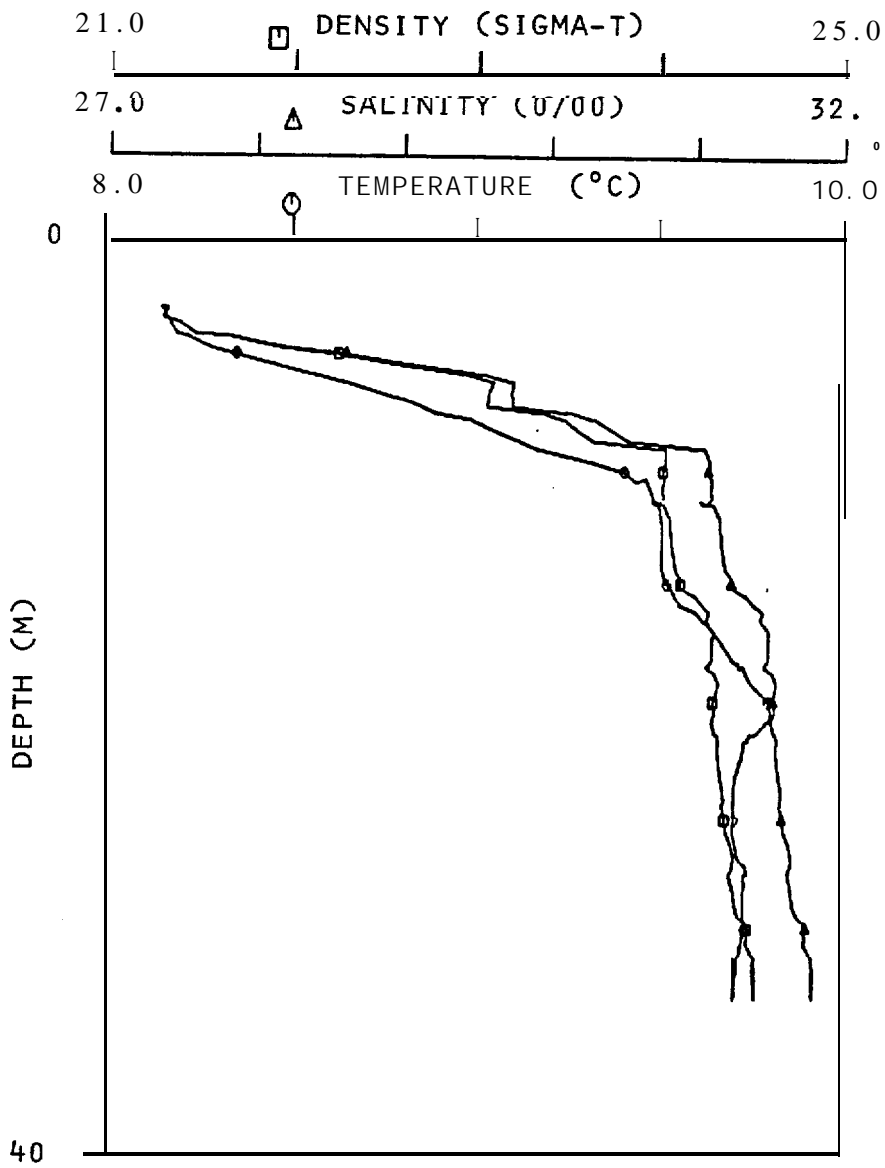


Figure 13. Vertical profiles of temperature, salinity, and density at Station **B1** just off Ocean Cape. Station location is shown on Figure 6.

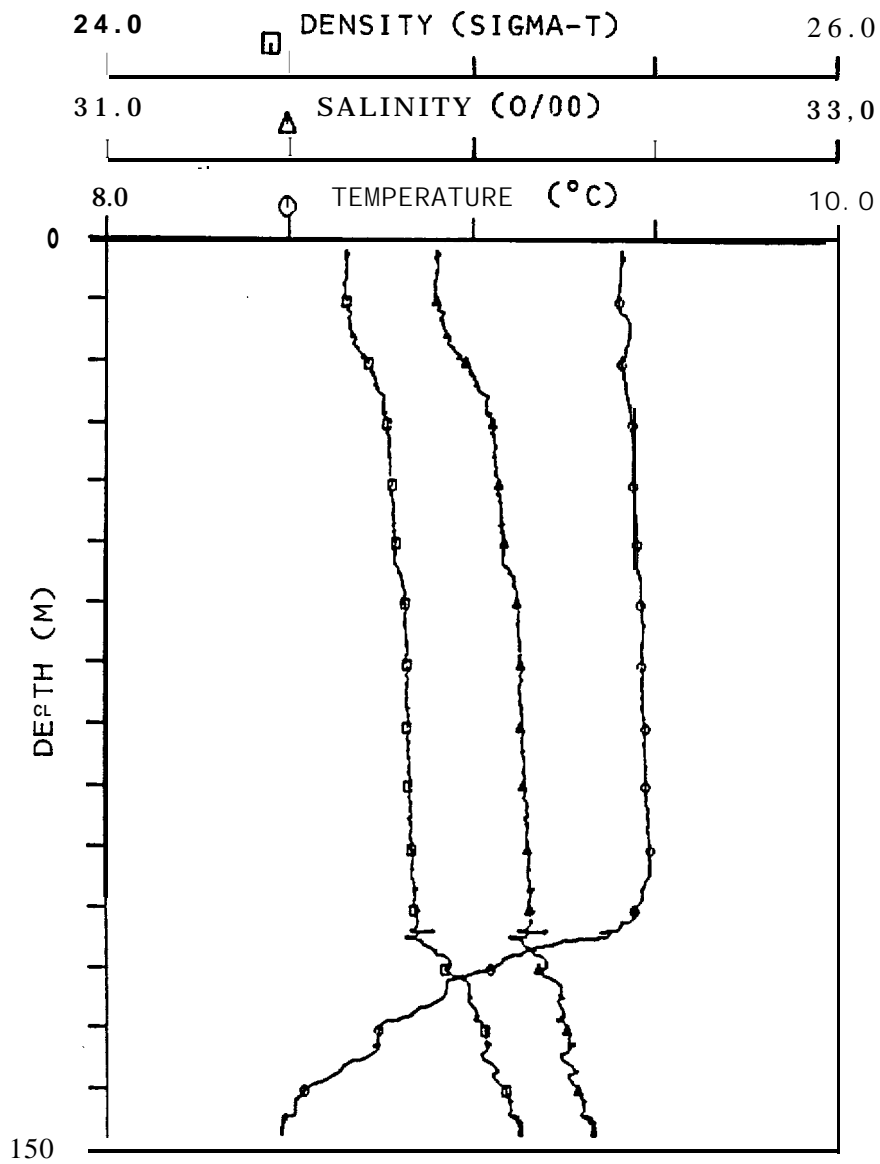


Figure 14. Vertical profiles of temperature, salinity, and density of Station D5 on mid-shelf. Station location is shown on Figure 6.

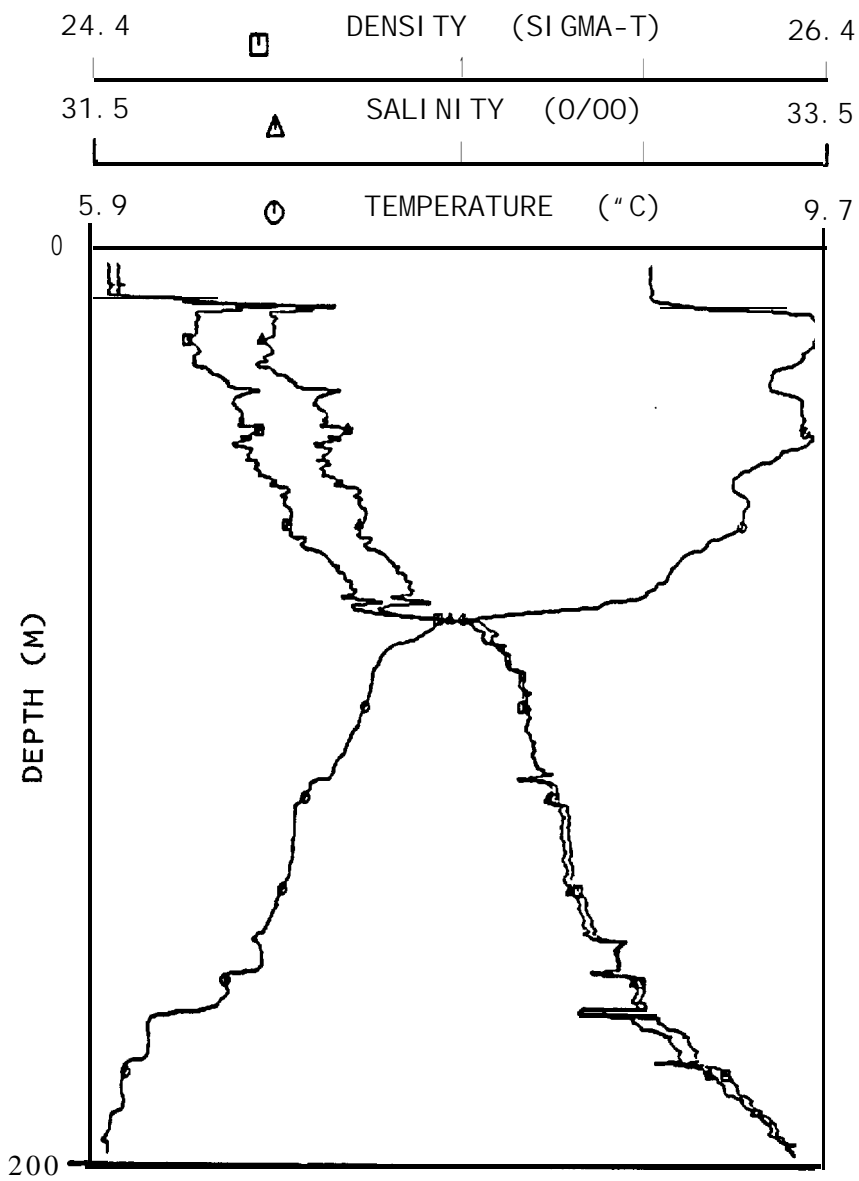


Figure 15. Vertical profiles of temperature, salinity, and density at Station 13 near the shelfbreak. Station location is shown on Figure 6.

To summarize, regional temperature and salinity distributions during October-November 1980 were typified by a two-layered structure seaward from a near-coastal band 10 km from shore. The lower layer was colder and more saline than the upper layer, and the interface between layers occurred at 75-125 m depths. There was a general tendency for salinity to increase, and temperature to decrease, in the offshore direction. Superposed upon this regional distribution was a narrow (< 7 km in most locations), shallow (< 20m) coastal band of water which was low in salinity and temperature relative to that water immediately beneath and to seaward.

### 3.2 Observed Autumn Near-Shore Circulation

Water circulation was observed in October-November 1980 using current meters on taut-wire moorings, drogued buoys, and seabed drifters (see Section 2). Results of each of these observation sets will be discussed separately, because each yielded a different type of circulation information.

#### 3.2.1 Autumn Moored Current Observations

There was considerable similarity between the results from near-shore Moorings 1 and 4 (cf. Figure 2), each of which was between 3 and 4 km offshore. Time series from these moorings are presented in Figures 16 and 17. The two **records show three prominent flow characteristics**. First, cross-shelf current speeds were **small** relative to longshore current speeds. Second, the **along-shore** flow was **bimodal**, with flow to the southeast nearly as frequently as to the northwest (Figure 18). Finally, the currents at each location were dominated by a relatively high speed ' (about 70 **cm/sec** at Mooring 4 and slightly less at Mooring 1) along-shore northwest flow event or pulse beginning on 27 October. At both Moorings 1 and 4, flow had been to the southeast prior to this pulse. Another similar event also occurred late on October 31 at Mooring 1, when simultaneous fluctuations in both the along-shore and cross-shelf components indicated a current pulse at the mooring.

Mooring 2, located about 10 km offshore (Figure 2), **had** current meters at 40m and 129 m. Data from these meters are presented in similar format (Figures 19 and 20), except that a time series is presented of density instead

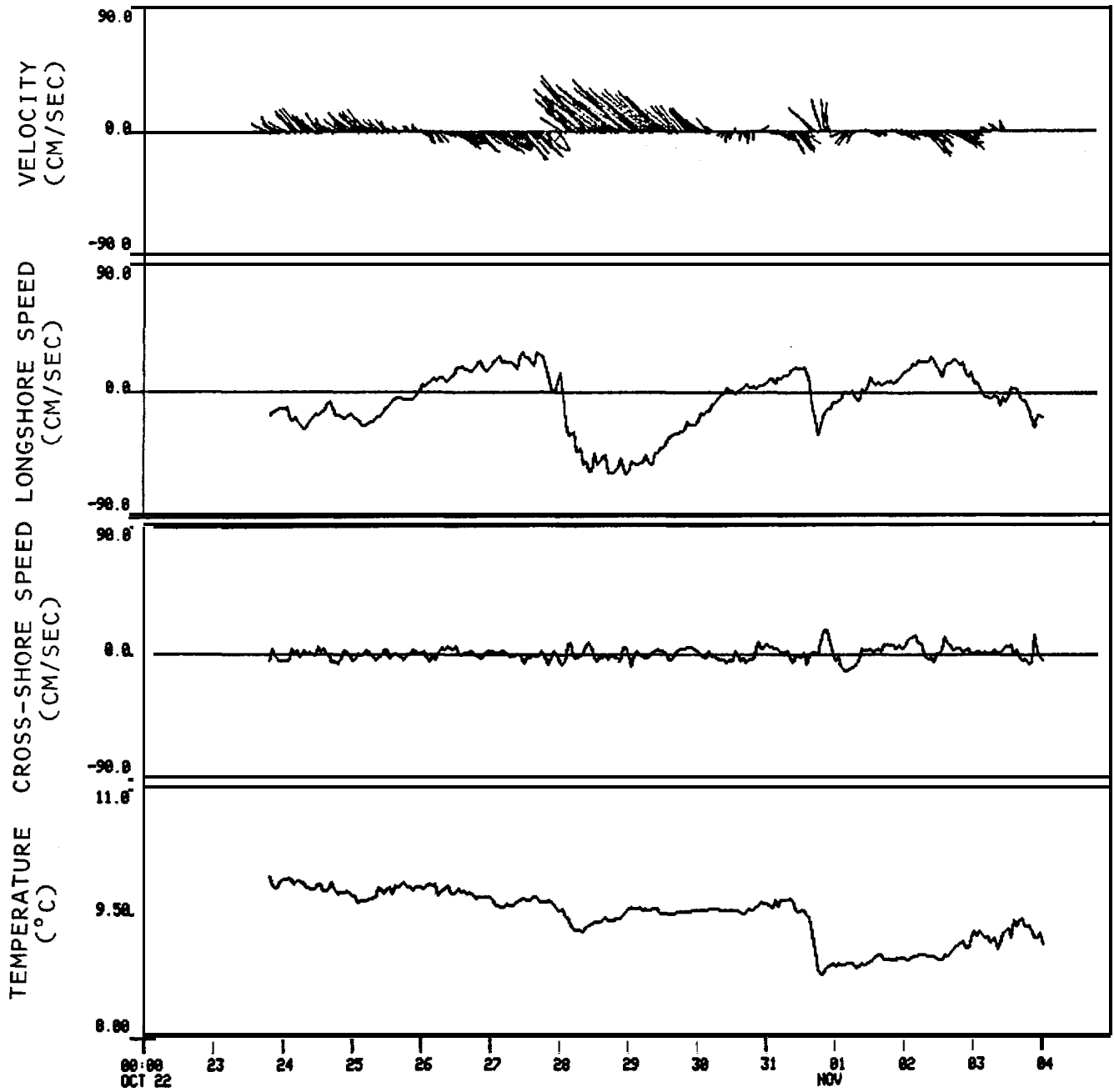


Figure 16. One-hour **lowpass-filtered** time series of currents (as time-stick vector plot, with vertically upward being north) from autumn Mooring 1. Mooring location is shown on Figure 2.

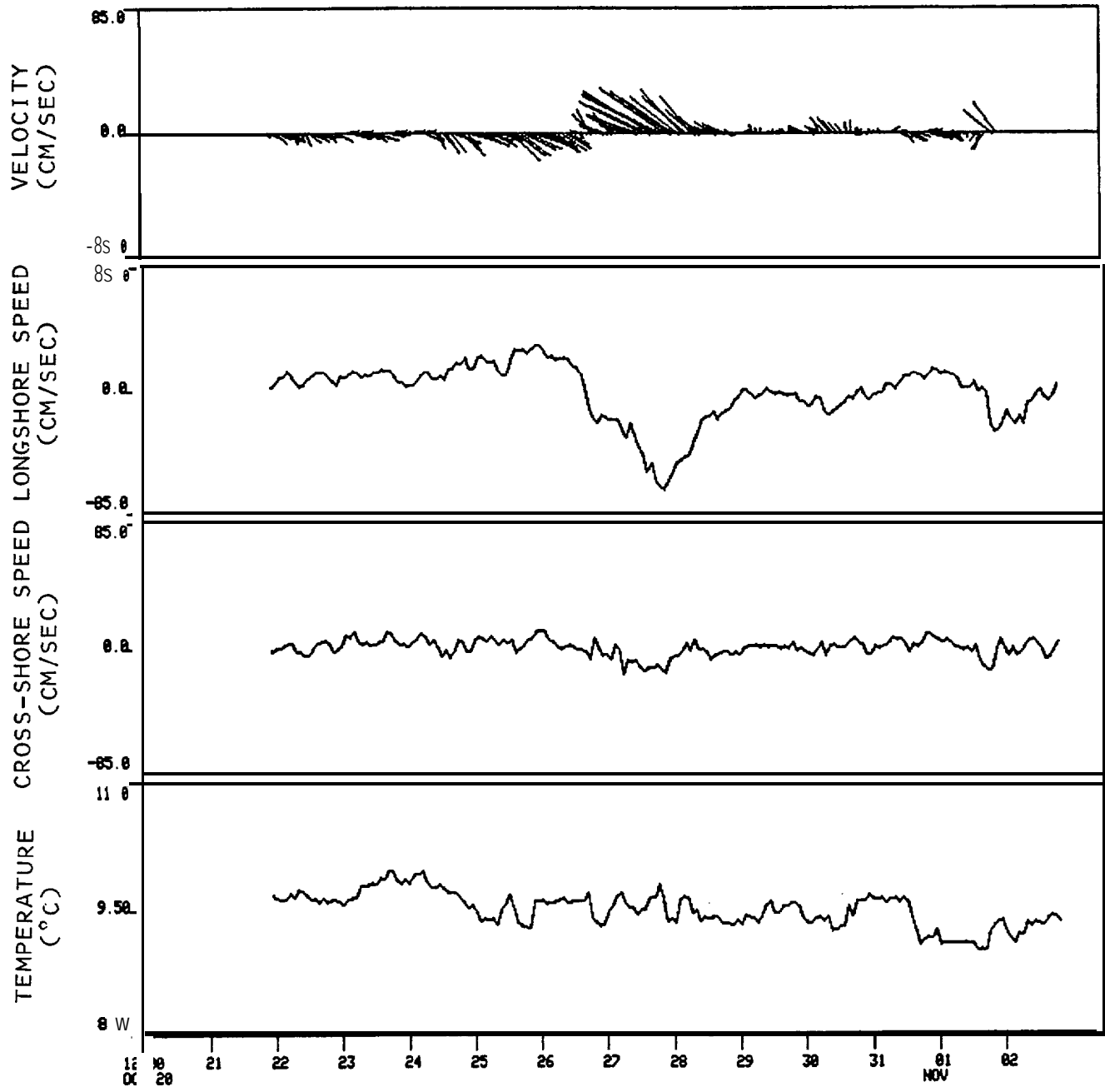


Figure 17. One-hour lowpass-filtered time series of currents (as time-stick vector plot, with vertically upward being north) from autumn Mooring 4. Mooring location is shown on Figure 2.

DIRECTION  
MOORING 1 - FALL

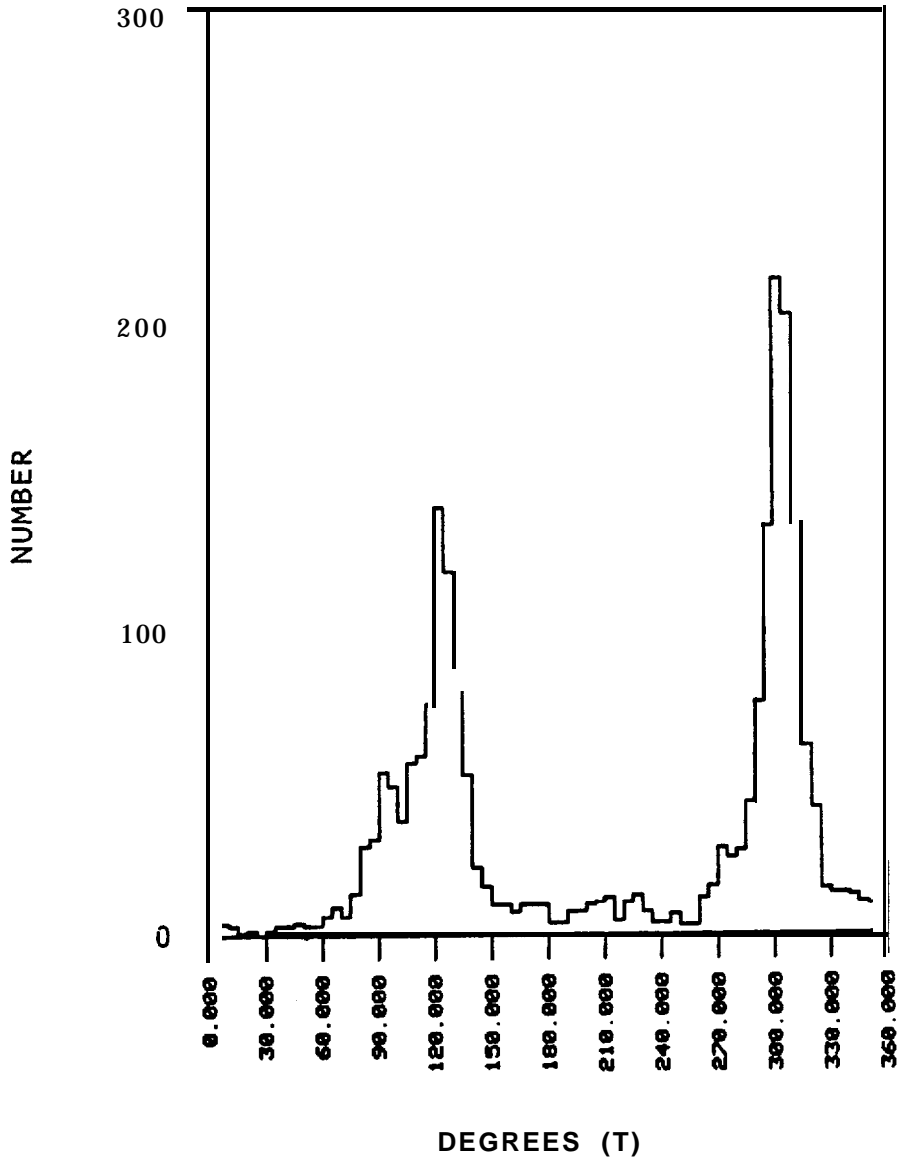


Figure 18. Direction histogram illustrating the **bimodal** flow direction at autumn Mooring 1. Mooring location is shown on Figure 2.

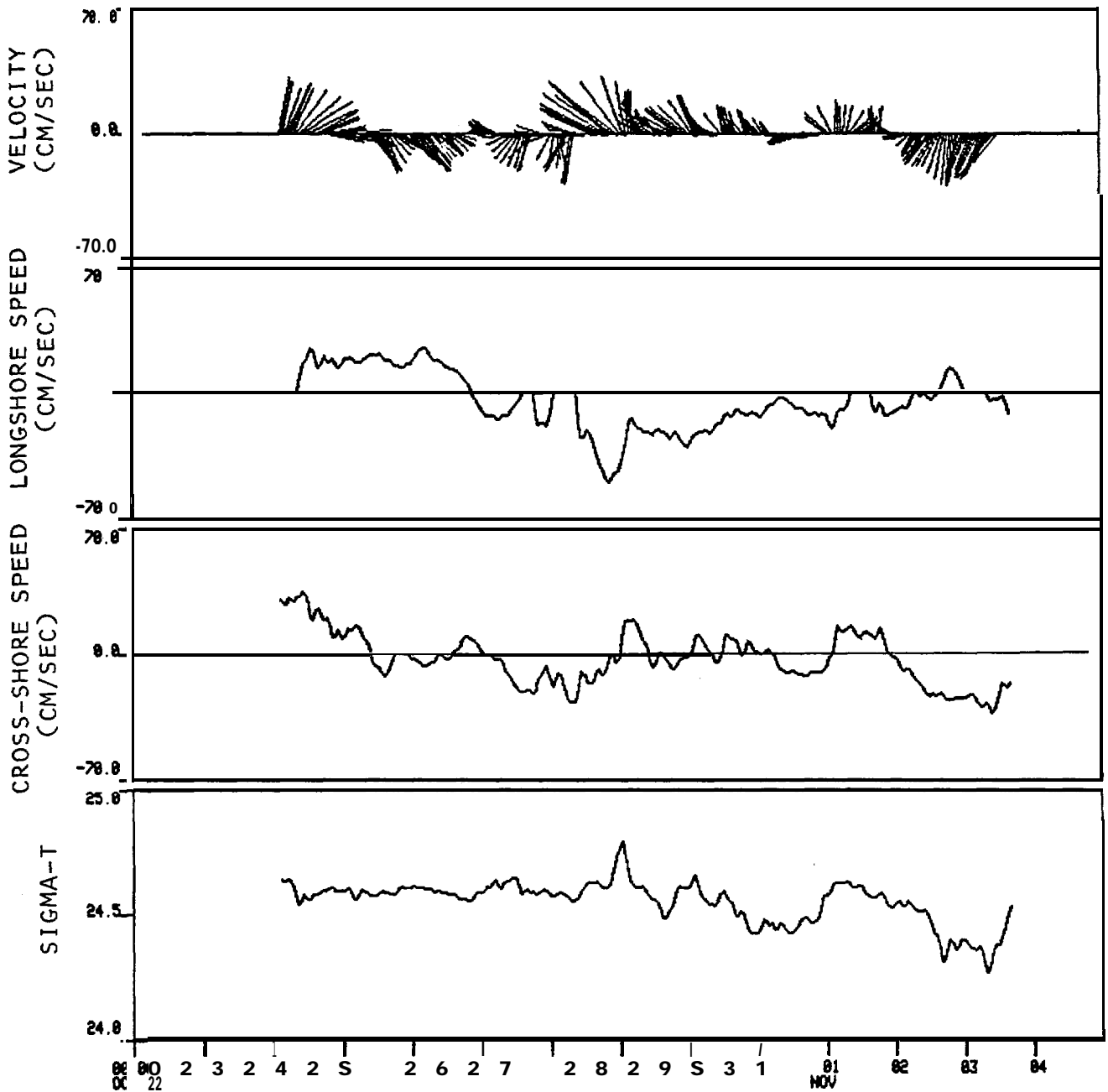


Figure 19. One-hour lowpass-filtered time series of currents as time-stick vector plot, with vertically upward being north, from the 40-m deep meter at autumn Mooring 2. Mooring location is shown on Figure 2.

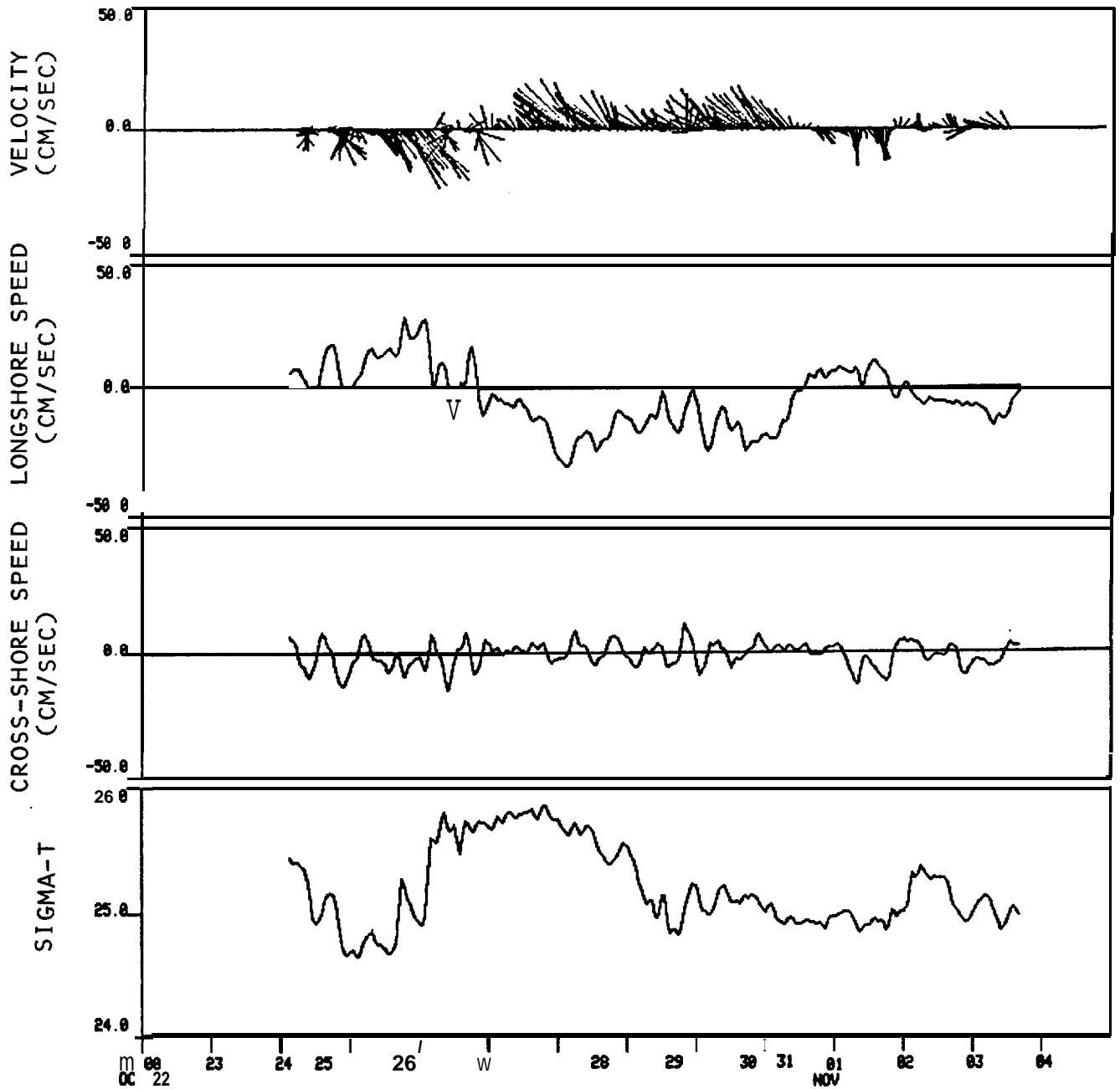


Figure 20. One-hour lowpass-filtered time series of currents as time-stick vector plot, with vertically upward being north, from the 129-m deep meter at autumn Mooring 2.

of temperature as for Moorings 1 and 4. Characteristics of the **flow at** Mooring 2 were similar to those at Moorings 1 and 4. At the deeper current meter, cross-shelf speeds were very small relative to along-shore **speeds**, while at the shallower meter this was less evident than at either the deeper meter or at Moorings 1 and 4. The along-shore flow was **bimodal** at all depths, although the **bimodality** was far stronger at the upper current meter (Figure 21). Finally, the same current pulse observed at Moorings 1 and 4 on 27 October occurred at the upper meter at Mooring 2 a few hours after it was observed at Mooring **1**, reaching peak speeds of about 50 **cm/sec**. The along-shore pulse was followed by a smaller peak in cross-shelf speed. The current pulse was **also** observed at the deep current meter at Mooring 2, but was smaller than at the surface and occurred somewhat earlier. The large fluctuations in density which were apparent at the deep meter at Mooring 2 will be discussed in Section 3.3.

Mooring 5 was located about 9.4 km offshore at 65 m depth and had one operational current meter at 17 m; the deeper current meter deployed on this mooring malfunctioned and thus yielded no record. The most apparent difference **between the flow at the upper meter at Mooring 5 and those discussed above was the relatively large cross-shelf** flow at Mooring 5 (Figure 22). Mooring 5 also detected the northwesterly pulse which was present at the other near-coastal moorings, with a peak speed of about 50 **cm/sec**. A separate feature, unique to Mooring 5, was a strong (> 50 cm/sec) current to the southeast persisting from October 25 to October 27 prior to the northwesterly pulse.

Mooring 6 was considerably farther offshore -- about 70 km -- than Moorings 1-5. Because it was so much farther offshore than the moorings discussed above, it recorded **currents** within a basically different mid-shelf current regime than the older moorings discussed above. Results from the Mooring 6 observations are shown on Figures 23 and 24. Both speed and direction at the upper (29 m) meter showed considerable variability; a speed pulse on one occasion (17 November, after the other moorings had been recovered) was greater (nearly 80 cm/sec) than had been recorded elsewhere. Along-shore and cross-shelf speed fluctuations were of the same order, unlike conditions at the moorings nearer the coast where (except for Mooring 5) the flow was predominantly along-shore. Tidal fluctuations are evident on the plots, but these fluctuations were secondary in significance to the longer period (**~ 4 days**)

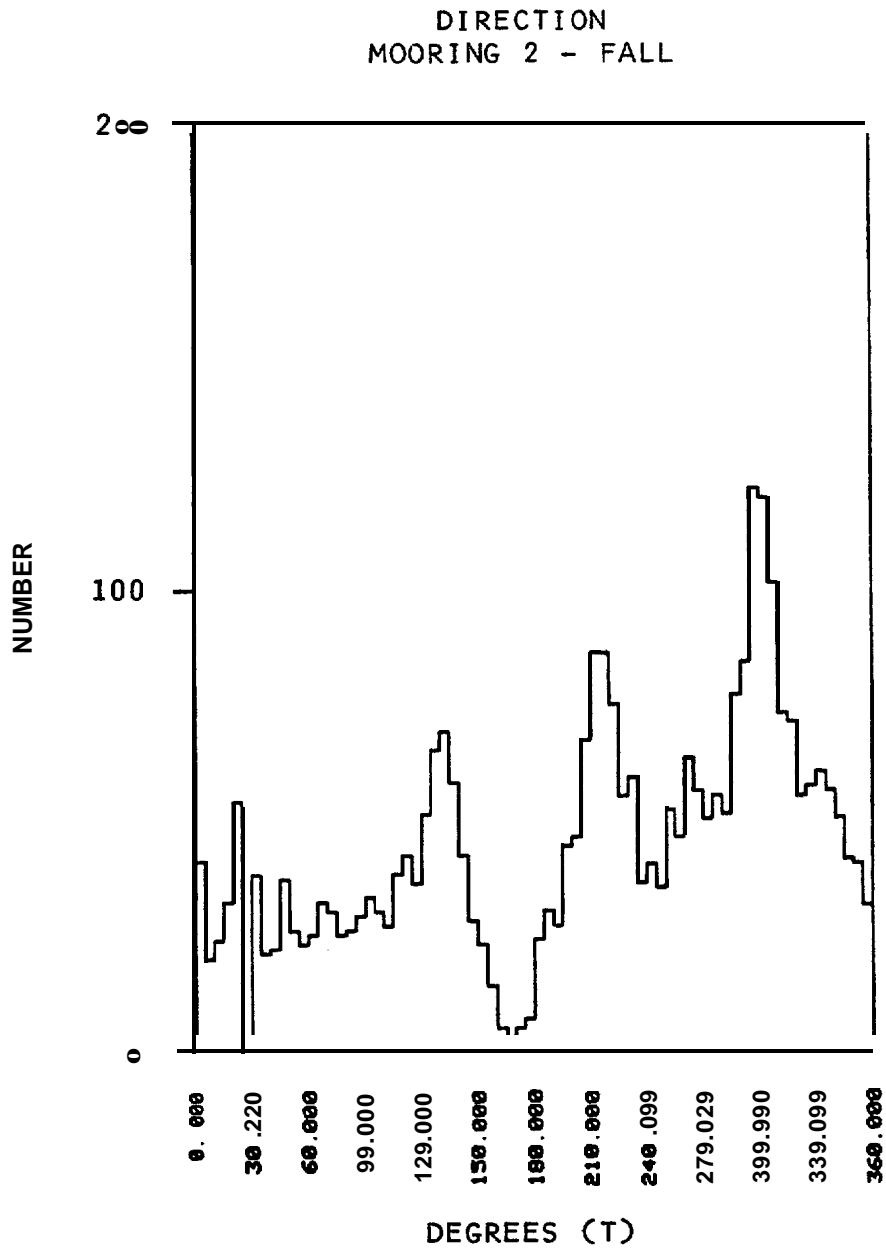


Figure 21. Histogram illustrating the flow direction tendencies at the shallow meter on autumn Mooring 2.

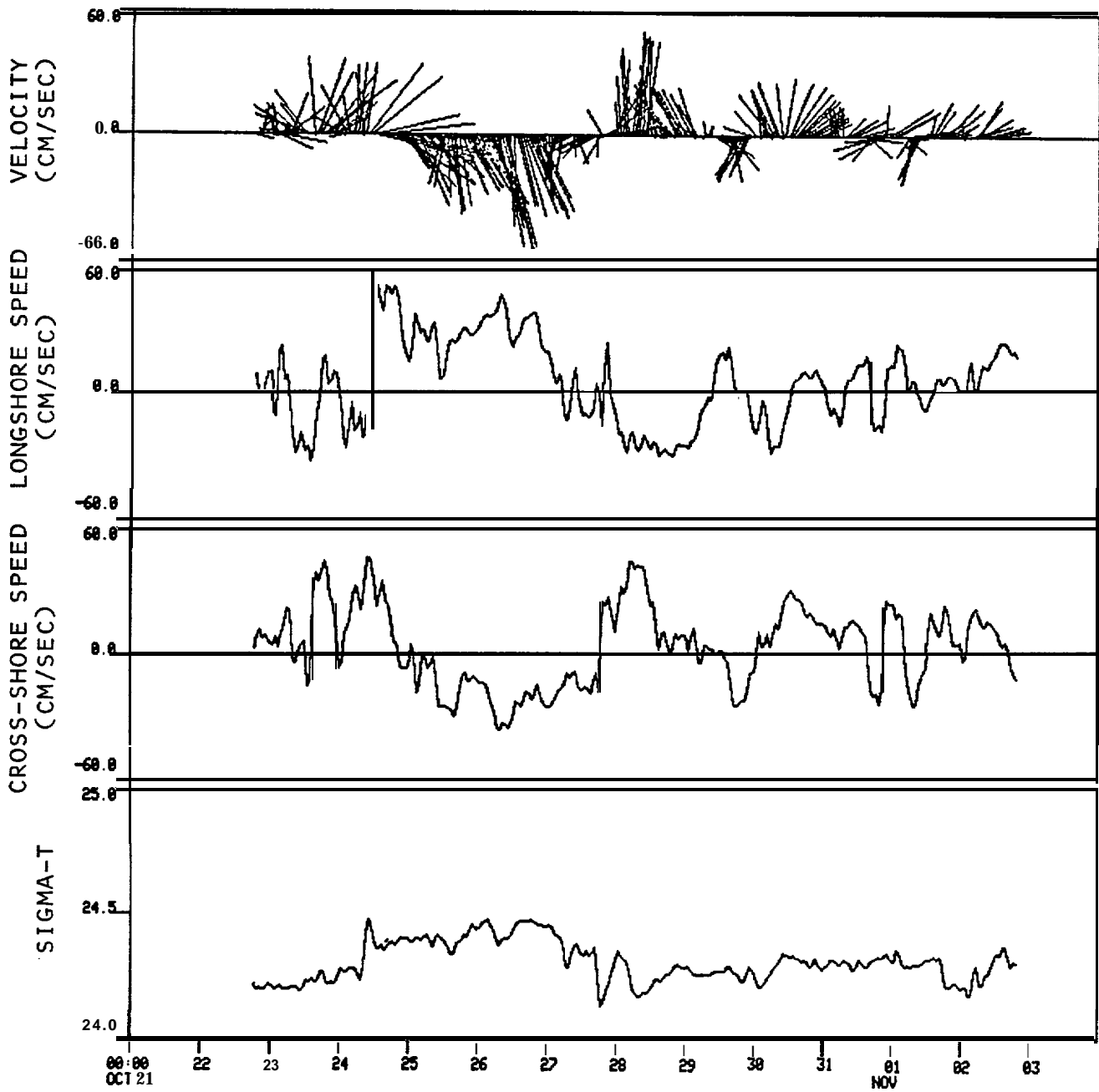


Figure 22. One-hour lowpass-filtered time series of currents as time-stick vector plot, with vertically upward being north, from the 17-m deep meter at autumn Mooring 5. Mooring location is shown on Figure 2.

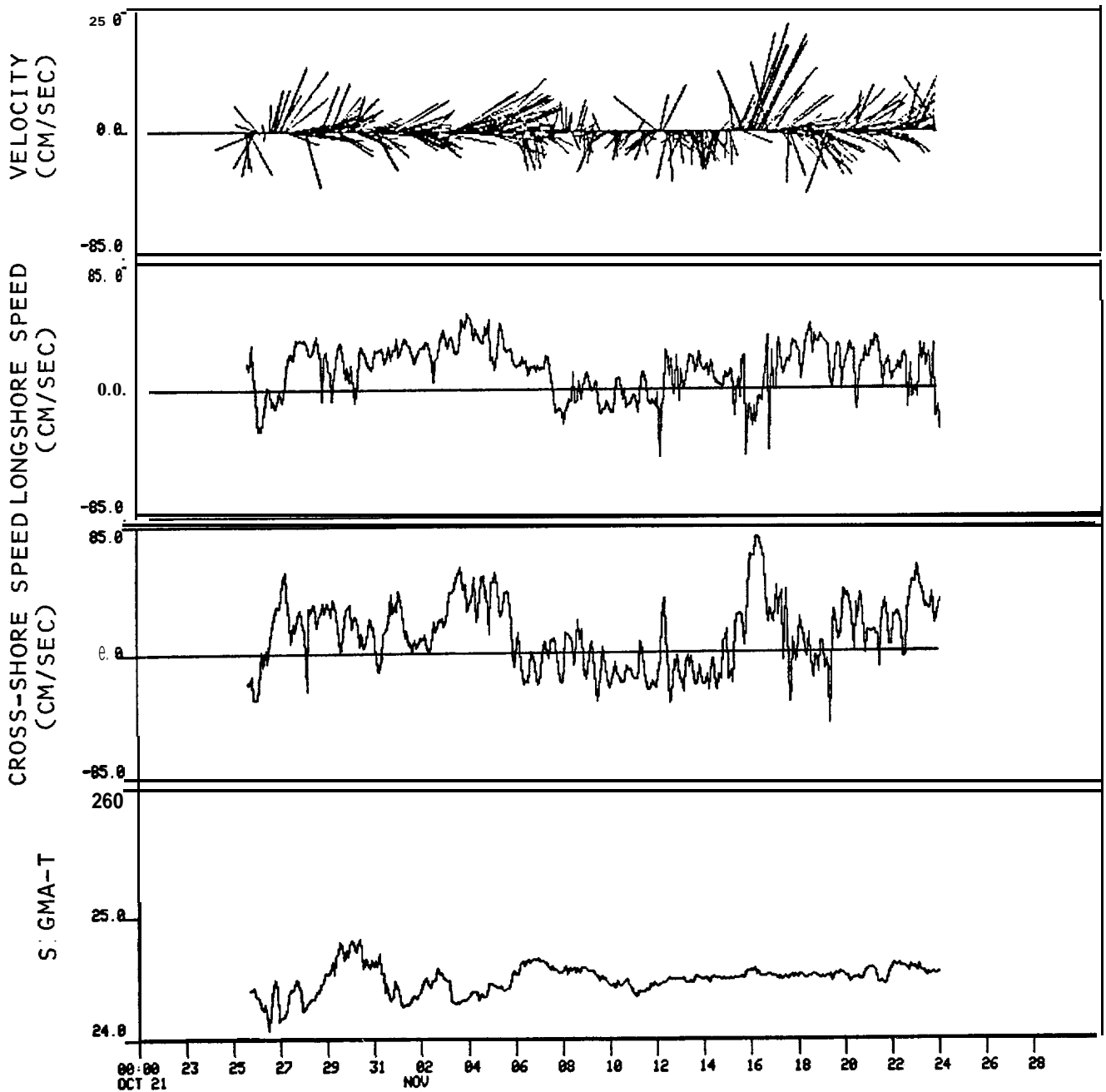


Figure 23. One-hour **lowpass-filtered** time series of currents as time-stick vector plot, with vertically upward being north, from the 29-m deep meter at autumn Mooring 6. Mooring location is shown on Figure 2.

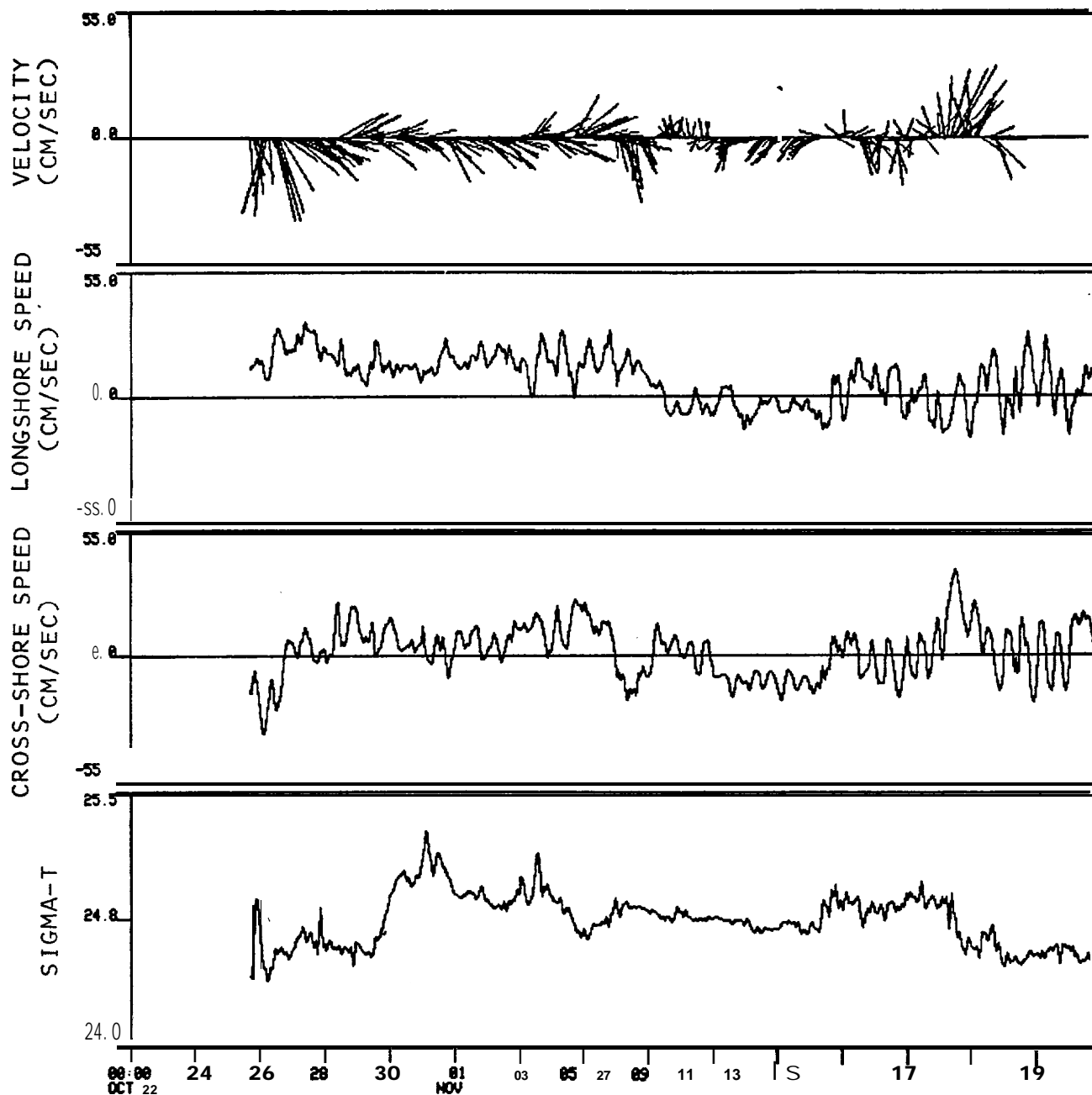


Figure 24. One-hour **lowpass-filtered** time series of currents as time-stick vector plot, with vertically upward being north, from the 102-m deep meter at autumn Mooring 6. Mooring location is shown on Figure 2.

fluctuations such as that which resulted in the **along-shore** speed peak on 17 November. The net flow during the period of the autumn experiment was easterly, with a great deal of directional fluctuation. Current speeds at the lower (102 m depth) meter were lower than at the upper meter, and the tidal signal was therefore relatively more significant. Visual inspection of the plots suggests that coherency between the upper and lower records was poor. At Mooring 6 there was no detectable signature of the along-shore current pulse which had been a prominent feature of the nearer-shore records on 27 October.

### 3.2.2 Autumn Drogued Buoy Observations

The first autumn drogued buoy experiment was conducted 26-28 October 1980. The buoys were deployed within a 0.5-km radius and tracked for approximately one day, after which Buoy 1 was retrieved and the ship broke off operations to drop personnel in Yakutat. Tracking of the remaining two buoys was resumed after a hiatus of approximately 23 hours due to storm conditions. The buoys were subsequently tracked for 15 hours and then retrieved. A composite **dia-**gram of all fall buoy tracks is displayed in Figure 25, and more detailed individual buoy tracks are shown in Figures 26 and 27.

During Phase I of the first experiment, the buoys moved briefly in unison due north then reversed direction, turning toward the southeast (Figure 25). **Statistically the buoy speeds (Table 3) for Phase I are essentially** identical with a mean speed for all three **drogues** near 13 **cm/sec** and peak speeds of 20-25 **cm/sec**. All three buoys initially traveled in the same water parcel for this phase, and the **separation** distance between the buoys (Figure 28) decreased during the first 12 hours (to **~50 m at some times**). By 1600 hours **on 26 October**, 15.5 hours after deployment, the buoys started to disperse more rapidly. The mean separation rates for this last part of Phase I ranged from 1.4 to 5.1 **cm/sec**.

Buoy 1 was now retrieved and the ship left the area as described above. During its absence current conditions changed considerably. Both remaining buoys (2 and 3) reversed direction and were traveling northwestward with considerably higher speeds (Table 3). In Phase II of the experiment, peak speeds of 47 and 105 **cm/sec** were reached at approximately 1100 hours on 28 October, thus

Table 3

AUTUMN **DROGUED** BUOY SPEED STATISTICS

	MIN SPEED (cm/sec)	MAX SPEED (cm/sec)	MEAN SPEED (cm/sec)	SPEED STD DEV (cm/sec)
EXPERIMENT 1				
<u>Phase I: 10/26/80 (0030 hrs) - 10/27/80 (0230 hrs)</u>				
Buoy 1	4.0	24.9	13.3	4.9
Buoy 2	5.0	21.2	13.5	3.9
Buoy 3	4.4	20.2	12.2	3.6
<u>Phase II: 10/28/80 (0200 hrs) - 10/28/80 (1630 hrs)</u>				
Buoy 2	12.5	46.9	29.4	10.6
Buoy 3	24.4	104.7	62.6	28.4
-----				
EXPERIMENT 2				
<u>Phase I: 10/29/80 (0230 hrs) - 10/29/80 (1730 hrs)</u>				
Buoy 2	0.6	18.7	8.5	4.4
Buoy 3	4.0	21.7	14.0	5.1
<u>Phase II: 10/29/80 (1800 hrs) - 10/30/80 (1730 hrs)</u>				
Buoy 1	12.3	42.1	28.1	8.3
Buoy 2	13.0	43.7	29.1	8.7
Buoy 3	6.8	49.1	24.1	9.6

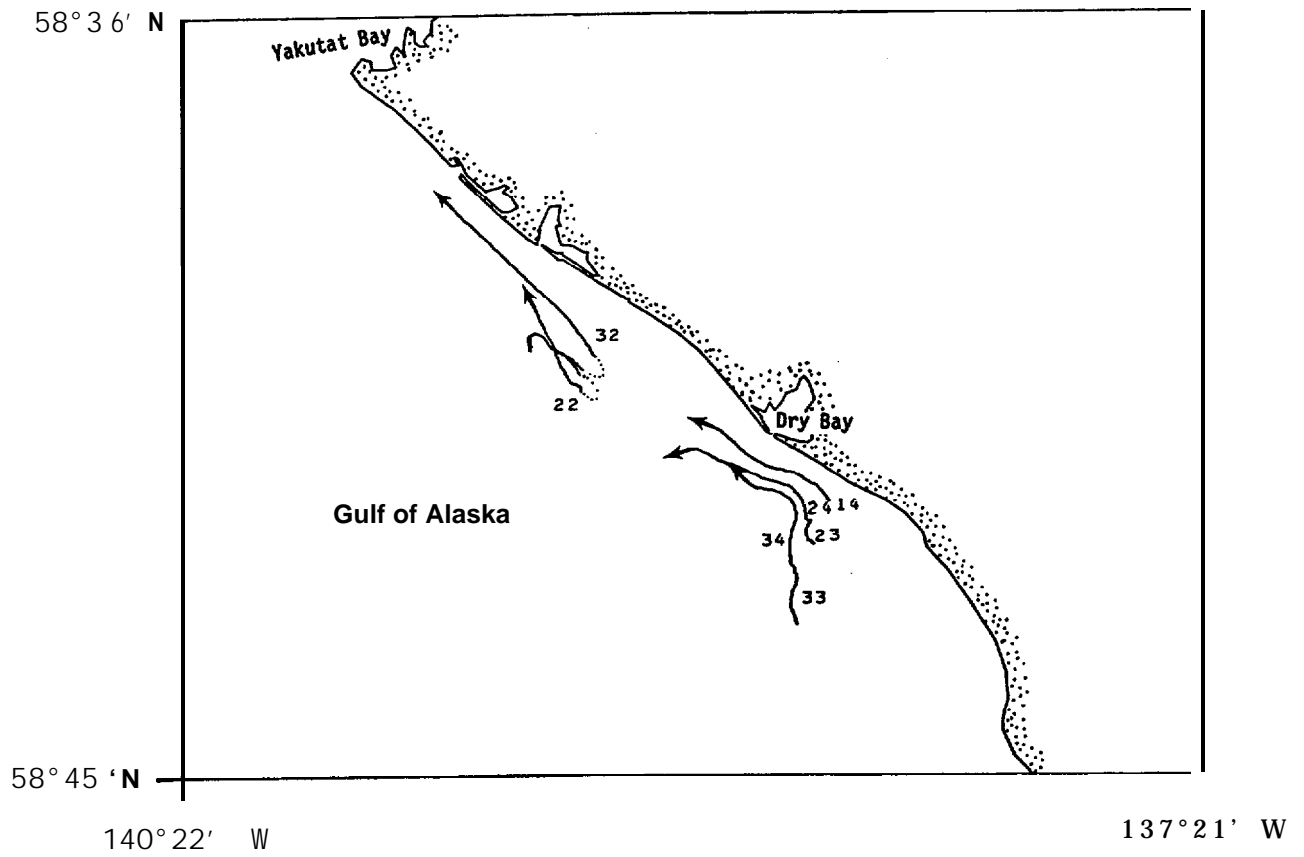
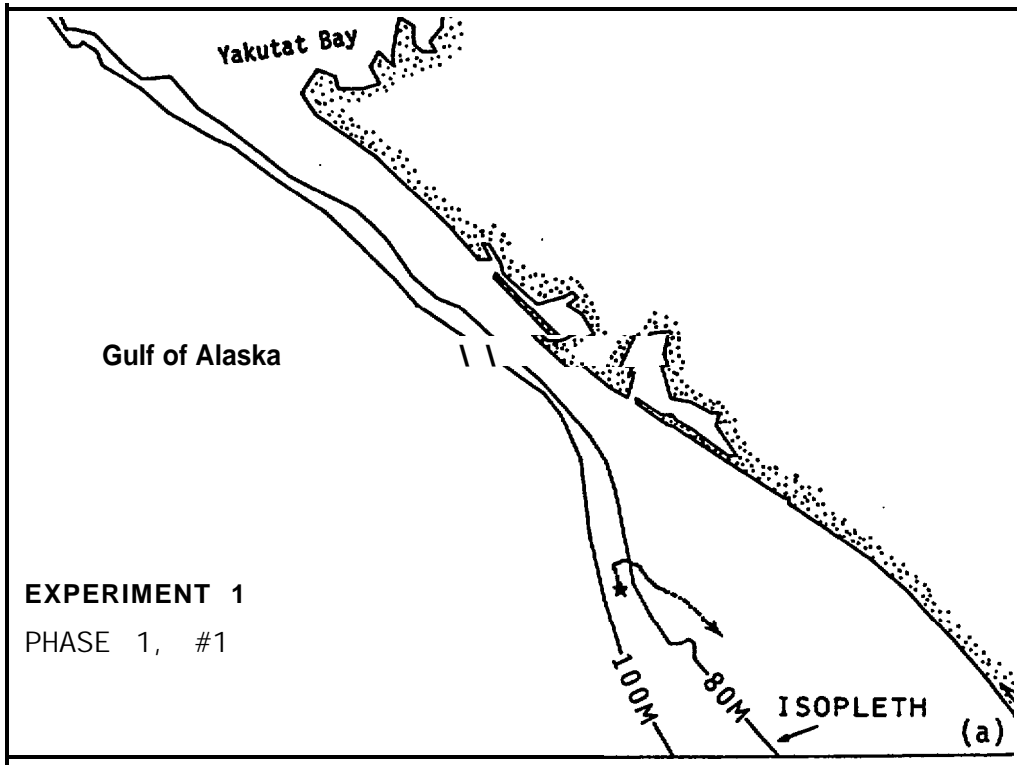


Figure 25. Composite picture showing all **drogued** drifter tracks observed in autumn 1980.

59°36'N

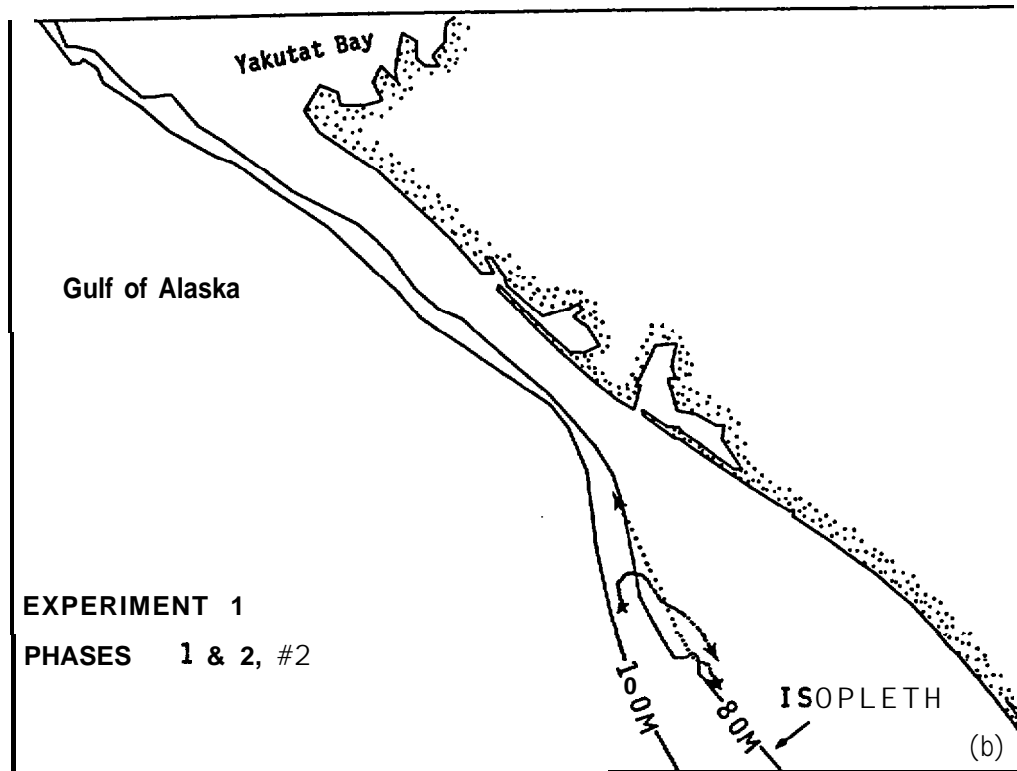


58°45'N

140°22'W

137°21'W

59°36'N



58°45'N

140°22'W

137°21'W

Figure 26. Individual drogue tracks (a), (b), (c) followed by Drifters 1, 2, 3 respectively in the first autumn 1980 drogue experiment. Stars mark start points for each drift track segment.

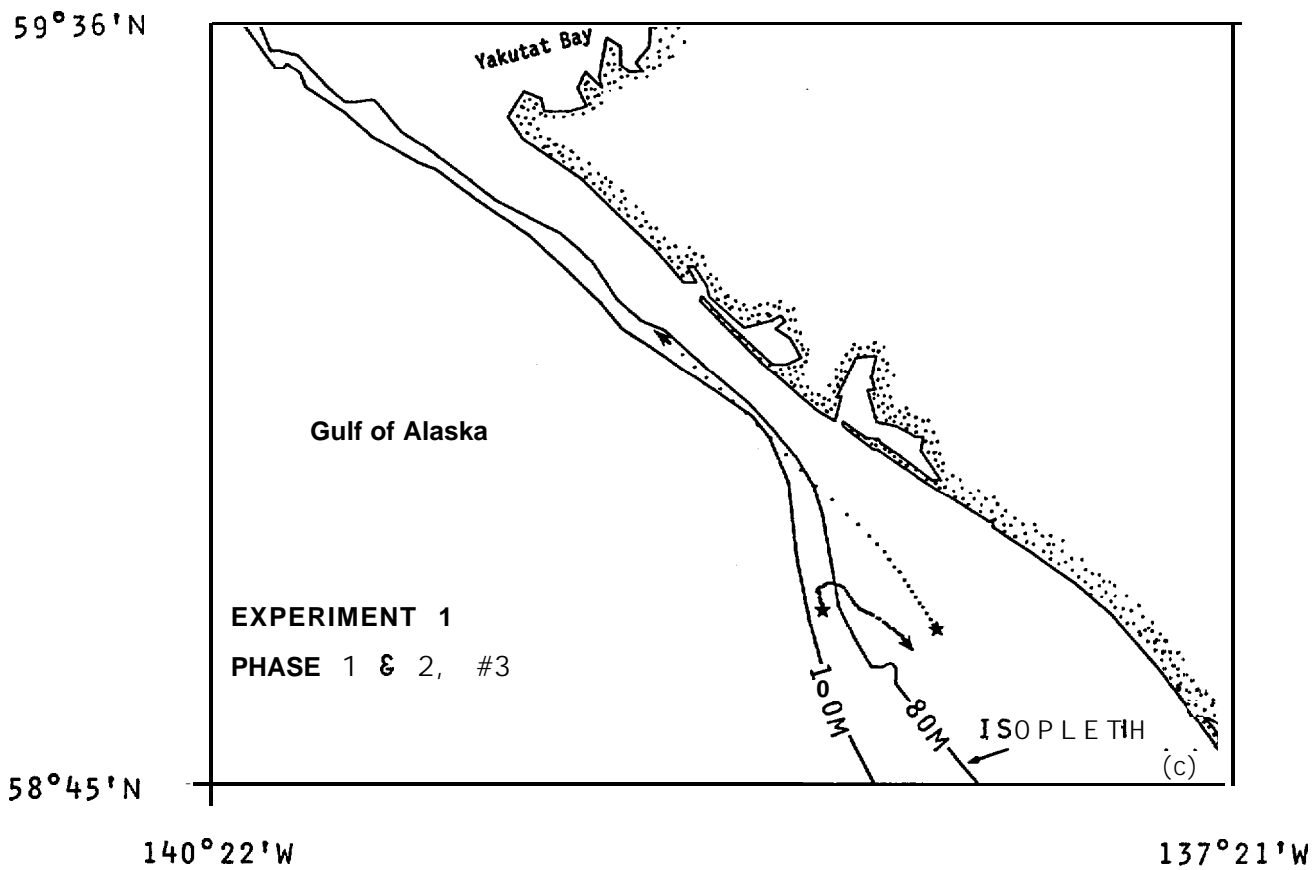
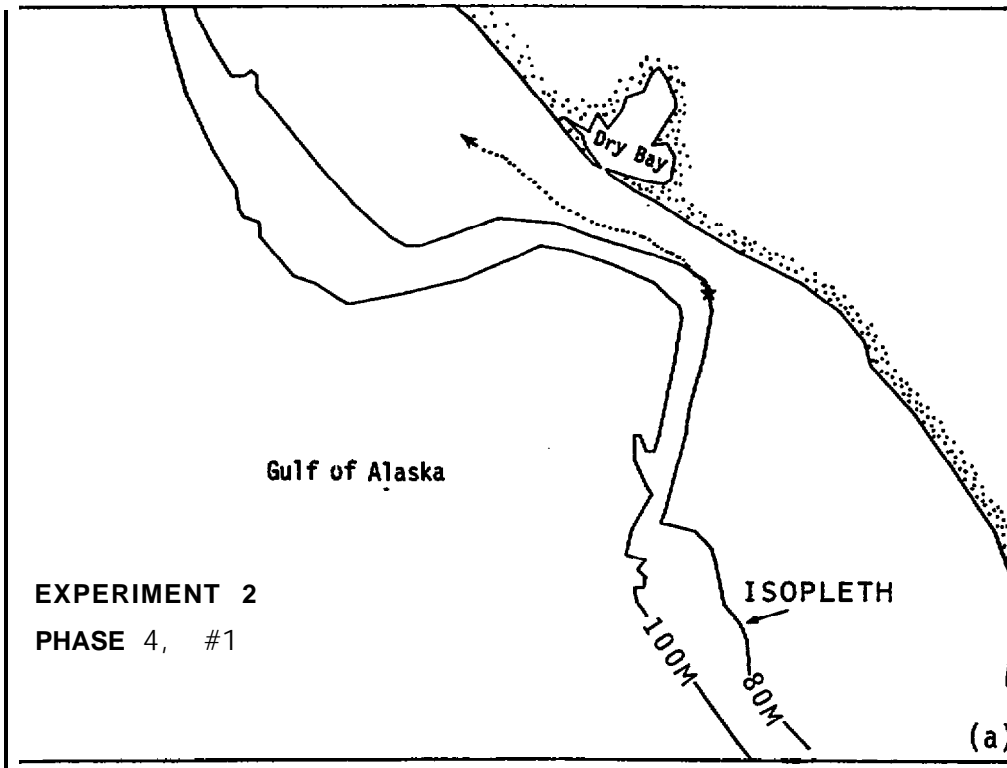


Figure 26 (continued).

59°36'N

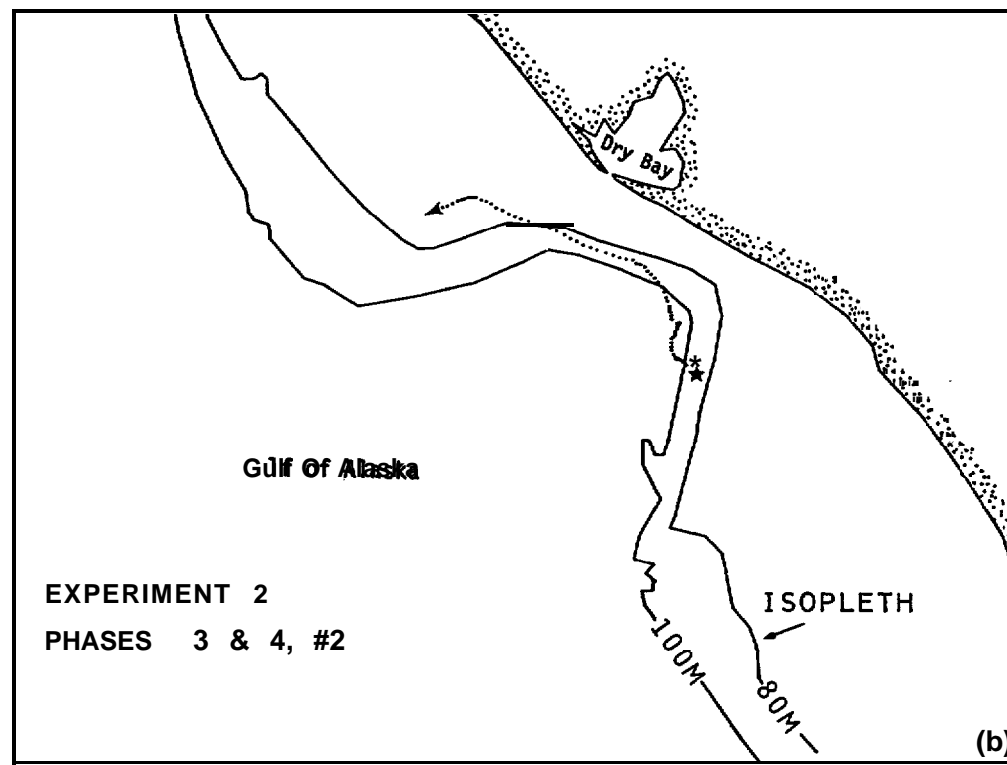


58°45'N

140°22'W

137°21'W

59°36'N



58°45'N

140°22'W

137°21'W

Figure 27. Individual drogue tracks (a), (b), (c) followed by Drifters 1, 2, 3 respectively for the second autumn 1980 drogue experiment. Stars mark start points for each drift track segment.

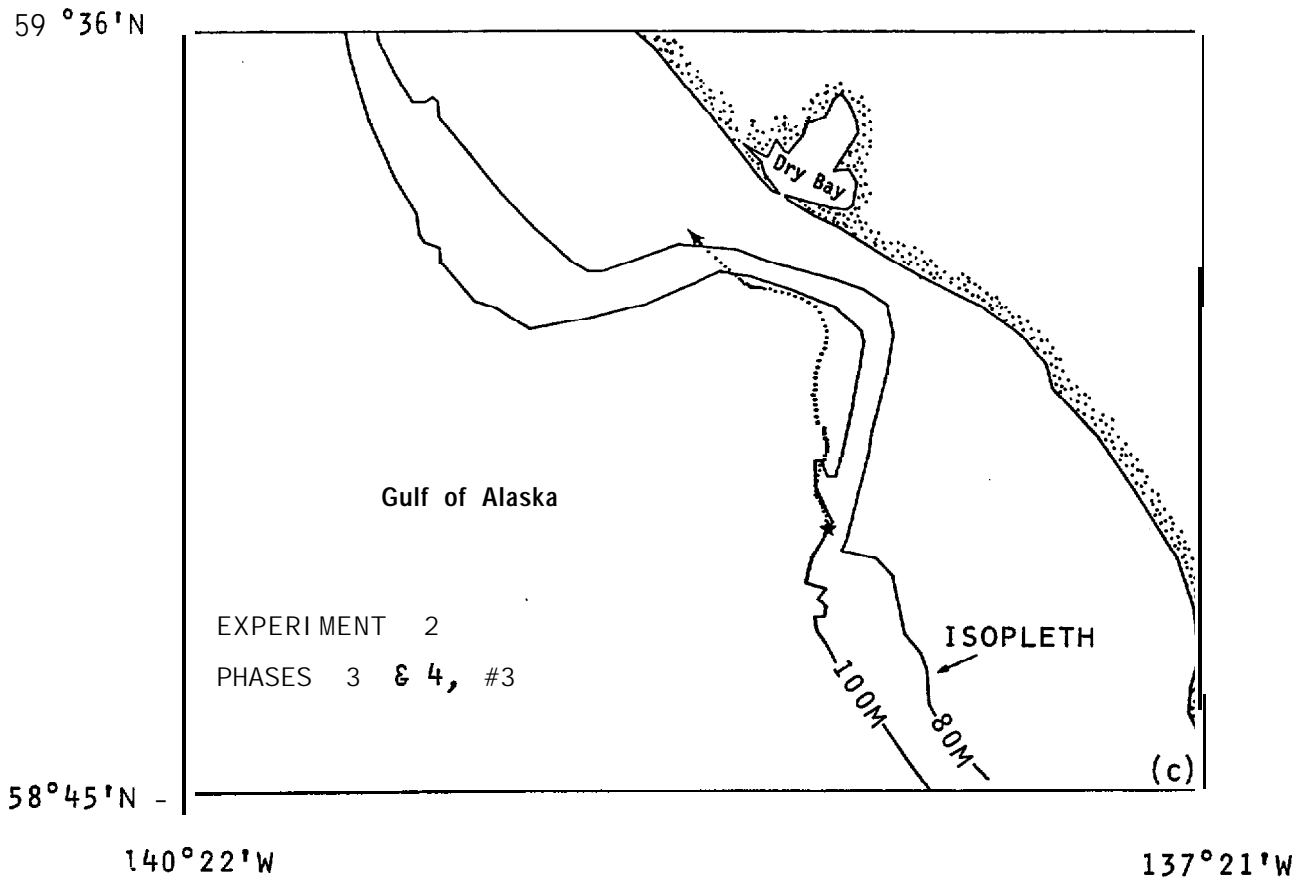


Figure 27 (continued):

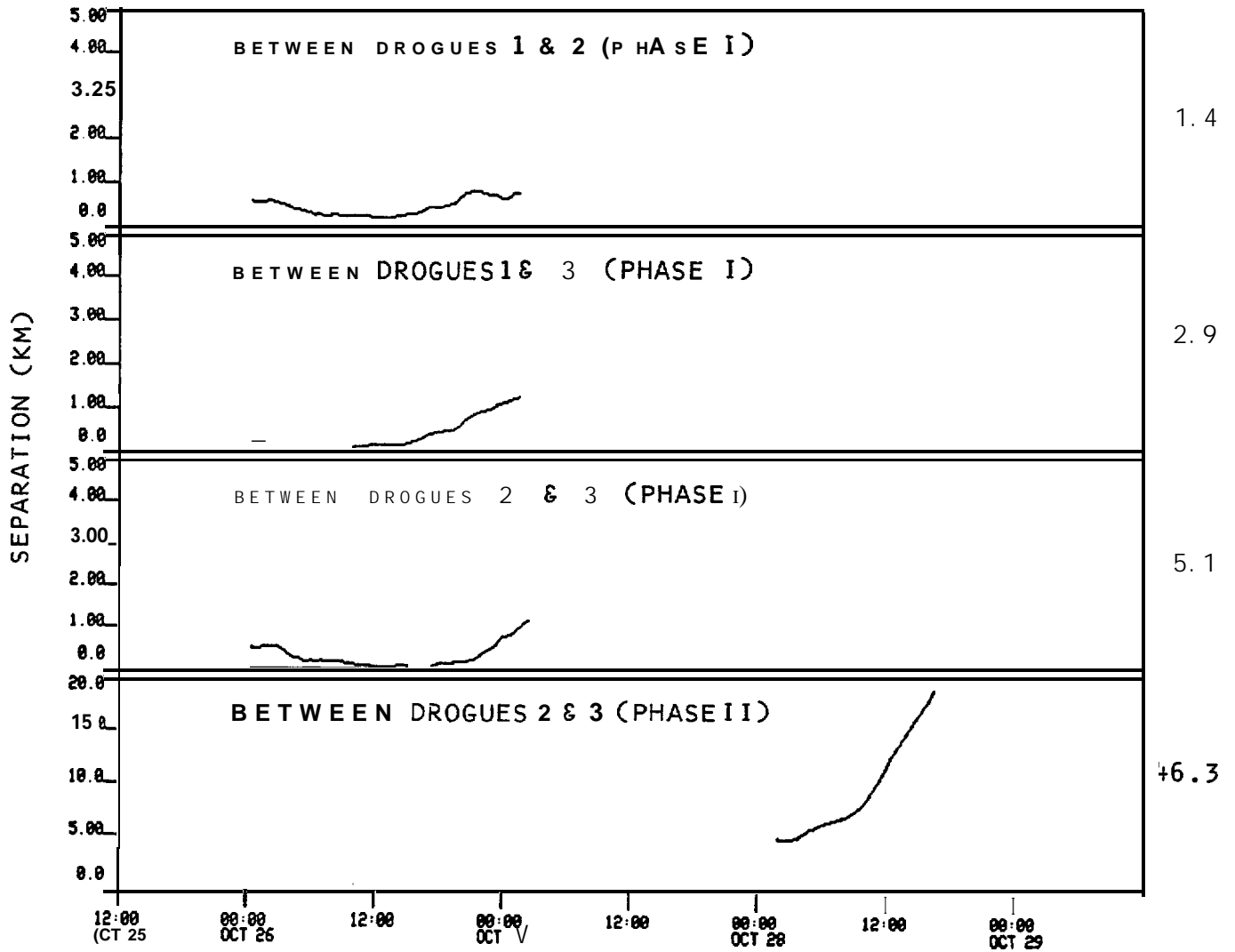


Figure 28. Plot of separation between **drogues** as a function of time for the autumn 1980 drifter experiment.

lagging the peak **winds** by **10-12** hours (Figure 29). As Buoy 3 was subjected to higher speeds, the average **separation rate between** the buoys reached **20 cm/sec** (Figure 28). Buoy 2, **which was slightly offshore of** Buoy 3 at the beginning of Phase II, traveled **~ 50** percent slower and had a stronger northward component than Buoy 3 (Figure 26), suggesting entrainment into a strong near-shore current feature. After 14 hours of tracking, the buoys were retrieved and the ship proceeded southeast for the second experiment.

For the second experiment, the buoys were deployed in a line roughly normal to the coastline (Figure 25). Buoys 2 and 3 were deployed initially (Phase I) with Buoy 1 being deployed approximately 15 hours later (Phase II). The buoy tracks followed the bathymetry closely for both phases of this experiment (see individual buoy tracks in Figure 27). This observed pattern of motion was due to the steering influence of the sharp topography at the head of the **Alsek** Canyon on the longshore current. Mean speeds (Table 3) **were lower for Phase I than** for Phase **II**, as the **buoys were turning** under the influence of the topographic effect. All three **buoys** showed increased speeds during Phase II, when mean speeds ranged from 24 to 29 **cm/sec** and peak **speeds reached** 40 to 50 **cm/sec**.

Summarizing the **drogued** buoy data for the fall **survey, considerable variability was found in current speed and direction**. A slow (**~ 13** cm/sec) mean drift to the southeast was found to **reverse and become quite intense** (**~ 63** cm/sec) concurrent with the onset of a storm event. Topography was observed to have considerable influence on current direction at the head of a **deep "submarine** canyon. Buoy drift speeds increased by factors of two to three as buoys appeared to be entrained from offshore into a stronger near-shore along-shore current. *Presence* of this accelerated flow was probably **due in part to shoreward packing of** streamlines as the water movement parallels **isobaths** shoreward along the upstream (southeast) side of **Alsek** Canyon.

### 3.2.3 Autumn Littoral Currents

During the period of the littoral zone current **study** (28-30 October 1980), strong northwestward currents were observed both in surface surf zone (**~ 200** cm/sec) and along the bottom (**~ 30** cm/sec) as estimated using wave measurements and as shown by seabed drifters, respectively. The strong currents were evidently caused

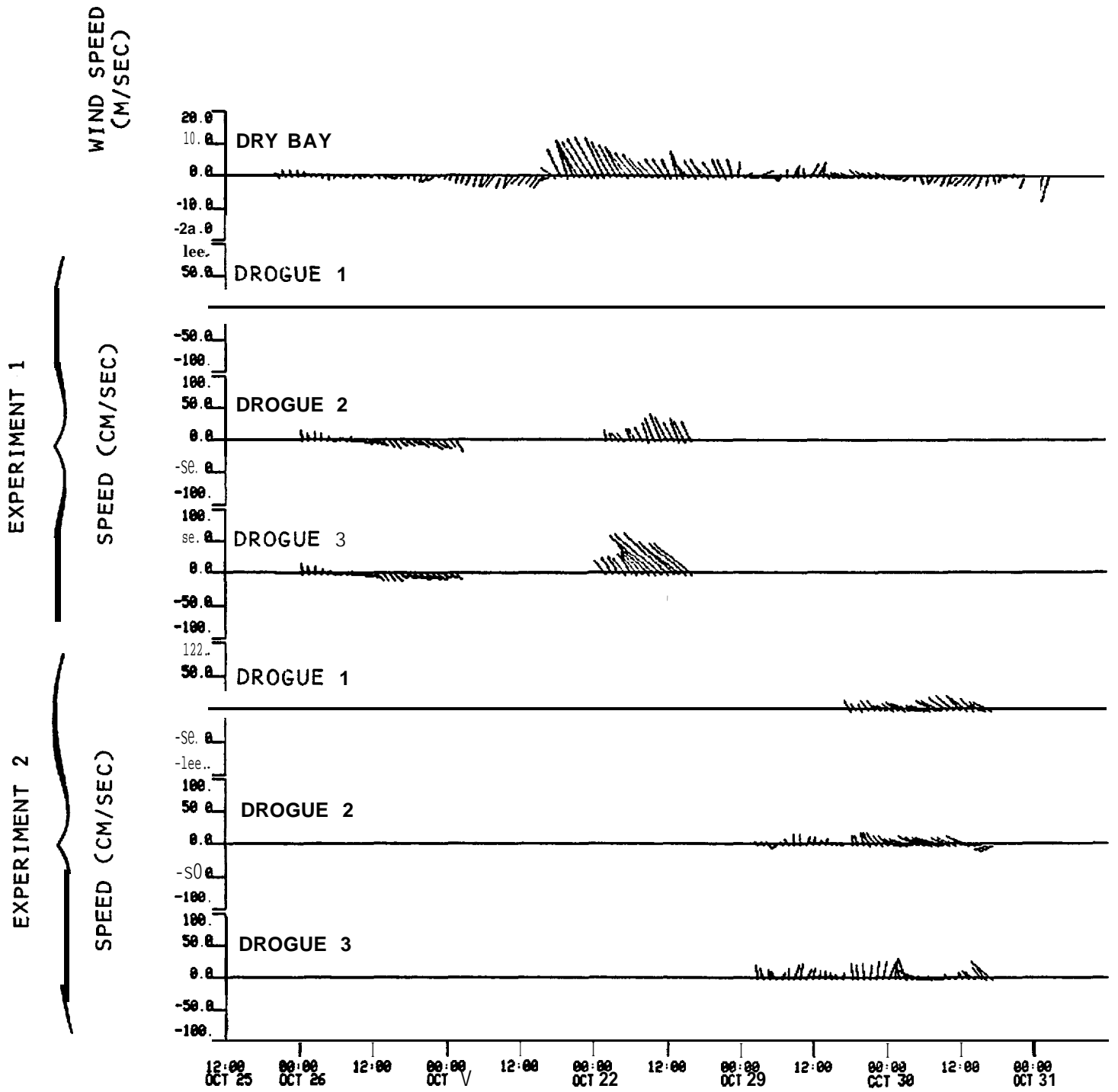


Figure 29. Plot of **drogue** speeds as a function of time and vector wind observed at Dry Bay.

by storm-induced wave action **which was maximum on 28 October**, the day the seabed drifters were launched.

The longshore surface currents (Table 4) were computed as described in Section 2. They were highest the day of the launch ( $\sim 196$  cm/sec), were lower the next day ( $\sim 93$  cm/sec), and eventually reversed direction on the last day ( $\sim -154$  cm/sec) (these **speed estimates are peak values valid only in the region of breaking waves**). Also displayed in Table 4 are vector-averaged along-shore velocity values which should be more easily compared with the bottom velocity values from the seabed drifters. **The vector-averaged velocities do show a strong northwestward current pulse on the day of the launch and a subsequent decrease to levels similar to that seen in the seabed drifter velocities discussed below.**

Three groups of seabed drifters were also launched on 28 October, and strandings were recorded as described above (Section 2). The three groups of drifters will be discussed progressing from near-shore to offshore. **The recoveries from Group 1F occurred generally on the first day close to the launch site, resulting from mean along-shore speeds to the northwest from 0 to 3 cm/sec (Figure 30a); two drifters from this group were recovered on the second day and reflected similar speeds and no seabed drifters from this group were recovered on the third search day.**

The recoveries from Group 2F **showed a distinct bimodal distribution of mean speeds** for the first day (Figure 30b). The lower speed peak ranged from 2 to 30 cm/sec, with a weighted mean value of 15 cm/sec. The higher peak showed speeds **ranging from 24 to 34 cm/sec, with a mean value of 29 cm/sec**. The **second day of recoveries for this group showed two-day mean speeds to be similar to the lower speed peak** seen on **the** first day of recoveries, with speeds to the northwest ranging from 2 to 16 cm/sec with a weighted mean of 12 cm/sec. Again, no drifters were recovered on the third day.

The outermost group, 3F, had a recovery pattern similar to Group 2F (Figure 30c). The first day of recoveries displayed a speed peak at 18 cm/sec with some drifters having speeds up to 35 cm/sec. On the second day, the two-day average speed was 12 cm/sec with values ranging from 8 to 16 cm/sec. No drifters were recovered the third day.

Table 4

AUTUMN SURFACE CURRENT VELOCITY  
ESTIMATED FROM WAVE PARAMETERS\*

	WAVE ANGLE ( $^{\circ}$ )	WAVE HEIGHT (m)	LONGSHORE SURFACE VELOCITY (cm/see)	VECTOR- AVERAGED VELOCITY (cm/see)
Launch	24 ( $\pm 3$ )	2.0 ( $\pm 0.5$ )	196 ( $\pm 42$ )	196
Day 1	15 ( $\pm 3$ )	1.0 ( $\pm 0.5$ )	93-(*40)	127
Day 2	-28 ( $\pm 3$ )	1.0 ( $\pm 0.5$ )	-154 ( $\pm 50$ )	15

\* Error estimates in velocity are those resulting from the uncertainties in angle and height.

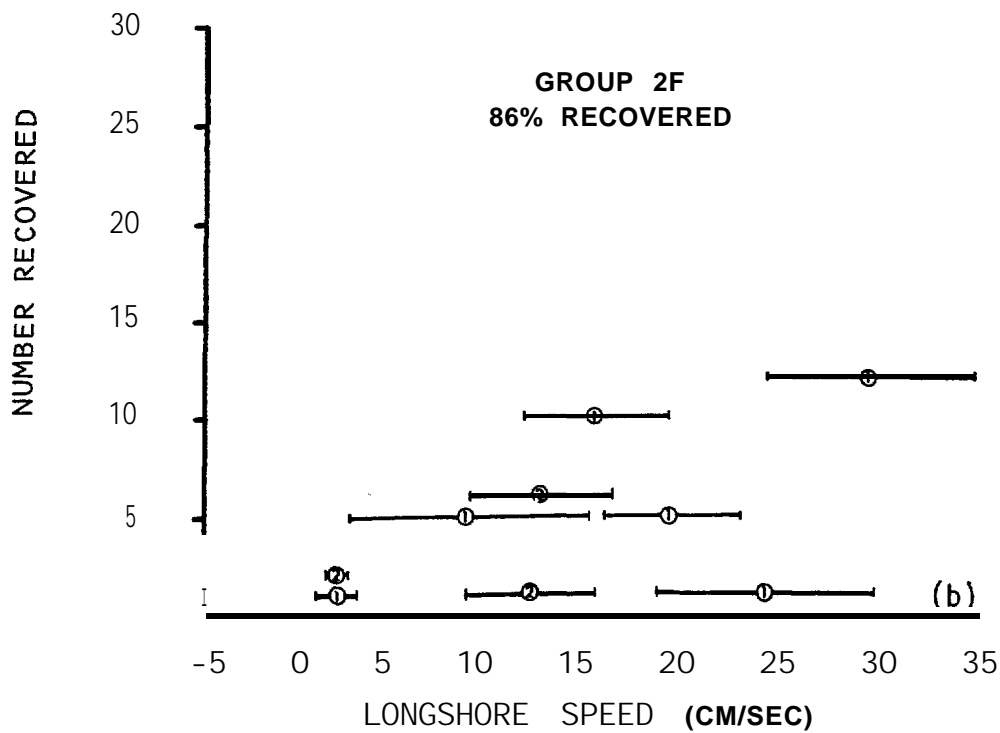
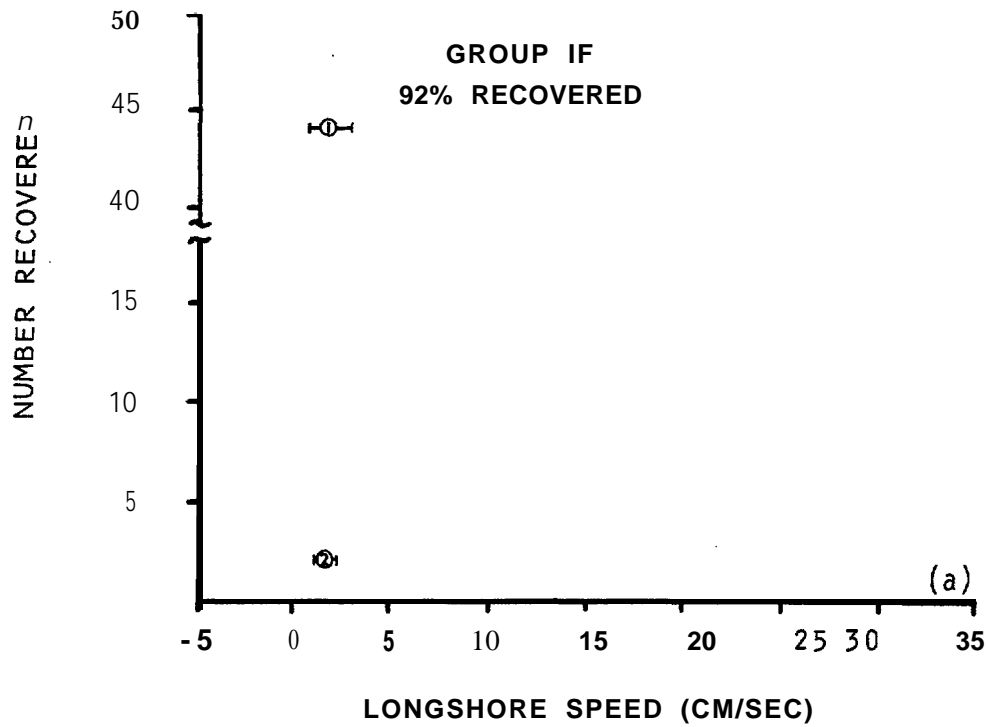


Figure 30. Histograms of **longshore** speed for Group 1 (a), Group 2 (b) and Group 3 (c) fall 1980 seabed drifter studies. Positive **longshore** speed is to the northwest. **Circles show mean speed for a particular grouping of drifters, and height above horizontal axis reflects number in group.** Numbers within circles indicate number of days over which speed was averaged (i.e. day of **recovery**). **Error bars allow for positional uncertainty, release time uncertainty and error in time of stranding (usually the major source of error).**

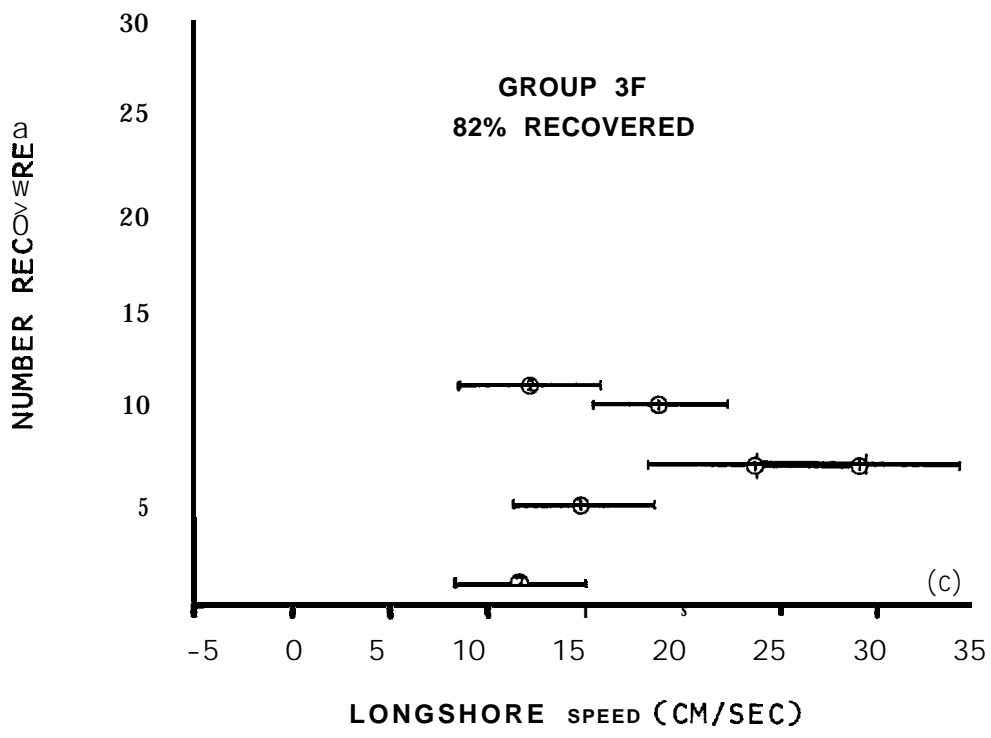


Figure 30 (continued).

The similar recovery patterns for Groups 2F and 3F suggest that some drifters from these groups were subjected to higher current speeds on the first day. The remaining drifters showed similar speeds for the two-day period.

### 3.2.4 Autumn Wind Observations

The autumn 1980 wind data from the coastal meteorological stations are presented in Figure 31. Coincident winds obtained from Yakutat Airport and as computed geostrophic winds are presented within the context of discussion of the over-winter time series in Section 5. Since these records all show the same features during the autumn field program, it was not felt necessary to include the longer-term time series plots at this point.

The scalar total and cross-shelf speed at Dry Bay (Figure 31a) showed a great deal of fluctuation. In contrast, the along-shore speed showed relatively small values except for three pronounced high-speed ( $> 20$  m/sec) events which occurred on about 17 October, 27-28 October, and 4 November. The wind speed at Ocean Cape had smaller fluctuations than at Dry Bay, both in the along-shore and cross-shelf directions except for the same wind events as observed at Dry Bay -- those on 28 October and 4 November (the Ocean Cape record did not start early enough to have recorded the 17 October pulse which was observed at Dry Bay). As at Dry Bay, the wind pulses were primarily along-shore to the northwest, though there was also a pronounced (7-8 m/sec) on-shore component present during each such event. Since the 4 November wind events occurred after the current moorings (except for Mooring 6, which was relatively far offshore) had been recovered, the 27-28 October wind pulse is of primary concern here. Relations between this pulse and the coincident observed current events are discussed in Section 3.4.

### 3.3 Discussion of the Autumn Experiment

The foregoing description of the temperature, salinity, and current fields observed in the study region during autumn 1980 reveals a regime which was characterized by strong vertical and horizontal property gradients and by rapid time variability. Prominent features of the temperature and salinity fields included a low-salinity coastal wedge and a persistent deep pycnocline. The

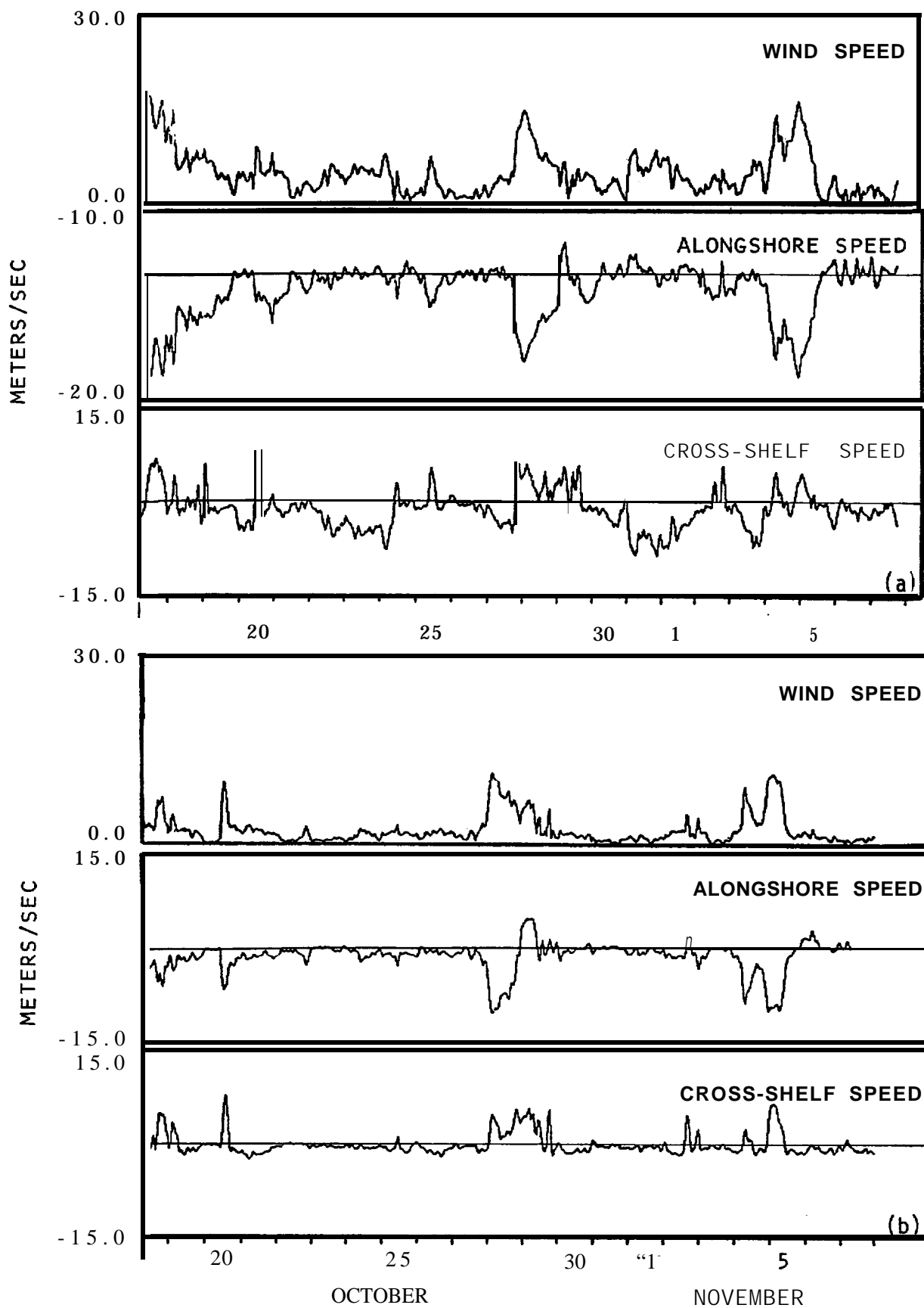


Figure 31. One-hour lowpass-filtered time series plots of wind speed, alongshore and cross-shelf components at the Dry Bay (a) and Ocean Cape (b) meteorological stations during the autumn field program.

variability of the currents, particularly close to the coast, was a prominent feature. These features are discussed below using temperature-salinity and time series analyses.

### 3.3.1 Temperature-Salinity Analyses

A composite temperature-salinity (T-S) plot has been constructed for the shelf waters off the northeast Gulf of Alaska during autumn 1980 using all stations obtained during the field program (Figure 32). This T-S diagram suggests that the shelf waters may be divided in autumn into three separate masses: (1) coastal water, having salinities of  $< 28$  ‰ and temperatures of 7-8 °C; (2) shelf water, having salinities of 31-32 ‰ and temperatures of 9-10 °C; and, (3) deep ocean water, having salinities of  $> 32.5$  ‰ and temperatures of  $< 7$  °C. The remaining waters in the region can be derived through mixing of these three basic masses.

Coastal water was contained in the low-salinity/low-temperature band which was a permanent feature throughout the study region along the coastline. The **temperature-salinity** characteristics of this water resulted **from admixture of fresh water** into the **shelf** water from the adjacent land. The northeast Gulf of Alaska coastal **region is characterized by extremely high rainfall**, particularly in autumn just prior to the period when the **temperature/salinity data were acquired (cf. Royer, 1979; 1981b; 1981c)**. Major fresh water **sources for this coastal band were Cross Sound (which enters the shelf** region to the southeast of the study region and contains freshwater input from southeast Alaska), the **Alesek** River, the Dangerous River, and the various glacial streams entering Yakutat Bay (cf. Figure 1 for locations). While satellite imagery suggests that freshwater input from these rivers may retain its identity as a plume over a relatively short distance from the source, the horizontal salinity distribution (Figure 8) suggests that bottom topography was as important **in controlling the configuration of the coastal band as the locations of major freshwater inputs**. For instance, the offshore bulge in the coastal band off the **Alesek** River was probably due as much to the tendency for the along-shore flow to parallel **isobaths** around the head of **Alesek** Canyon, as to the increased local freshwater **input** from the river. Farther northwest, a steeper bottom topography coincided with a narrower band configuration.

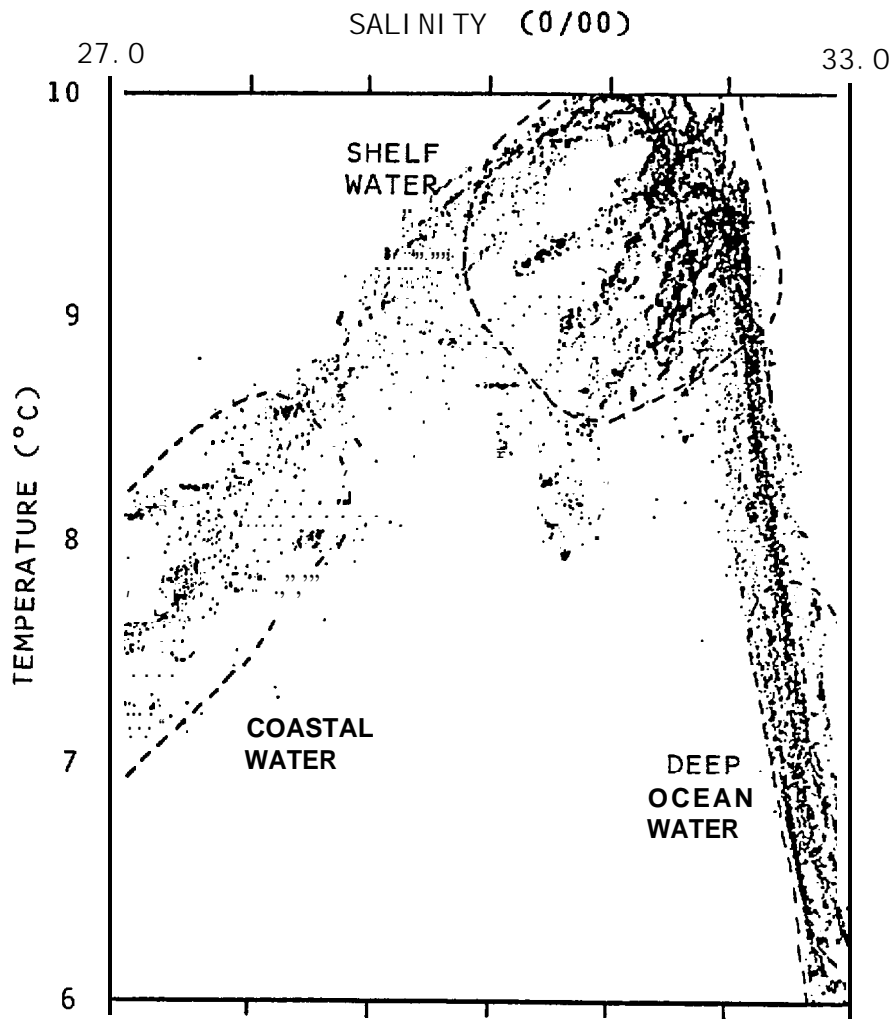


Figure 32. Composite temperature-salinity diagram for autumn 1980, showing the relationships between near-shore, shelf and deep ocean water masses.

These waters defined by their temperature-salinity characteristics as "shelf water" showed considerable variability toward their lower-salinity/lower-temperature ranges, whereas there was a sharply defined cutoff for temperature and salinity values at the high-temperature/high-salinity end (Figure 32). This variability was probably due to the variable nature of the **inputs; freshwater, which mixes into the shelf water as low-salinity coastal water, is highly variable in quantity as compared to the relatively constant T-S character of the deep ocean waters.** Shelf water occurred throughout the shelf above depths of 75-125 m, where the **pycnocline** described above in Section 3.1 separated it from deep ocean **water.** Only in one instance, **in the near-surface layers about 50 km south of Dry Bay (Figure 8),** was there an indication that coastal water was present at mid-shelf.

Deep ocean **water, which was characterized by a relatively narrow range of salinity values, occupied the deeper portions of the shelf and the oceanic regions seaward of the shelfbreak.** In particular, it was present in the deeper portions of Yakutat Canyon. Based upon results of other research (**Hsueh, 1980; Lavelle et al., 1975; Nelson et al., 1978), a deep up-canyon flow would be expected to occur in response to certain along-shore wind conditions which would advect deep ocean water onto the shelf. The preponderance of along-shore wind events in the study region suggests that such mechanisms were probably responsible in part for shoreward flow of deep ocean water in the cross-shelf valleys.** Where shelf bottom depths exceeded about 100 m, a thin layer of deep ocean water was evident in many instances near the bottom (cf. "Figure 10). The seaward boundary between deep ocean and shelf waters was marked in some instances by a frontal structure where the shelf water intersected the surface. Such a structure occurred between CTD Stations 37 and 38. Regions of mixing between these water masses *were* characterized in addition by vertical **fine-structure, as illustrated in particular by the zone of interaction between the coastal and shelf waters (Figure 13) and the shelfbreak region where deep ocean and shelf water were interacting (Figure 15).** Fine structure is, in a general sense, indicative of dynamic mixing processes associated with sharp property gradients such as occur in this region.

The above depiction of water mass interactions in the study region may be used to speculate qualitatively upon circulation. The general large-scale mass boundaries -- coastal/shelf and shelf/deep ocean -- with local isobaths suggests that the time-mean flow also parallels isobaths except for such instances as on-shelf flow in the deeper portions of the cross-shelf valleys. Such a mean advective regime is necessary for maintenance of these water mass boundaries. This supposition is supported by the current observations except for those at Mooring 6, although except for Mooring 6 these records are too short to rigorously define a "mean" flow. (Lagerloef et al. (1981) have shown that in this region a minimum current record length of 60 days is required to obtain a mean flow value in which we may have confidence at the 95 percent level.) Dynamic considerations also lend credence to our observations; high-latitude conservation of potential vorticity dictates that streamlines of the three basic water mass types parallel isobaths.

Superposed upon the distribution depicted above, there was considerable scatter in the mid-shelf region, as shown particularly clearly on Figures 8 and 9. Of particular interest is the "lens" of coastal type water which occurred 40-50 km south of Dry Bay and was approximately outlined by the 31.5°/00 isohaline at 5m (Figure 8b). This lens may have originated from Cross Sound to the southeast and been advected by the mean flow northwest to its observed location. Alternatively, it may have been a remnant of coastal water which was originally present in the coastal band off Dry Bay and was then advected to the observed location by offshore surface flow resulting from relaxation of the shelf waters following a wind-driven downwelling event. (This latter possibility will be more thoroughly discussed below in Section 3.3.2) Because no data were acquired prior to the time when the feature was observed, it is impossible to determine which of these two mechanisms was responsible. Whatever the source, these irregular features are reflected in the composite temperature-salinity plot (Figure 32) as "streamer-like" sets of points extending toward lower temperature/lower salinity values from that portion of the plot defining shelf water. It is possible that the locations of these streamers relative to the portions of the curves connecting shelf water/deep ocean water and shelf water/coastal water reflect the ages of the features, Older features which had been on mid-shelf for a longer period of time, especially those farther seaward, might reflect a greater admixture of shelf-deep ocean water.

### 3.3.2 Circulation Analyses

This section considers the circulation features observed using the drogues and moorings, and the observed features are correlated with winds and fluctuations in the temperature and salinity fields. Because the moored current records were relatively short compared with the time scale for events -- 12-day records as compared with an event time scale of 5-6 days (cf. Section 5) -- no attempt was made here to compute "mean currents." The main **current vectors presented** in Section 6, for comparison with a diagnostic model, should be viewed with caution because of the high variability which was observed. To reiterate (see Section 3.3.1 above), Lagerloef et al. (1981) found a minimum recording period of 60 days necessary to obtain meaningful "mean" currents in the northeast Gulf of Alaska shelf region. Therefore, this section will concentrate instead upon the nature of the time variations and will attempt to link these with dynamical processes which may aid in explanation and predictability.

As for computation of "mean" currents, no attempt has been made to construct dynamic topographies. Again, this decision was based on the observed high temporal variability coupled with non-synoptic temperature-salinity sampling. The temperature and density time series observed at the moorings (Figures 16, 17, 19, 20, 22, and 24) reveal that large (as great as 1 °C and 1 sigma-t unit) rapid (time scales of a few hours) fluctuations occurred, particularly at Moorings 2 and 6. Since several days were required to occupy the CTD grid with frequent breaks in the sequence to track drogues, for bad weather and for other operational reasons, significant variations probably occurred in the density **field** during occupation of the grid. In conjunction with non-synoptic nature of the temperature and salinity data, the noise level introduced by these time variations would be expected to introduce an unacceptable level of uncertainty into an estimate of dynamic topography. These effects would be particularly bad in the near-shore region within about 10 km of the coastline, where the observed fluctuations were greatest and also where experimental results are of most interest to this program.

Near-shore Moorings 1 and 4 exhibited flow which was strongly constrained to flow in the along-shore direction. The flow was thus **bimodal**, being either to the northwest or to the southeast for about equal portions of the 12-day

record obtained **from each mooring**. Flow constraint in the along-shore direction was governed by topographic influences both by the sloping bottom and due to the close proximity ( $< 4$  km) to the beach. The small cross-shelf velocity **fluctuations** appeared upon **visual** -inspection to be due primarily to the tidal currents. Only in one instance (27-28 October at Mooring 4) was there a small ( $\sim 20$  cm/sec) offshore current event which coincided with the large ( $\sim 70$  cm/sec) north-westward pulse (Figure 17).

Offshore Moorings 2, 5, and 6 showed far less tendency toward solely **along-shore** flow. Because they were farther from the beach ( $> 10$  km) than Moorings 1 and 4, they were subject to less topographic control. The deeper current record from Mooring 2 is an exception because it was **close** enough to the bottom that control was imposed by the sloping bottom topography. The near-surface records from Mooring 6 (Figures 23 and 24) showed the greatest cross-shelf fluctuations. In both these cases, the moorings were located in areas where the **isobaths** were at large angles to the coastline; for Mooring 5, **isobaths** were nearly normal to the coast as they formed one side of Alsek Canyon. It is likely that a portion of the fluctuations at Moorings 5 and 6 were due to eddy motions resulting from the interaction of a weak mean flow with complex bottom topography.

The reasons for the strong southeasterly flow in the near-shore region (Moorings 1 and 4) are uncertain. The major northwestward current event which was observed at Moorings 1, 2 (upper meter) and 4 on 27-28 October correlated with a storm center which passed over the region and generated strong ( $\sim 15$  m/sec) along-shore winds to the northwest (Figure 31). The spatial distribution, magnitude, and along-shore propagation speed of the current event suggested that it behaved as a continental shelf wave generated by the storm (Temple and Muench, 1981). Flow just prior to and (at Mooring 1) just after this northwestward pulse was lower in speed and to the southeast. It is possible that the southeasterly flow may have been due in part to a relaxation of the system following the northwesterly flow, abetted by the curvature of the northeast Gulf of Alaska coastline. This possibility is discussed to **greater extent below within the context of the current, temperature, and density time series**.

Presence along the coastline of the low-salinity/low-density band of water suggests that a northwesterly **along-shore baroclinic flow** should have been present rather than the observed **bimodal** flow with no significant net northwesterly

preference. Because the current meters at Moorings 1 and 4 were, respectively, at 26 and 38 m depths and the density signature of the coastal band did not extend appreciably below about 20 m, it is possible that a northwestward flow associated with the low-density band was present but undetected by our moorings. However, the drogued buoys were set to track water motion at about 15 m depth (cf. Section 2) and so should have detected northwesterly flow of the coastal water. Referral to the drogue velocities (Figure 29) shows that, except for a brief period (< 24 hr) on 26-27 October, the drogues traveled to the northwest with speeds as high as about 70 cm/sec occurring on 28 October. The drogue tracks (Figures 25) indicate the constancy of this northwestward flow except for the single reversal event, and Table 3 indicates mean speeds of order 30 cm/sec. The low mean speeds for Phase I of Experiment 1 reflected incorporation of the reversal into the mean speed computation, whereas the high average speeds for Drogue 3, Phase II were due to incorporation of the northwestward pulse into the means. The consistent 30 cm/sec northwestward drift recorded at 15 m depth by the drogues suggests that the near-surface coastal flow was characterized by speeds of about 30 cm/sec to the northwest.

In conclusion, northwesterly along-shore flow associated with the low density coastal water band (1) had speeds of order 30 cm/sec, (2) was limited primarily to depths above 20 m, and (3) occurred primarily within about 9 km (the approximate offshore distance for Moorings 2 and 5) of the coastline. These observations are consistent with theory, which predicts that this sort of coastal flow will occur primarily within a distance from the coast equal to the computed internal Rossby radius of deformation. In this case, this length scale is about 7 km or approximately the same as the observed width of the low-density band (Figure 11). Based upon observations in previous data bases, Reed and Schumacher (1981) concluded that there was no appreciable coastal flow in the northeast Gulf of Alaska. However, based upon the above analysis, it now appears that such a flow may in fact have been present at the time these data were collected, but was probably contained in too narrow a coastal band to have been detected by their temperature-salinity data, most of which were more than 10 km from the coastline.

### 3.3.3 Littoral Currents

In Section 3.2.3, results are presented from a **field** study of littoral currents which was conducted by a seabed drifter experiment and analysis through application of engineering equations to estimated incoming surface wave heights and directions. Both observed **longshore** seabed drifter speeds to the northwest, and **longshore** speeds predicted by the analytic equations were **greatest when waves approached the beach from the south-southeast, as would** be expected. In addition, there was also a southeasterly wind generally present which would have contributed to local wind forcing of a northwest current. At no time was a longshore littoral current observed in the southeasterly direction. This absence was a reflection of the wind stress and the resulting wave field, directed toward the northwest in this region in autumn-winter; in general, a northwesterly littoral current would be expected to exist through most of the winter due to the dominant southeasterly winds. The speeds observed with the seabed drifters -- of order 10-30 **cm/sec** -- may be considered as a representative estimate of the current speeds. Since these drifters tracked bottom water, this would also represent the longshore speed seen by contaminants which had been introduced into bottom sediments in the surf zone.

### 3.3.4 Summary

The results of the autumn field experiment can be briefly **summarized** as follows:

1. The regional temperature-salinity distribution defined coastal, shelf and deep ocean water masses. Coastal water was constrained primarily to a 20-m-deep layer within 10 km of the coast, except for isolated lenses which might be periodically advected well off the coast. **Shelf water** occupied the bulk of the region from the coast to the shelfbreak. Deep ocean water occurred seaward of the **shelfbreak** and beneath the shelf water on deeper portions of the shelf. The coastal water had the lowest temperatures and salinities observed; the shelf water had higher temperatures and intermediate salinities, and the deep ocean water had the lowest temperatures and highest salinities.

2. Circulation on **the** shelf was in general highly variable. Below the 20-m-deep coastal water in the near-coastal region, it was **bimodal** in the along-shore direction. The wedge of coastal water was characterized by a northwesterly flow of order 30 cm/sec, but was subject to occasional reversals to a southeasterly flow. Strong northwesterly current pulses were driven by southeasterly storm-related winds, with the magnitude of the pulse decreasing in the offshore direction. Currents near **A1sek** Canyon were particularly variable.
3. Littoral currents were along-shore to the northwest in response to wind waves from the south-southwest and sea surface set-up, and had near-bottom speeds of 10-30 cm/sec.

## 4. THE SPRING EXPERIMENT

### 4.1 The Spring Distributions of Temperature and Salinity

The temperature and salinity distributions were determined in the same way for the spring as for the autumn experiment (see Section 2). This section presents the spatial distributions of temperature and salinity observed using the CTD.

The regional temperature and salinity fields are presented as horizontal plan views at depths of **5 m** (Figure 33) and 100 m (Figure 34) and as vertical distributions along a transect across the shelf from the coastline to seaward of the shelfbreak (Figure 35). For comparison with the autumn distributions, the transect shown in Figure 35 was chosen to coincide spatially with that shown above in Figure 10 for the autumn distribution.

The 5-m temperatures in spring 1981 were characterized by values which were low relative to those observed in autumn: 6.3 and 7.1 °C compared to **8-9 °C** in autumn. Spatial variability in spring was similar to that found in autumn, or about 1 °C, **with** a tendency for lower temperatures near the coast. The 5-m salinities were about 0.2 ‰ higher off the **shelfbreak** in spring than **in fall** but were more than 1 ‰ higher in the coastal band. This was a major difference between the autumn and spring salinity distributions; the low-salinity near-coastal band was highly attenuated in spring.

Shelfbreak temperatures at 100m in spring were 6-7 °C (Figure 34a), similar to those observed in **autumn**. Farther onto the shelf, temperatures were 6-7 °C **in** spring whereas in autumn they had been 8-9 °C. Salinities at 100 m were similar in spring to those observed in autumn; they varied gradually from about **32.0 ‰** near-shore to about 32.8 ‰ near the shelfbreak (Figure **34b**).

As in autumn, both the 5-m and the 100-m temperatures and salinities were characterized by horizontal variability on mid-shelf and near the shelfbreak. At 5 m a region of low-temperature (6.5 °C) and low-salinity (31.9 ‰) water lay near the **shelfbreak** south of Dry Bay. The corresponding feature at 100 m (Figure 34) was characterized by high temperatures (7.3 °C) relative to colder

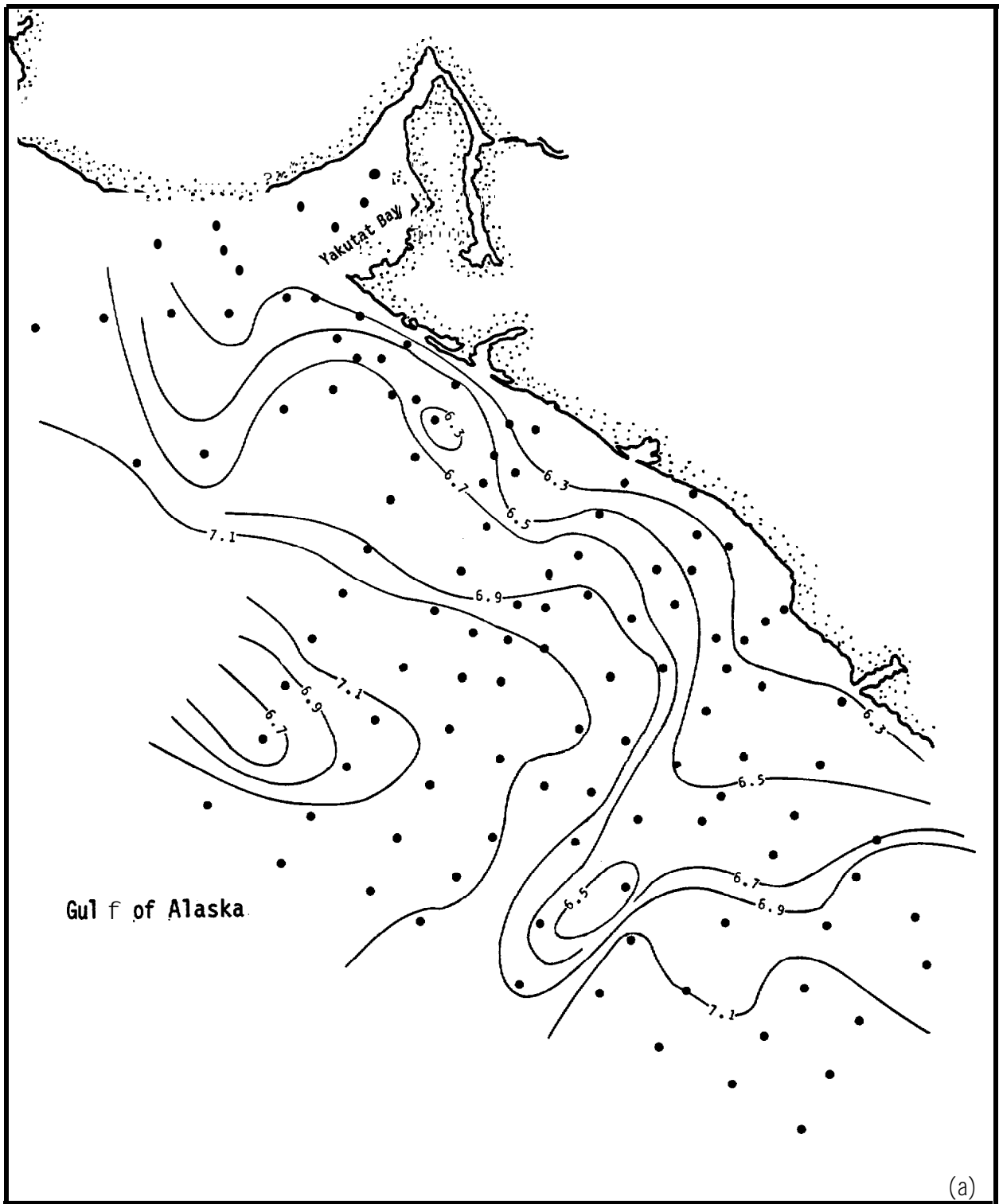


**Figure 33a.** Horizontal distribution of temperature (°C) at 5-m depth, 20 March-3 April 1981.

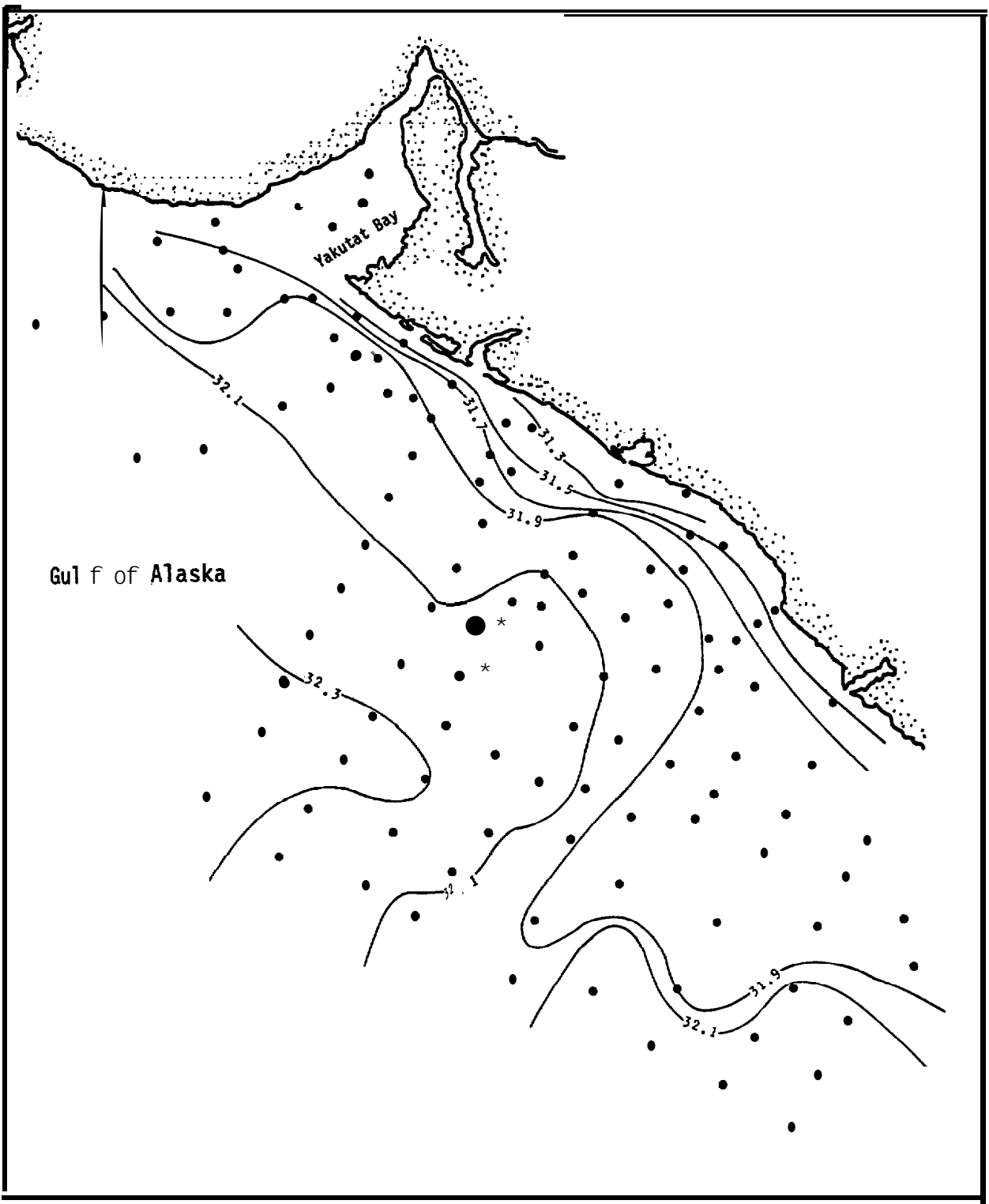
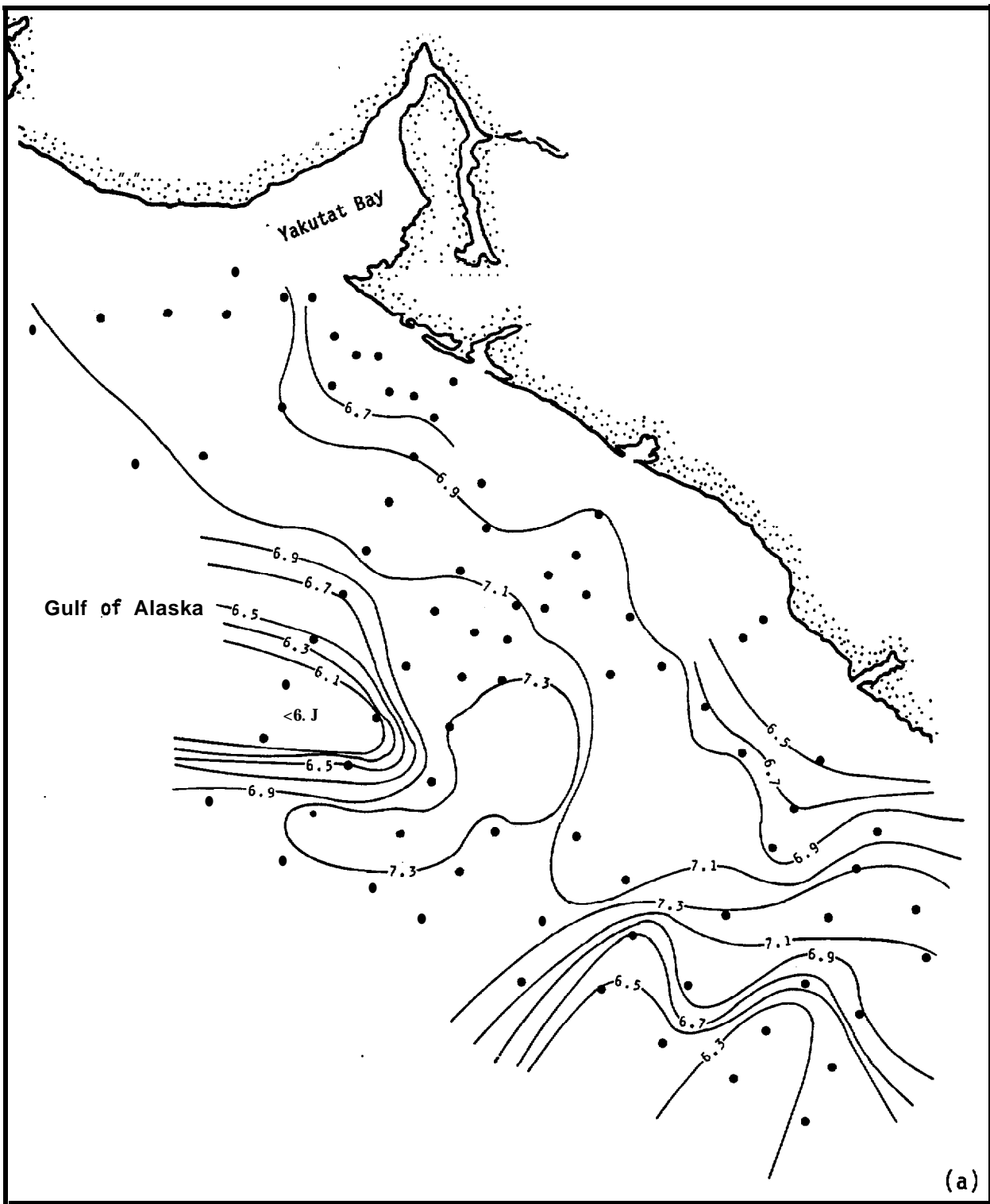


Figure 33b. Horizontal distribution of salinity ( $^{\circ}/_{\infty}$ ) at 5-m depth, 20 March-3 April 1981.



**Figure 34a.** Horizontal distribution of temperature (°C) at 100-m depth, 20-March - 3 April 1981.

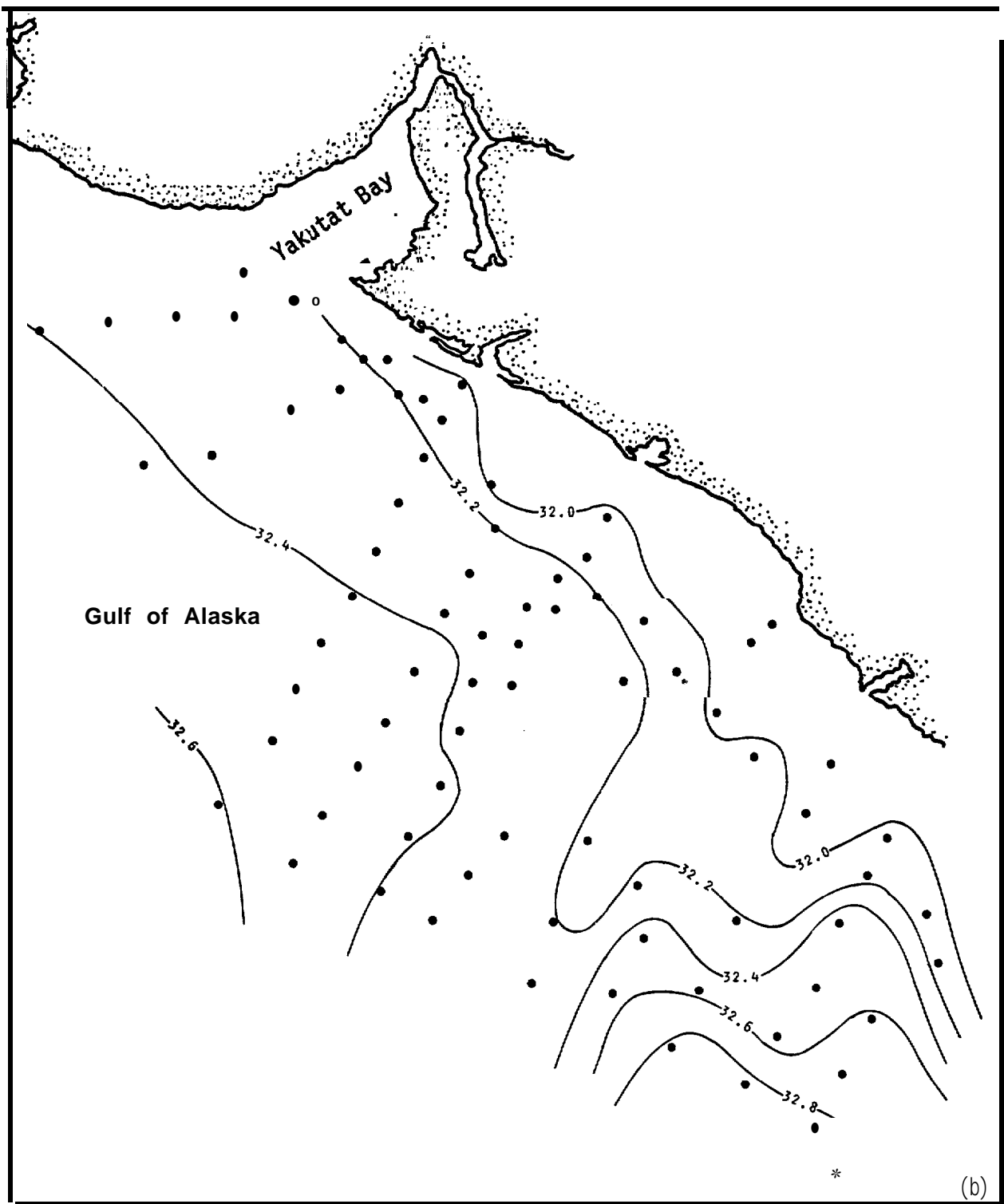


Figure 34b. Horizontal distribution of salinity ( $^{\circ}/_{\infty}$ ) at 100-m depth, 20 March - 3 April 1981.

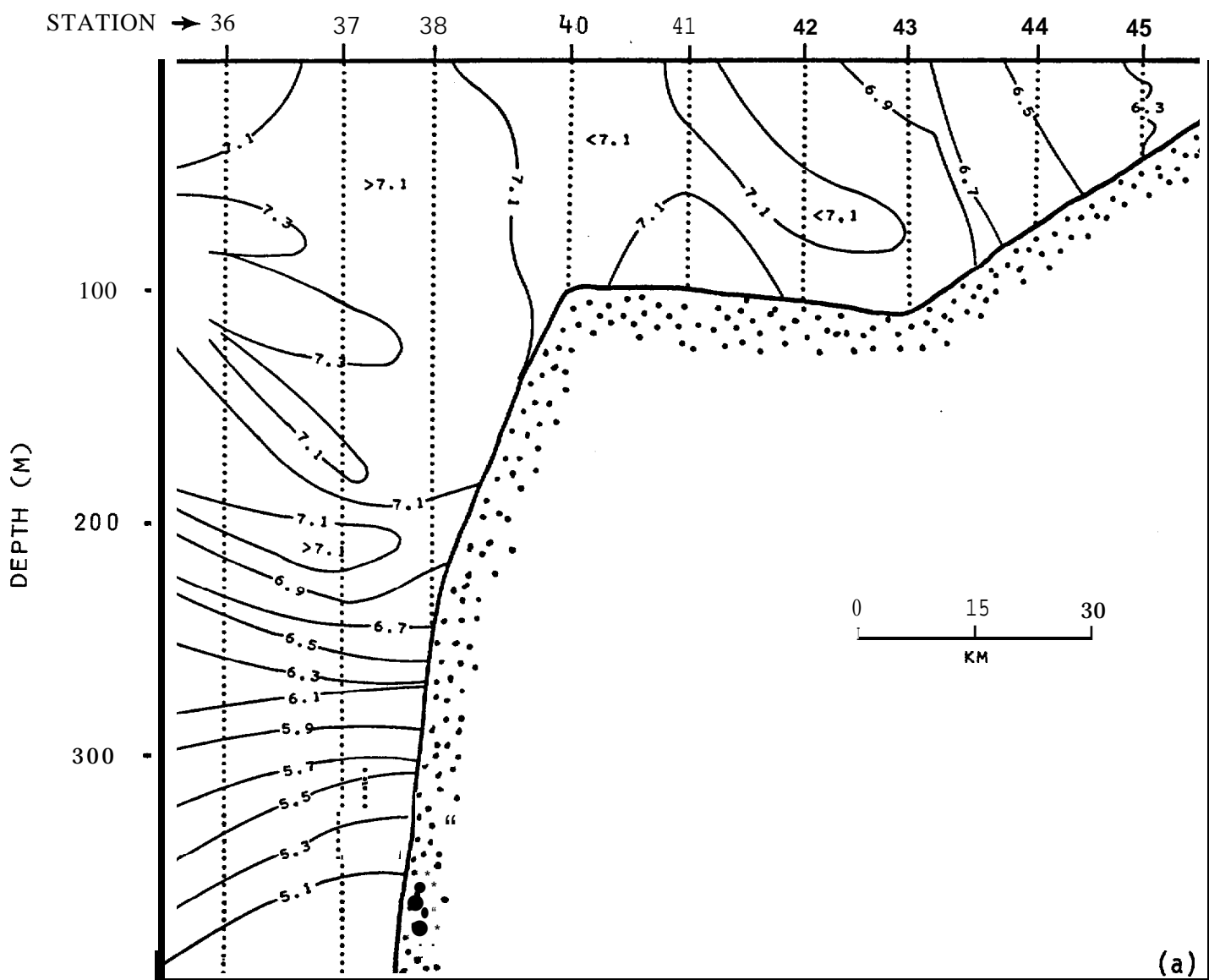


Figure 35a. Vertical distribution of temperature ( $^{\circ}\text{C}$ ) along a cross-shelf transect, 30 March 1981. Location of transect is indicated on Figure 7 by station number.

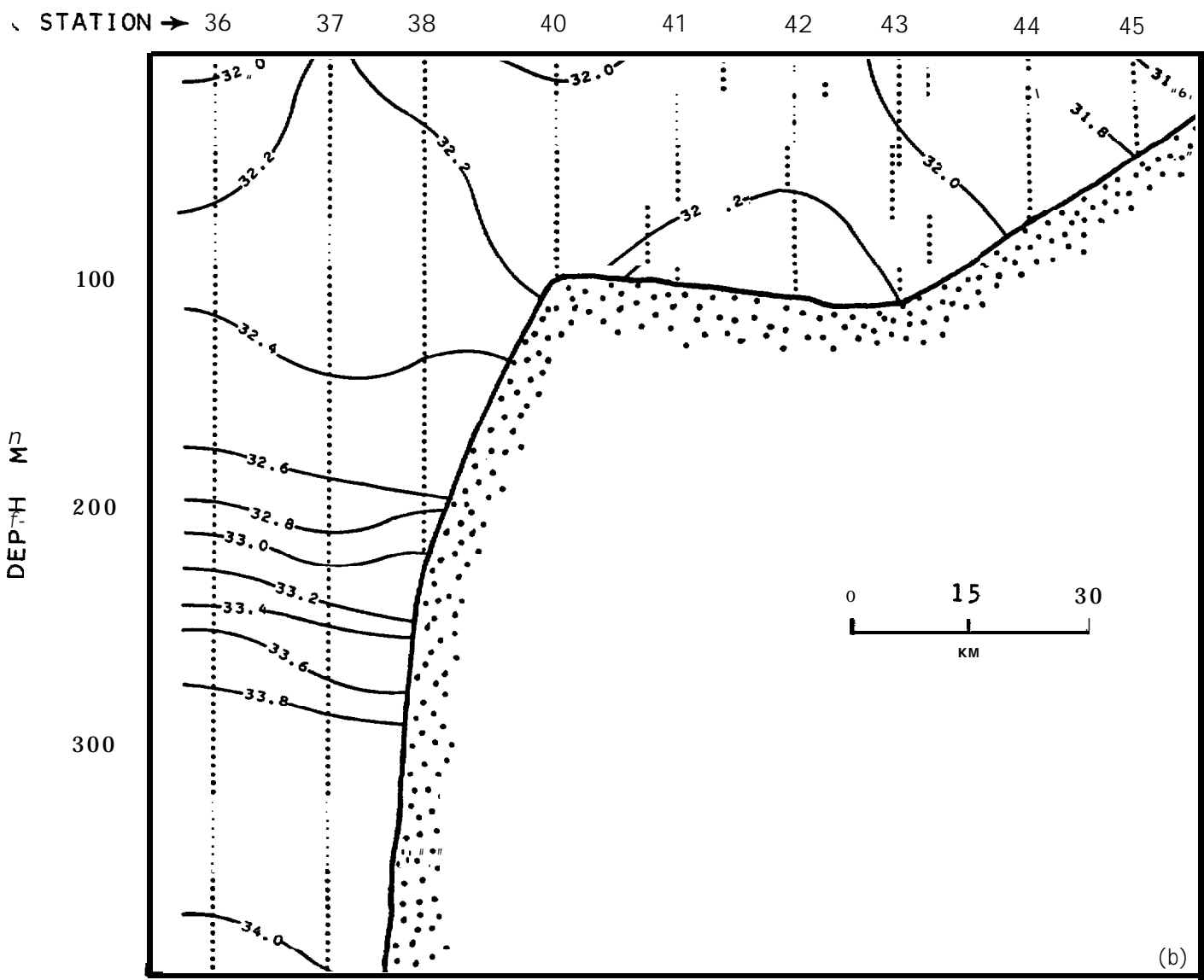


Figure 35b. Vertical distribution of salinity ( $^{\circ}/_{\infty}$ ) along a cross-shelf transect, 30 March 1981. Location of transect is indicated on Figure 7 by station number.

water to the northwest and southeast and by lower salinities (32.2 ‰). These features coincided approximately with the southeastern side of Aisek Canyon.

The vertical transects of temperature and salinity (Figure 35) indicate that most of the cross-shelf temperature and salinity gradient occurred within about 30 km of the coast. Temperature increased from 6.3 to 6.9 °C throughout the water column over this distance, and salinity increased from 31.6 to 32.0 ‰. Seaward of this zone of horizontal gradient, whose outer bounds were defined approximately by Stations 42-43 (Figure 35), temperature varied by less than 0.1 °C and salinity by less than 0.2 ‰ in either the horizontal or vertical. There was no indication in the shelfbreak region of the strong horizontal gradients which were present during autumn (Figure 10) between Stations 37 and 38. In the deeper water (> 100 m) off the shelfbreak, salinity increased to oceanic values of 33-34 ‰, similar to the autumn case. Temperatures below about 350 m were similar to those in autumn, i.e. approximately 5.0-5.5 °C. Temperatures between about 100 m and 300m were higher in spring (5.5-7.3 °C) than in autumn (5.2-5.0 °C), providing the only instance where higher temperatures were present in spring than in autumn.

As in the autumn case (Figure 11), near-shore closely-spaced CTD transects were occupied along the coastline in spring to better define coastal hydrographic features. The temperature distributions along these transects are presented in Figure 36, where B is the easternmost and E is the westernmost transect. Transects B, C, and D (Figures 36a-c) show little or no evidence of the low-temperature coastal wedge which was evident during autumn (Figure 11). Only at Transect E (Figure 36d) was there a region of strong horizontal temperature gradient, found at about 1 °C over 5 km between Stations E1 and E3. These closely-spaced transects therefore support the observation that the coastal wedge which was a prominent feature in the autumn temperature-salinity field was greatly diminished or absent, depending upon location along the coastline, in the spring.

Details in the vertical distributions of temperature and salinity can be seen, illustrating general features, by referring to selected vertical profiles (Figures 37-40). As in autumn, the maximum stratification was present in Yakutat Bay (Figure 37). The relatively low density of water above ~ 20 m was due primarily to its low salinity. Below 20 m the water was relatively uniform

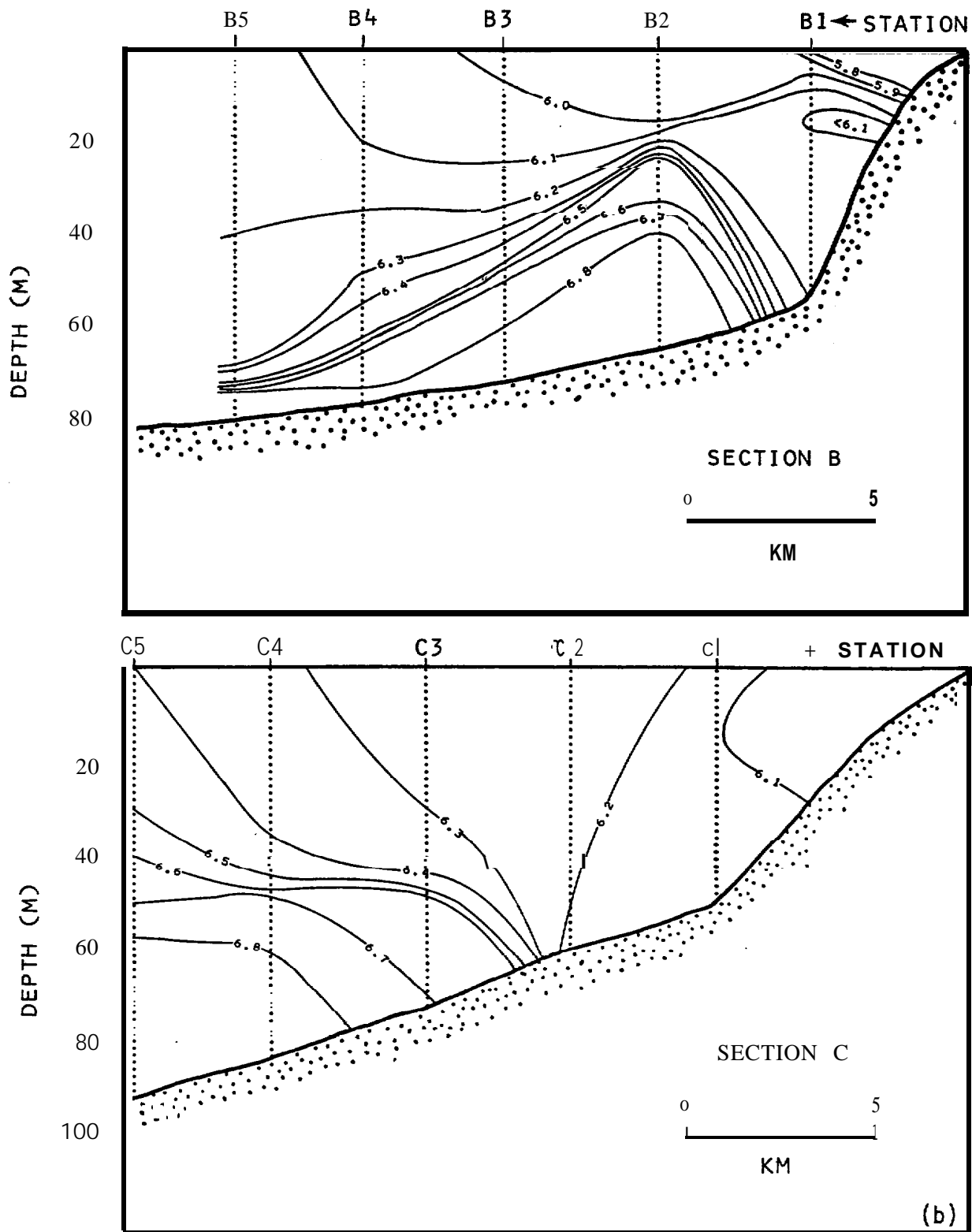


Figure 36. Vertical distribution of temperature ( $^{\circ}\text{C}$ ) at four transects normal to the coastline, 20 - 24 March 1981. Locations of transects are indicated on Figure 7.

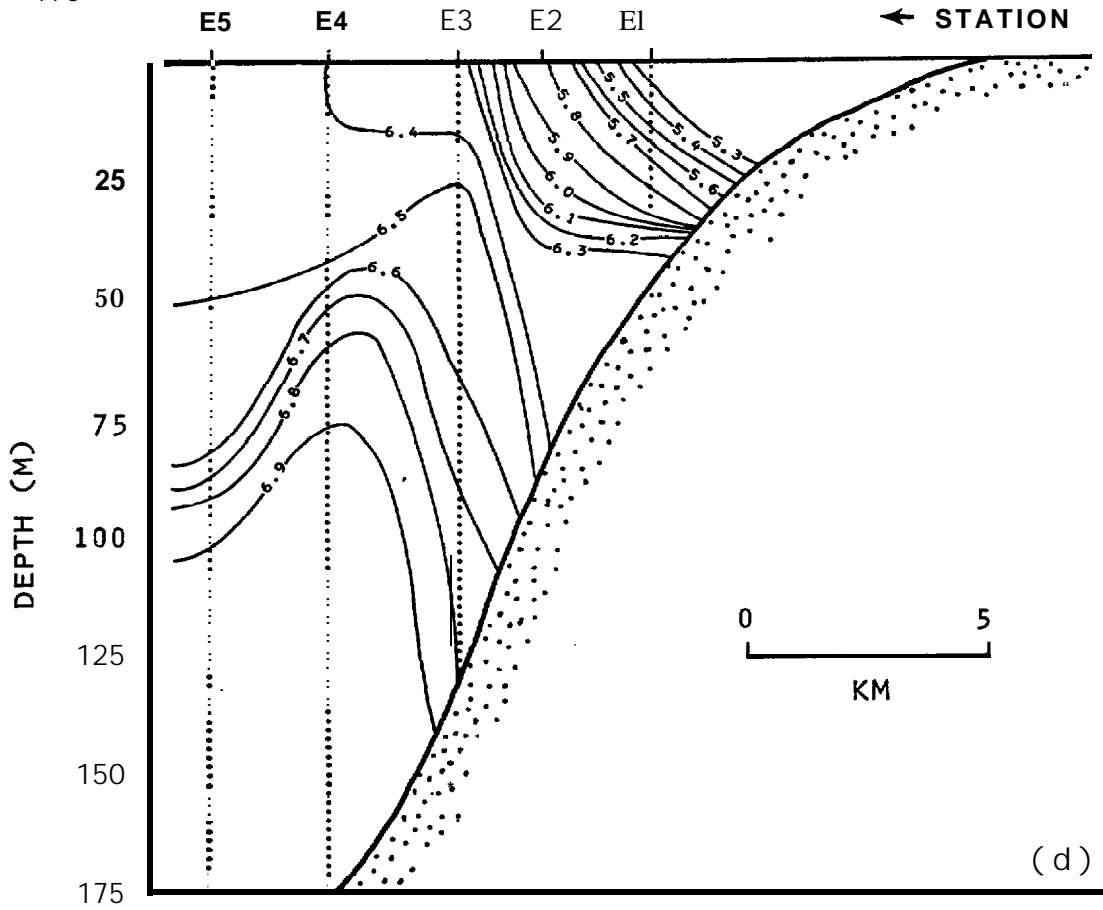
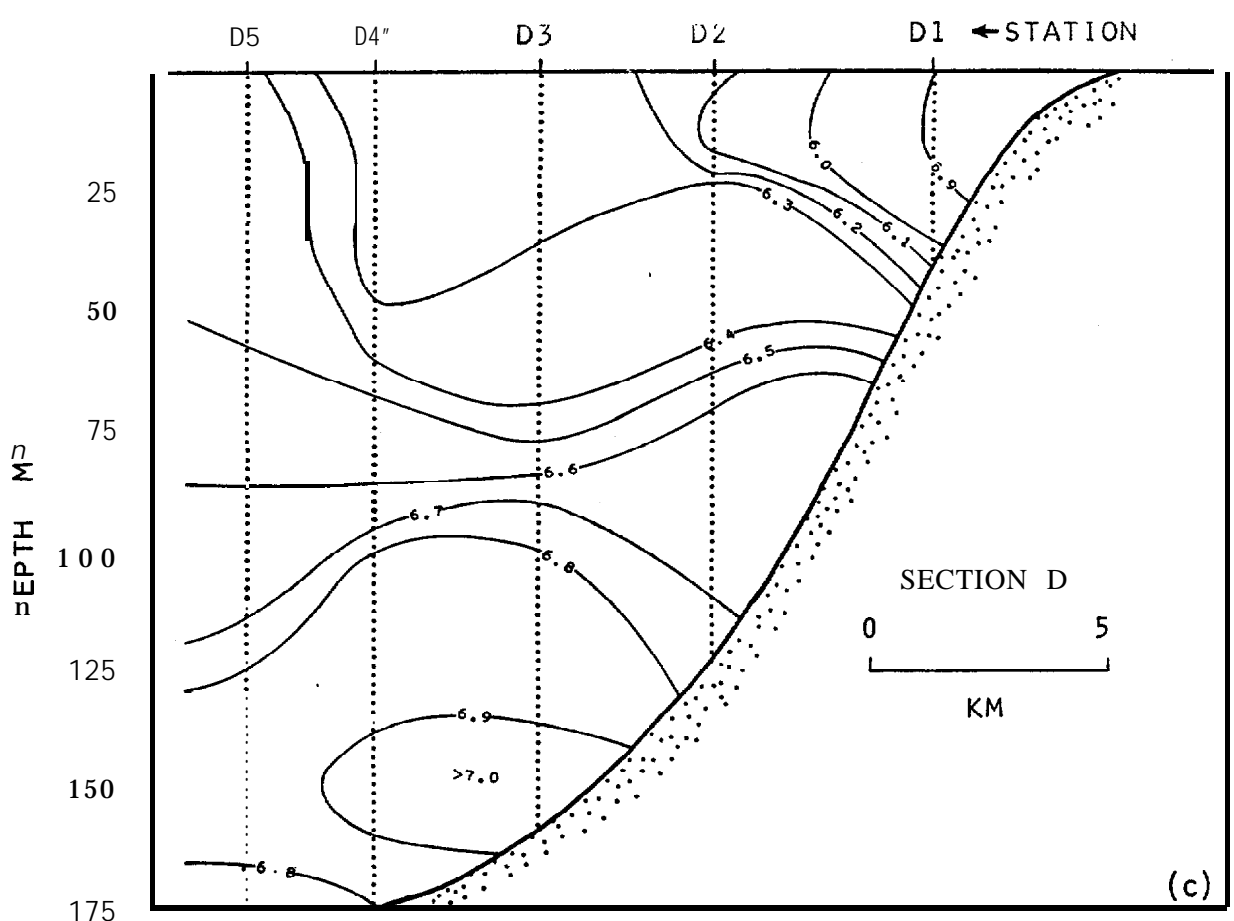


Figure 36 (continued).

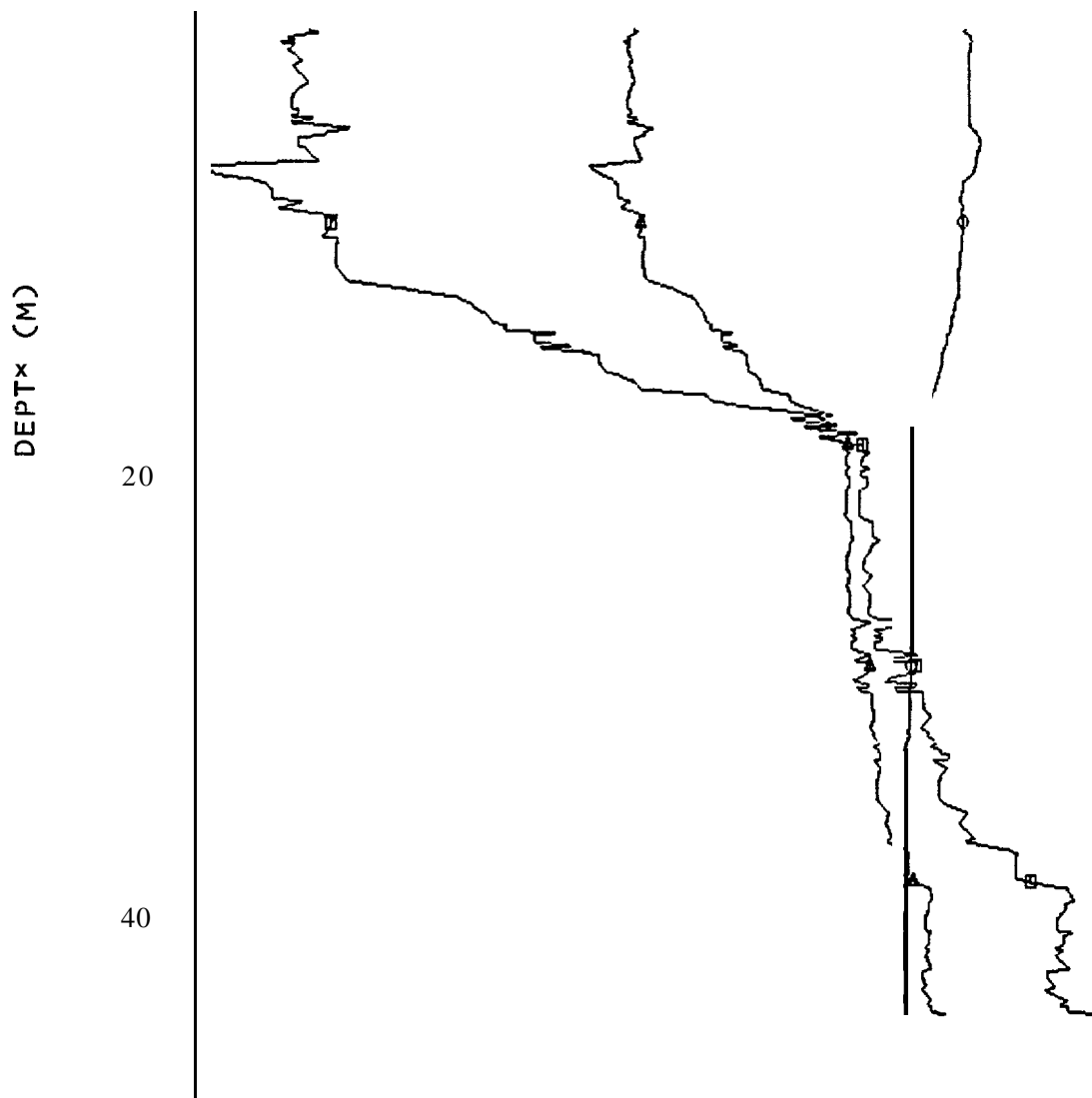


Figure 37. Vertical profiles of temperature, salinity and density **at** station 18 in Yakutat Bay. Station location is indicated on Figure 7.

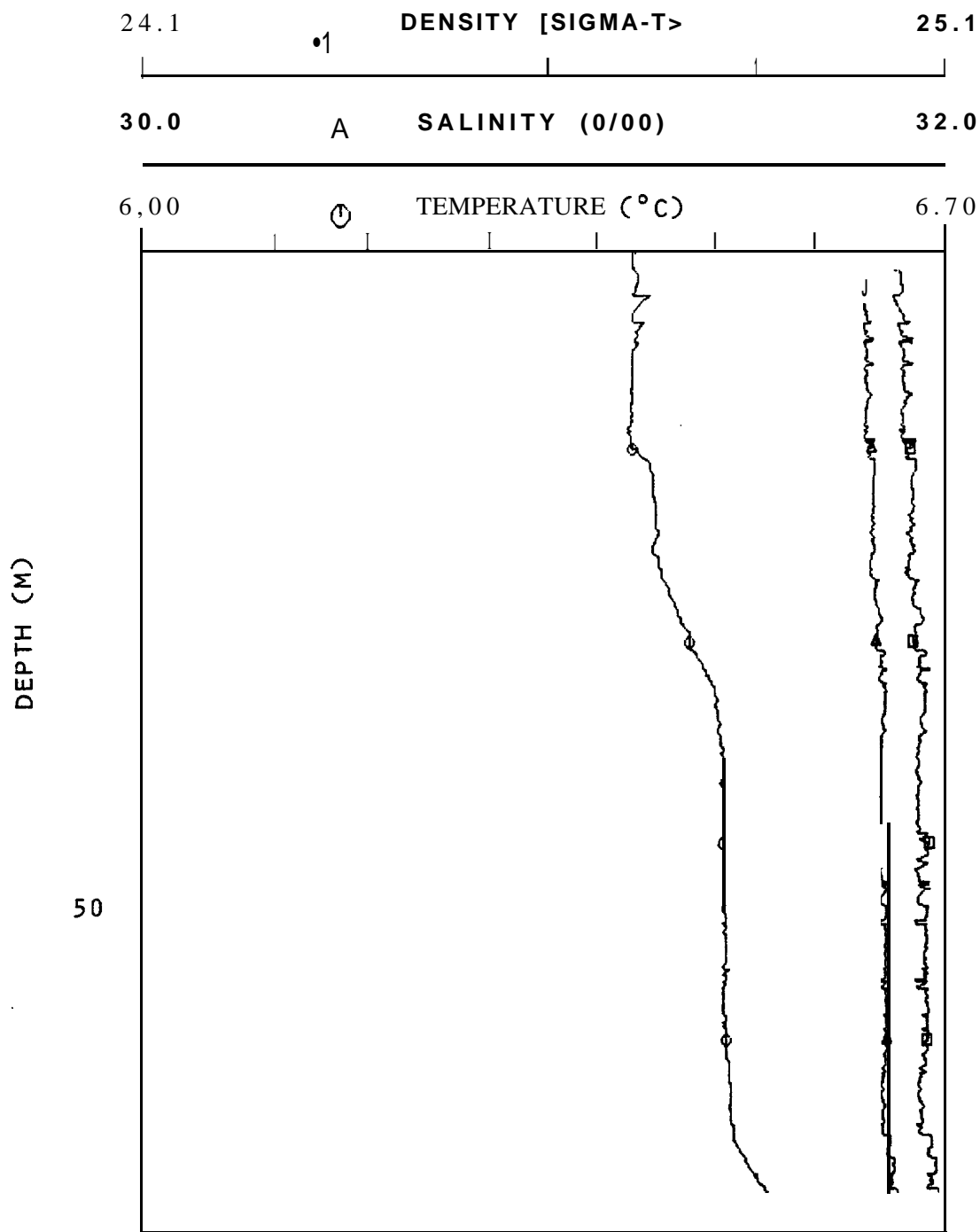


Figure 38. Vertical profiles of temperature, salinity and density at station 43 near the coast. Station location is indicated on Figure 7.

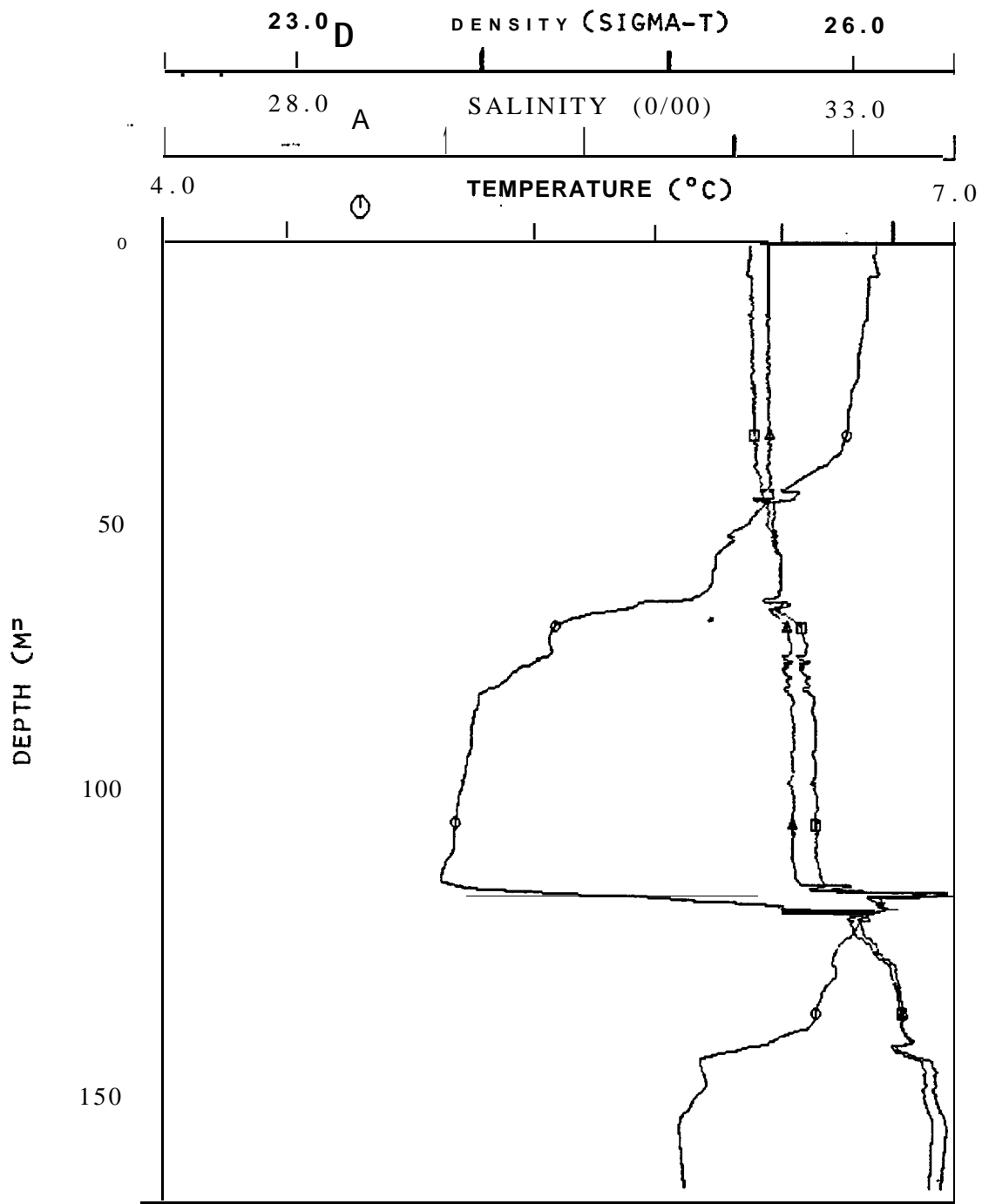


Figure 39. Vertical profiles of temperature, salinity and density at station 6 at mid-shelf. Station location is indicated on Figure 7.

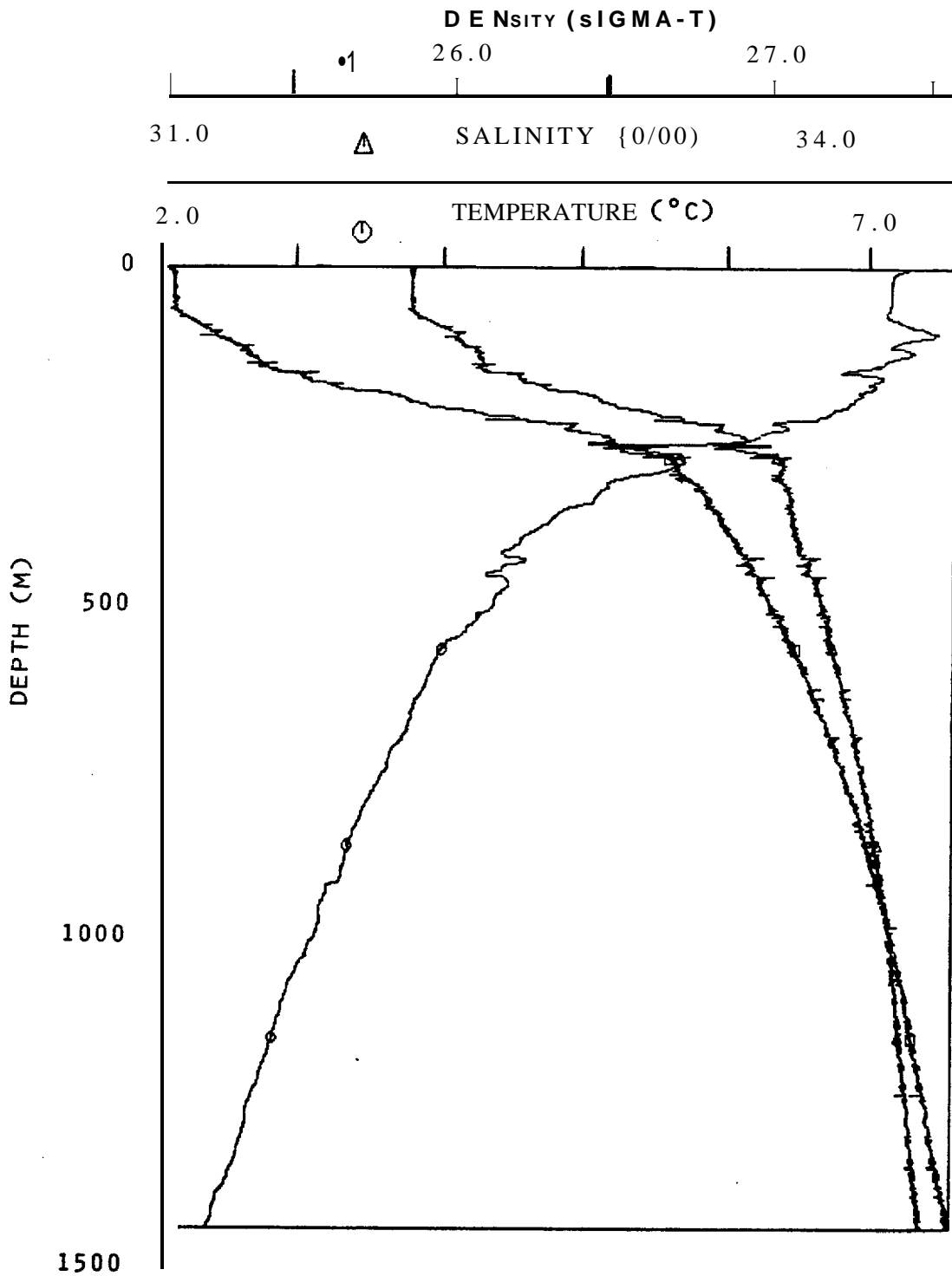


Figure 40. Vertical profiles of temperature, salinity and density at station 40 seaward of the **shelfbreak**. Station location is indicated on Figure 7.

in the vertical except for a slight near-bottom salinity (and hence density) increase. **Station 43** (Figure 38), in the coastal region off Ocean Cape, illustrates the lack of vertical structure in the coastal water. The only significant vertical gradient found was in temperature, which increased by about 0.1 °C from the surface to bottom; farther offshore, mid-shelf Station 6 (Figure 39) reveals that a low-temperature layer was present at about 100 m. Salinity increased by about 1 ‰ from surface to bottom. Finally, Station 33 seaward of the shelfbreak (Figure 40) illustrates the vertical transition to deep ocean water characterized primarily by the gradual temperature decrease with increasing depth and the relatively uniform density below about 200 m. The vertical profiles for spring showed far less fine structure than was observed in autumn.

To summarize, the regional temperature and salinity distributions in **March-April 1981** were typified by a far smaller variation in temperature and salinity than was observed the previous autumn, although considerable horizontal variability was still present off the shelfbreak. The autumn coastal band was nearly absent, being evidenced only weakly at Transect B and more strongly at Transect E. Water on the shelf away from the coast was nearly uniform except for perturbations which apparently coincided roughly with the southeastern border of Alsek Canyon. In general, temperature and salinity both decreased with increasing depth and offshore distance.

#### 4.2 Observed Spring Near-shore Circulation

As in the autumn case (Section 3.2), observations obtained using moored current meters, drogued buoys, and seabed drifters will be presented separately here.

##### 4.2.1 Spring Moored Current Observations

The records from **Moorings 1 and 4** showed considerable similarity to each other in spring (Figures 41 and 42). Both these moorings were located about 4 km from the coastline. The current meter on Mooring 1 was considerably shallower (17 m) than that on Mooring 4 (34 m), but despite the differences in deployment depth both showed a consistent along-shore flow toward the northwest with only a brief period (1-2 April) of weak reversal to southeasterly

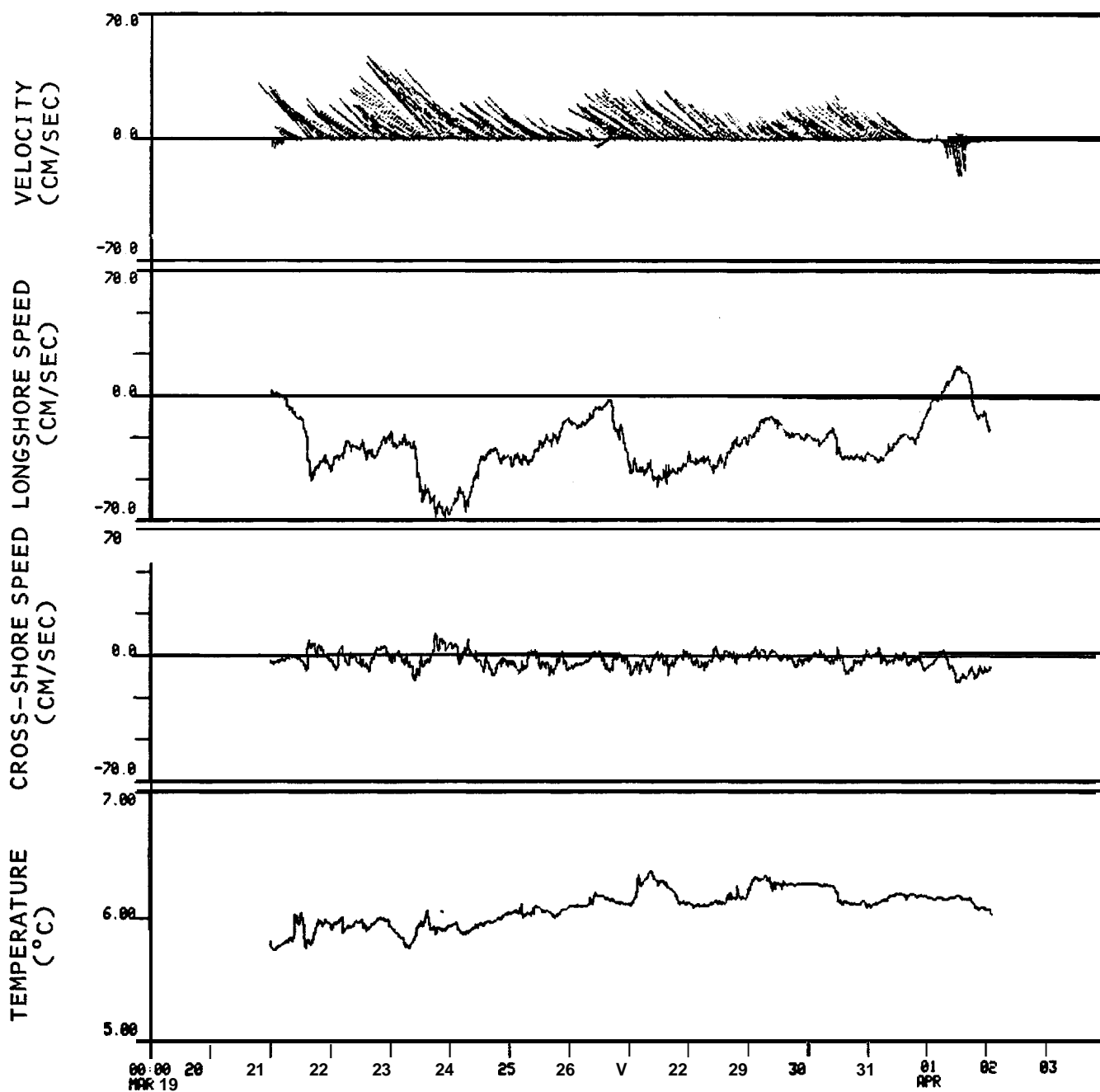


Figure 41. Time-series plots of 1-hour filtered current velocity (north is vertically upward), alongshore and cross-shore speed and temperature at 17 m, mooring 1. Mooring location is indicated on Figure 2.

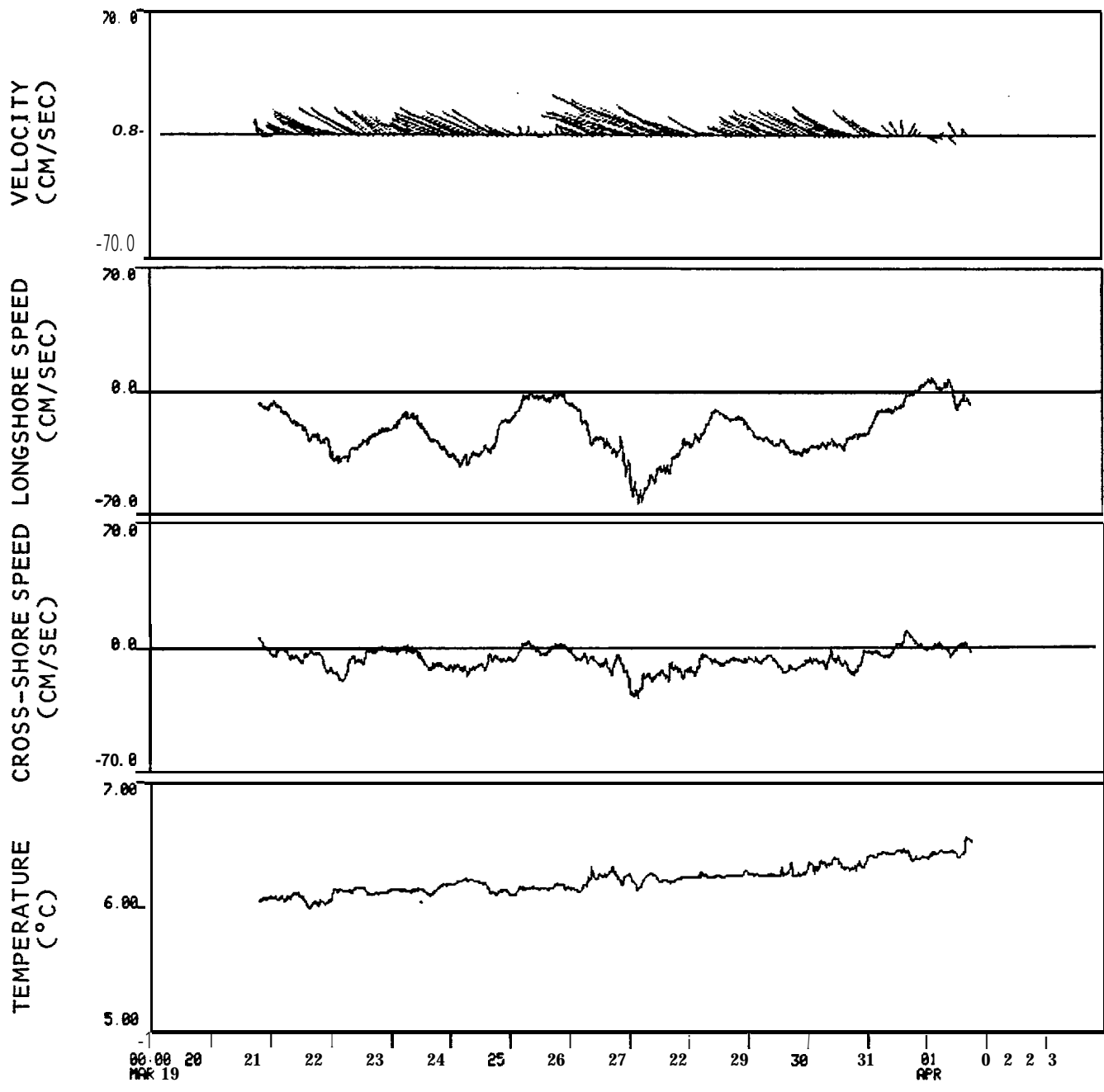


Figure 42. Time-series plots of 1-hour filtered current velocity, alongshore and cross-shore speed and temperature at 34 m, mooring 4. Mooring location is indicated on Figure 2.

flow. This behavior was in sharp contrast to the coastal flow in autumn 1980, when currents were **bimodal** with flow along-shore in either direction about 50 percent of the time. Flow speeds in spring were highly variable and reached maxima of nearly 70 cm/sec on **23-24** March at Mooring 1 (Figure 41) and on 26-27 March at Mooring 4 (Figure 42). Cross-shelf speeds were usually **below** about 10 cm/sec, though on 22 and 27 March they exceeded 20 **cm/sec** at Mooring 4. Visual inspection of the records suggests that a significant portion **of** the cross-shelf flow at Moorings 1 and 4 was tidal in nature. The records were, however, *too* short in duration for meaningful computation of energy spectra or tidal constituents. The along-shore flow was correlated at both moorings, with pulses on 22, 24, 27, and 30 March being evident in both records.

Both meters on spring Mooring 2 malfunctioned and yielded no records of significant length, and the upper meter on Mooring 5 also malfunctioned. Therefore, only the deeper (52 m) record from Mooring 5 is available as an indication of flow about 10 km from the coastline (Figure 43). Flow at this location was consistently toward the north, in rough alignment with local **isobaths** which at that location are strongly influenced by the presence of Alsek Canyon (see Figure 2). While there was some direction fluctuation about the northerly flow, only *on* 21, 25, and **31** March was there a weak reversal to southerly flow. Maximum flow speeds were about 30 cm/sec, and speeds were in the **15-20 cm/sec** range. The maxima in northward flow on 23-24 and 27-28 March coincided with northwesterly flow peaks which were also observed at Moorings 1 and 4 (Figures 41 and 42). Tidal fluctuations appeared to be secondary in magnitude relative to the **lower-**frequency pulses. As for Moorings 1 and 4, however, the record was too short for quantification of this observation.

Currents recorded on Moorings 3 and 6 provided documentation of mid-shelf currents during the spring field program (Figures 44-46). At Mooring 3 flow was consistently toward the north. Speeds were higher ( $\sim$  25 cm/sec) at the 37-m deep upper current meter (Figure 44) **than at** the 120-m deep lower meter (Figure 45) where speeds were 10-15 **cm/sec**. Reversals to southerly flow were infrequent, occurring only on 25 March, 6-7 April, and (at the deep meter only) 21-22 April. Visual inspection of the along-shore and cross-shelf speed plots reveals tidal currents which were appreciable but insufficient to reverse the flow from northerly to southerly.

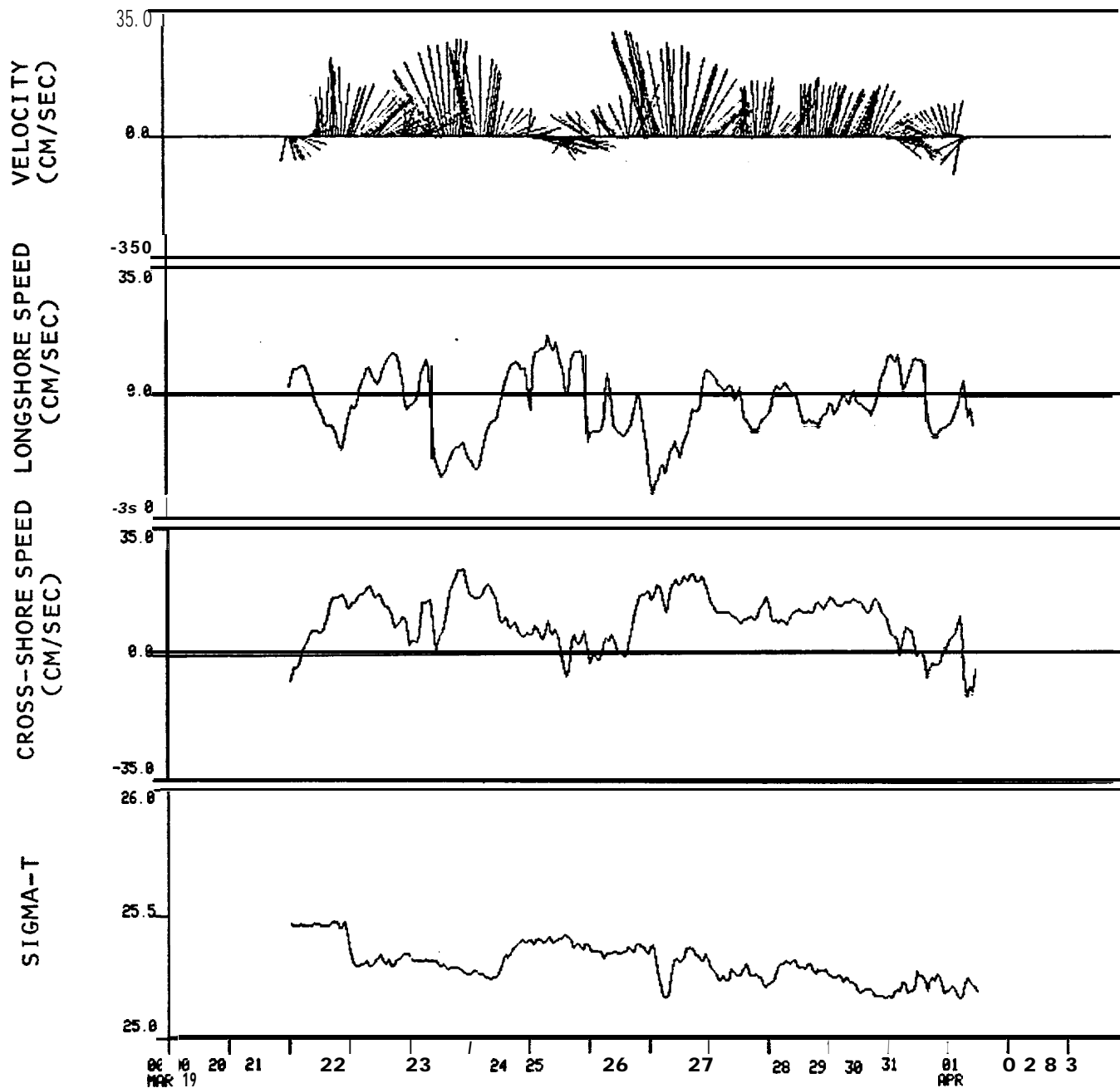


Figure 43. Time-series plots of 1-hour filtered current velocity, **alongshore** and cross-shore **speed, and** density (sigma-t) at 52m, mooring 5. Mooring location is indicated on Figure 2.

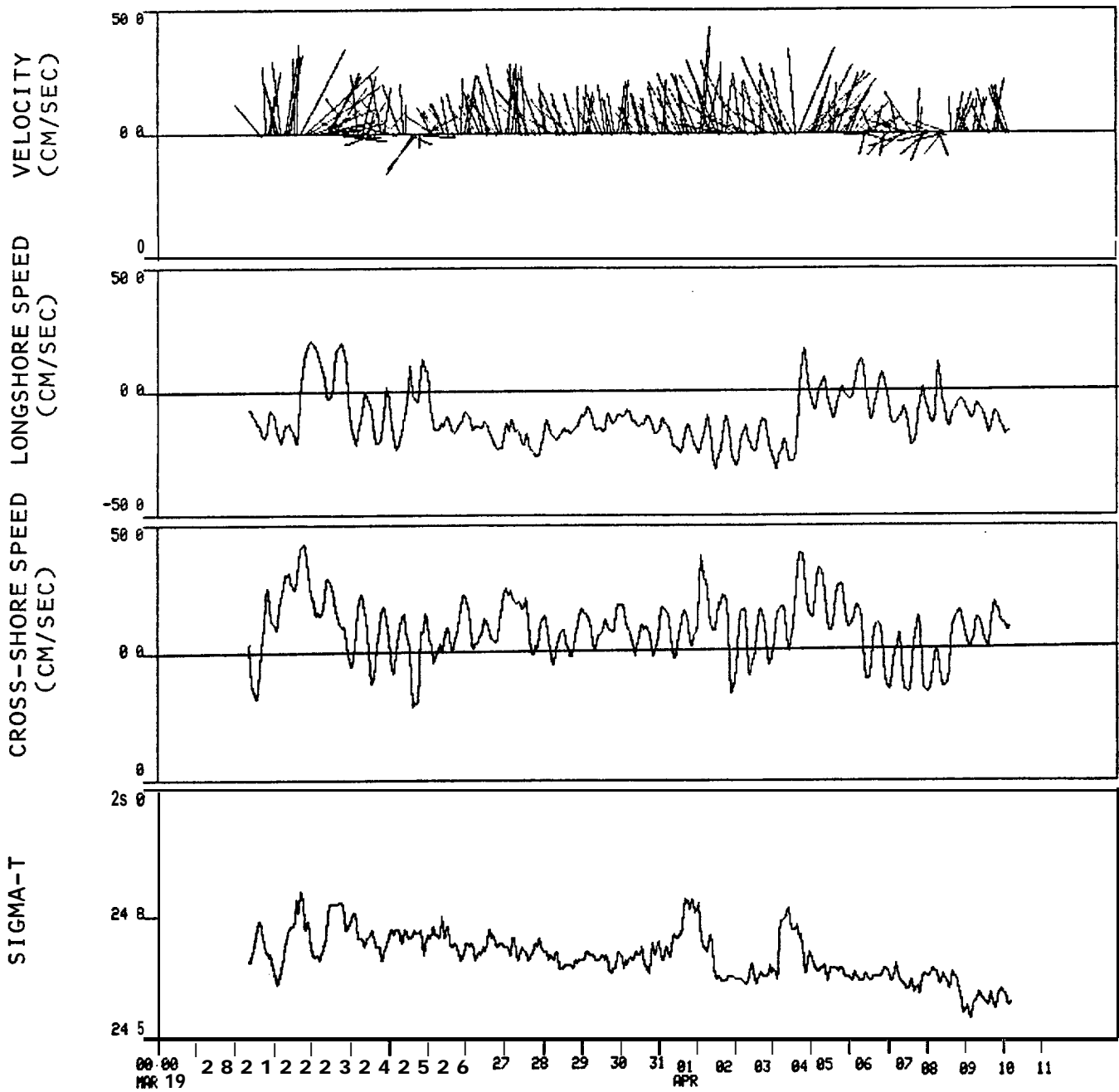


Figure 44. Time-series plots of 1-hour filtered current velocity, **alongshore** and cross-shore **speed**, and density (sigma-t) at 37m, mooring 3. Mooring location is indicated on Figure 2.

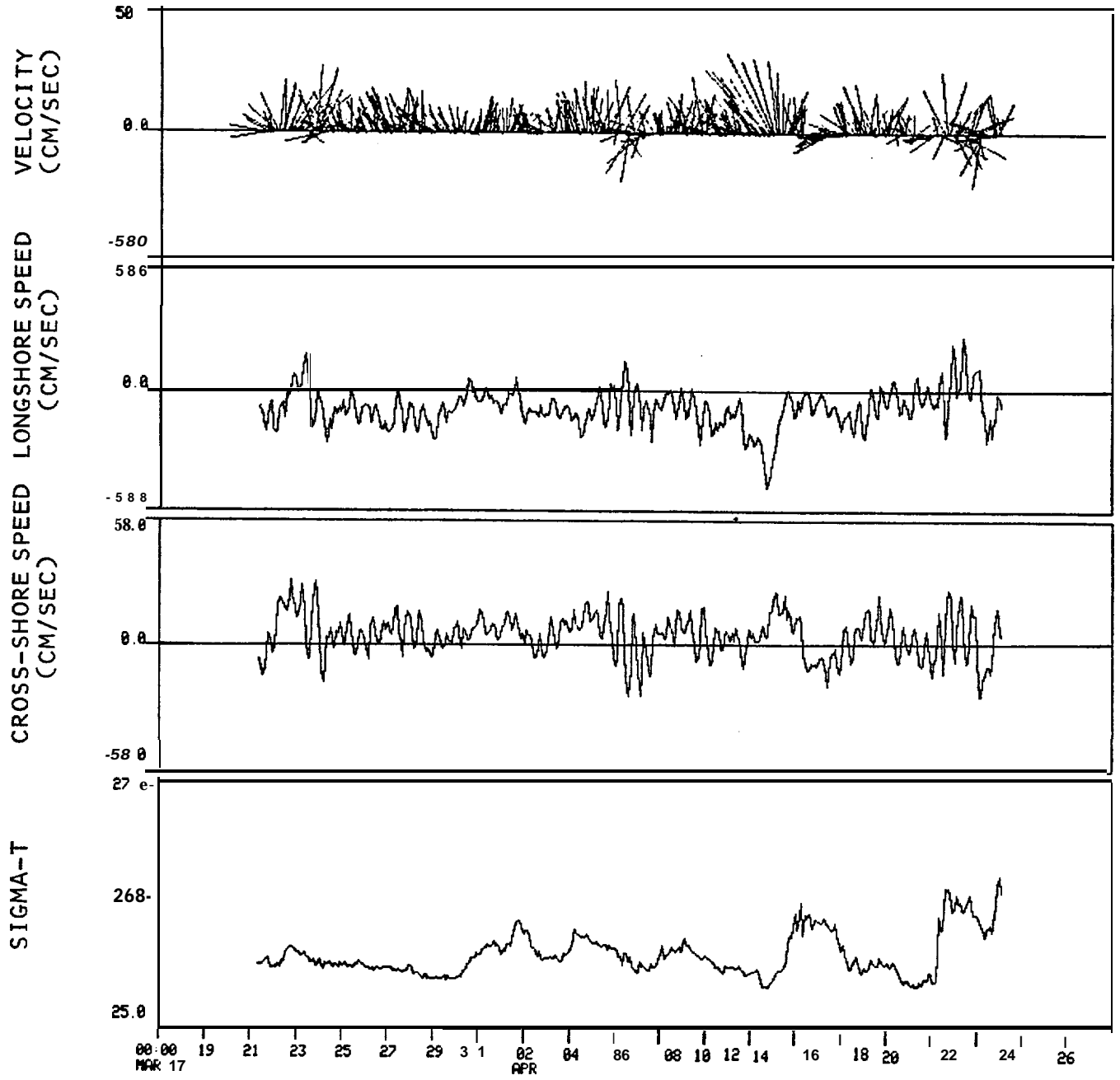


Figure 45. Time-series plots for 1-hour filtered current velocity, alongshore and cross-shore speed, and density (sigma-t) at 120 m, mooring 3. Mooring location is indicated on Figure 2.

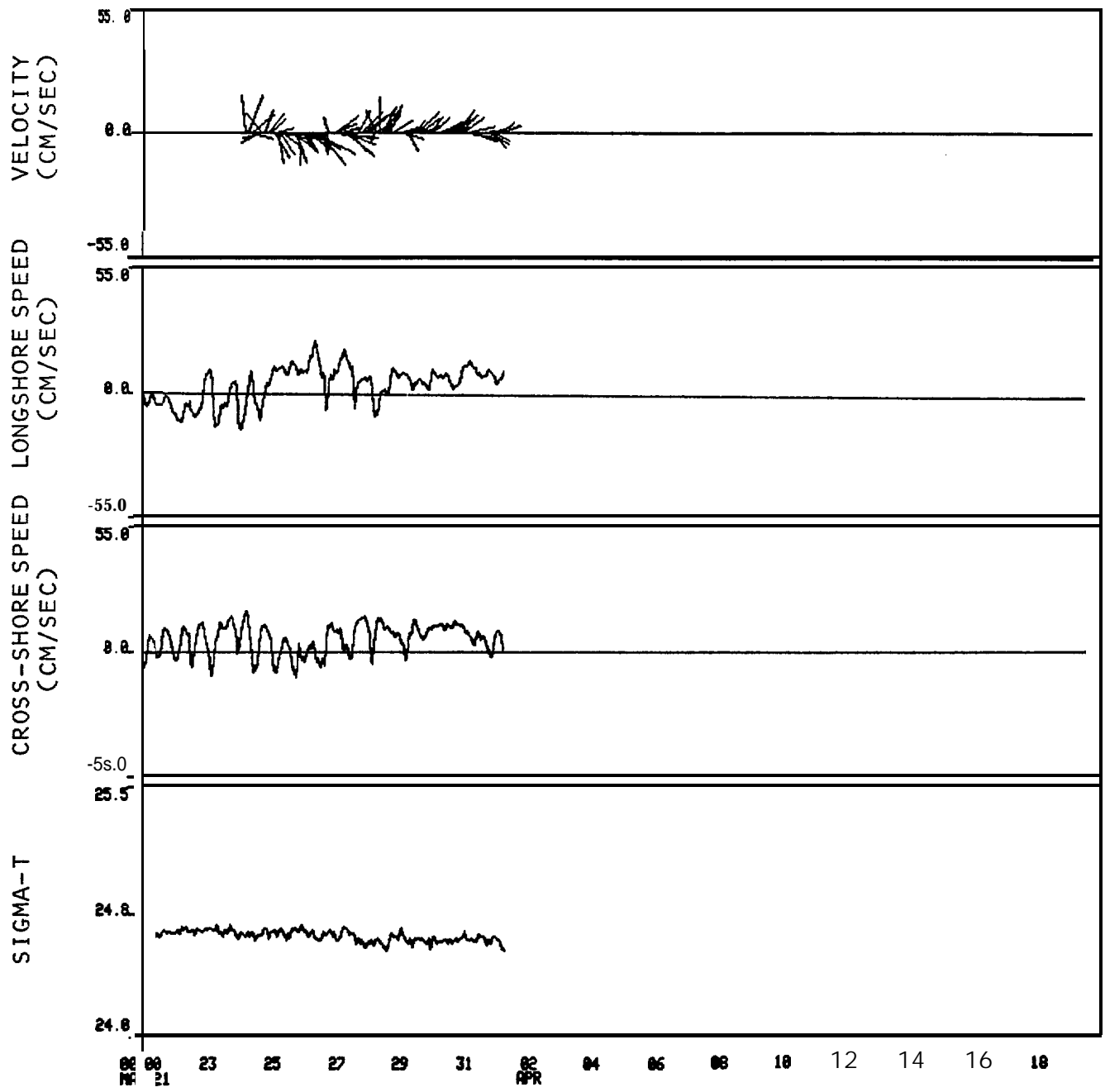


Figure 46. Time-series plots for 1-hour filtered current velocity, **alongshore and cross-shore speed, and density (sigma-t)** at 102 m, mooring 6. Mooring location indicated on Figure 2.

A current record was available only from the 102-m deep lower current meter on Mooring 6 (Figure 46). This record indicated that flow was fluctuating and generally easterly, varying from northeast to southeast in the same fashion as was observed during the autumn experiment (Figure 24). **Speeds** were 15-20 **cm/sec** with an obvious tidal signal as was recorded at Mooring 3. **This current record** showed by far the greatest directional variability of any of the spring moored current records.

#### 4. 2. 2 Spring **Drogued** Buoy Observations

The drogued buoys **in** the first spring survey were initially separated by 3.5 km (Figure 47), more than the autumn separation distance, to ensure a shorter time period before the buoys started to disperse. After an initial period of moving toward the southwest, both buoys changed to a northwestward direction, Buoy 6 first followed by Buoy 5 (Figure 48). The buoys had similar speed statistics (Table 5), with mean speeds near **20 cm/sec** and peak speeds of 40-45 **cm/sec**. The winds for this period were primarily out of the southeast at **4-5 m/sec**. After initially staying within 2-3 km of each other, the two buoys separated at a mean rate of **~13 cm/sec**; near the end of the experiment this rate returned to zero.

The second spring experiment, conducted from 24-27 March **1981**, has been broken up into four phases for statistical purposes. The three buoys were deployed out from the coast in a line approximately 20 km farther southeast than during the autumn survey. Buoy 4, nearest the coast, moved northwestward while Buoys 5 and 6 tracked towards the southwest (Figure 48). The two southwestwardly moving buoys had mean speeds similar to Buoy 4 (10-15 cm/sec), while their peak speeds were higher (34-35 cm/sec as compared to 22 cm/sec; see Table 5) and their directions were more erratic (Figure 50). Because Buoy 4 was moving toward shallow water where recovery would be difficult, **it** was retrieved and redeployed farther off shore (Figure 49). The frequent gaps in data taken during this experiment were due to equipment problems, position uncertainties, and buoys drifting out of radar range of each other.

Buoys 5 and 6 were redeployed for a short period (Phase 11). Although the statistics from this experiment are provided in Table 5, they are probably not particularly meaningful due to the short recording period (three hours).

Table 5  
 SPRING SURVEY DROGUE BUOY SPEED STATISTICS

	MIN SPEED (cm/see)	MAX SPEED (cm/see)	MEAN SPEED (cm/see)	SPEED STD DEV (cm/see)
<hr/> <b>EXPERIMENT 1</b>				
<u>Phase I: 3/22/81 (0300 hrs) - 3/23/81 (0900 hrs)</u>				
Buoy 5	6.6	45.8	18.1	7.4
<b>Buoy 6</b>	9.9	40.0	22.6	7.0
-----				
<b>EXPERIMENT 2</b>				
<u>Phase I: 3/24/81 (2000 hrs) - 3/25/81 (1600 hrs)</u>				
Buoy 4	1.0	22.1	<b>11.0</b>	6.2
Buoy 5	0.3	35.4	<b>10.3</b>	7.3
<b>Buoy 6</b>	2.1	33.8	<b>14.6</b>	7.2
<u>Phase II: 3/25/81 (2000 hrs) - 3/25/81 (2300 hrs)</u>				
Buoy 5	7.1	15.0	10.5	2.8
<b>BUOY 6</b>	2.1	7.9	5.0	1.9
<u>Phase III: 3/26/81 (0130 hrs) - 3/26/81 (1800 hrs)</u>				
Buoy 4	4.7	33.4	15.8	6.2
Buoy 5	2.4	16.9	6.9	3.2
<b>BUOY 6</b>	2.4	17.6	9.1	4.8
<u>Phase IV: 3/27/81 (0630 hrs) - 3/27/81 (2030 hrs)</u>				
Buoy 4	19.2	32.0	26.0	3.5
Buoy 5	4.4	34.8	20.8	9.1

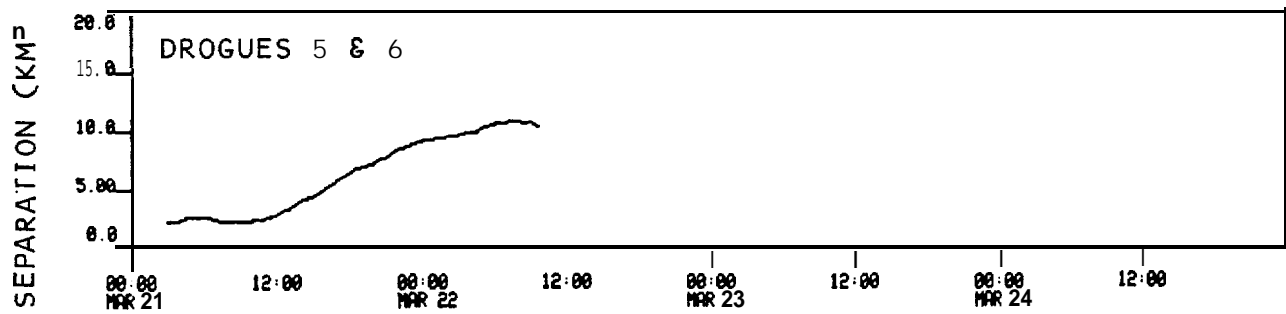


Figure 47. Plot of separation between **drogues** 5 and 6 as a function **of** time.

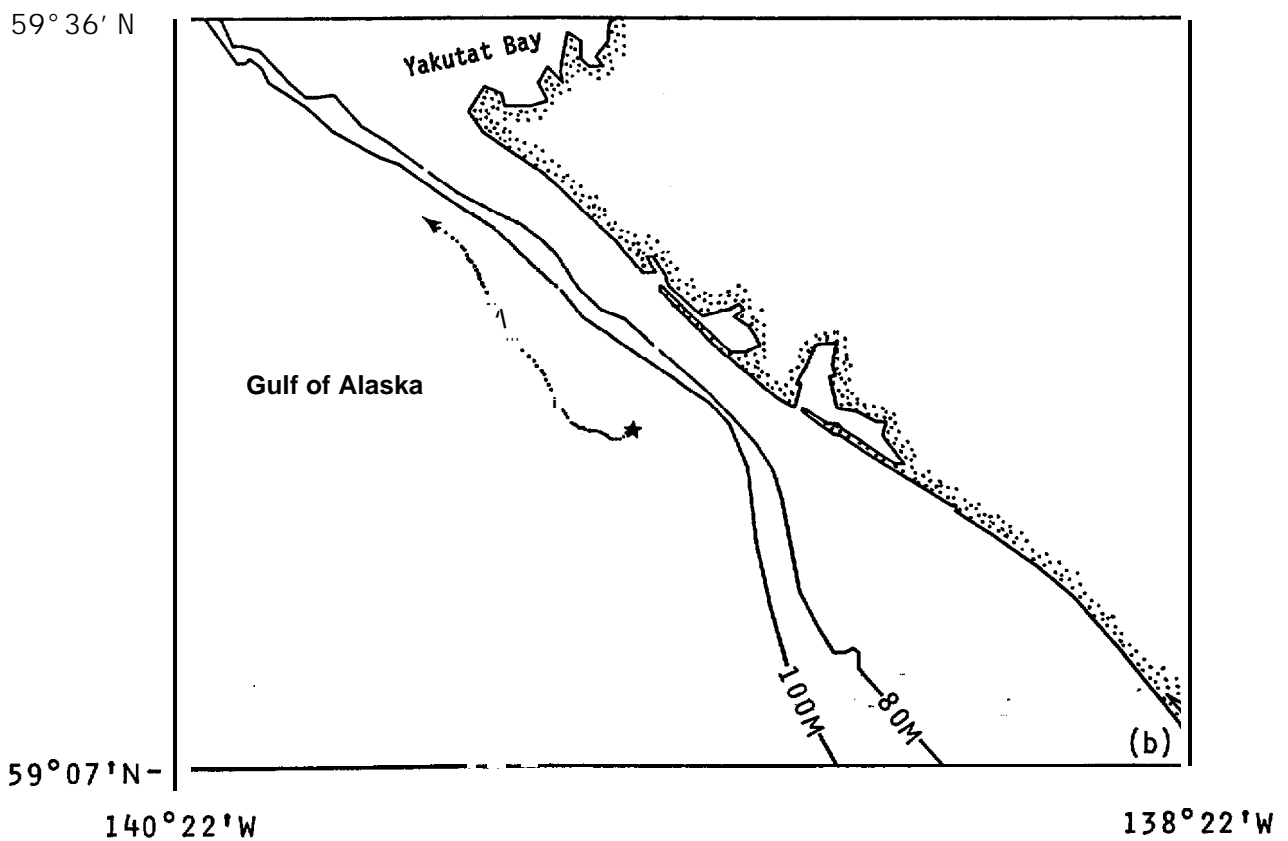
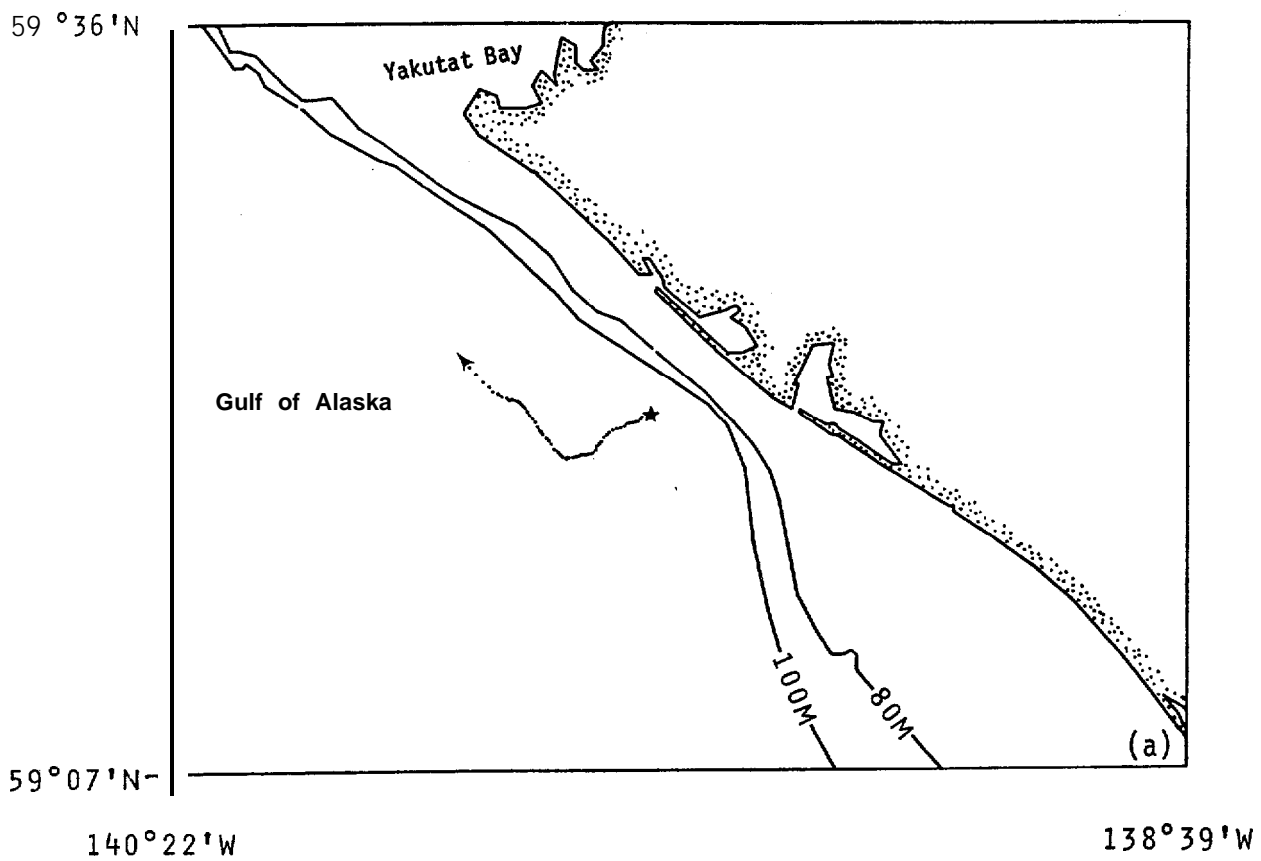


Figure 48. Drift tracks for **drogues** 5 (a) and 6 (b) during the first spring **drogue experiment**. Stars indicate deployment locations. See Table 5 for statistics.

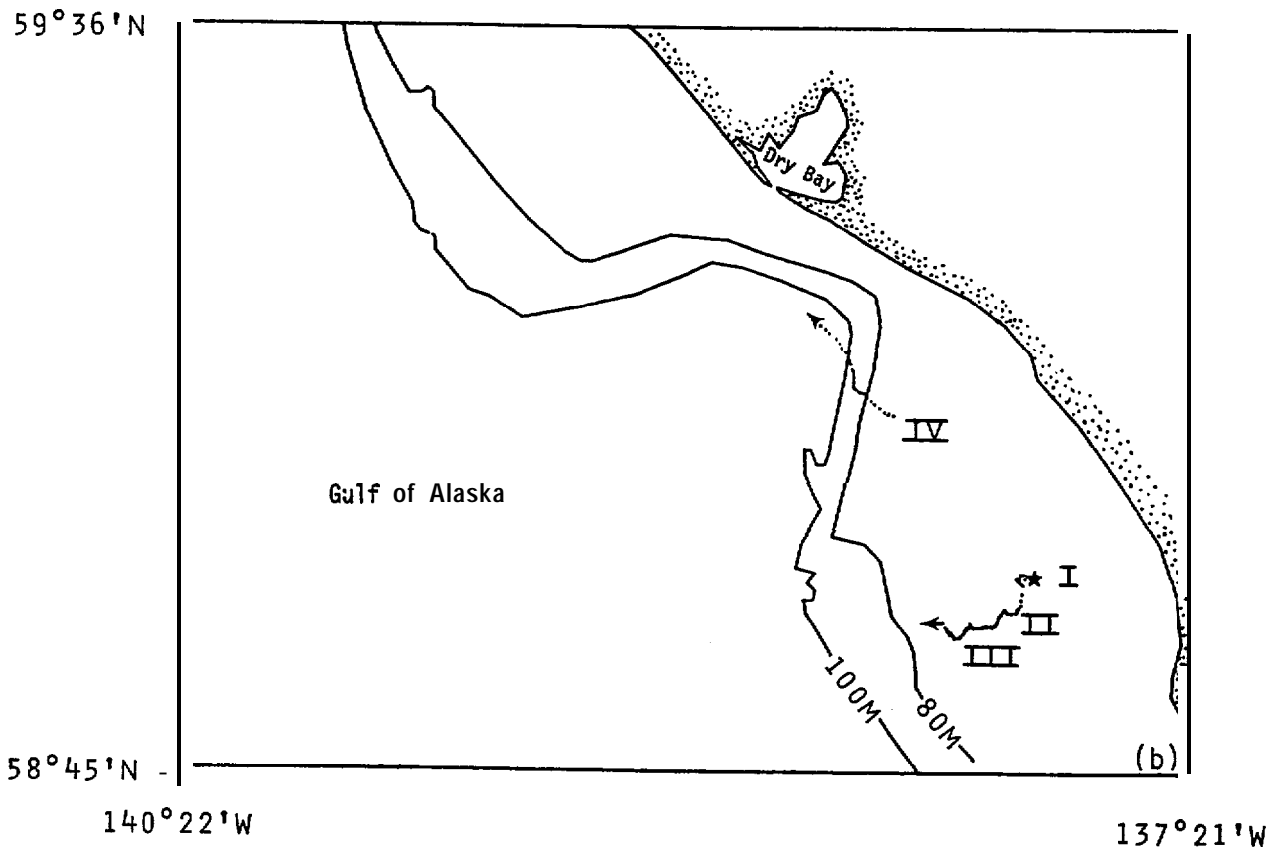
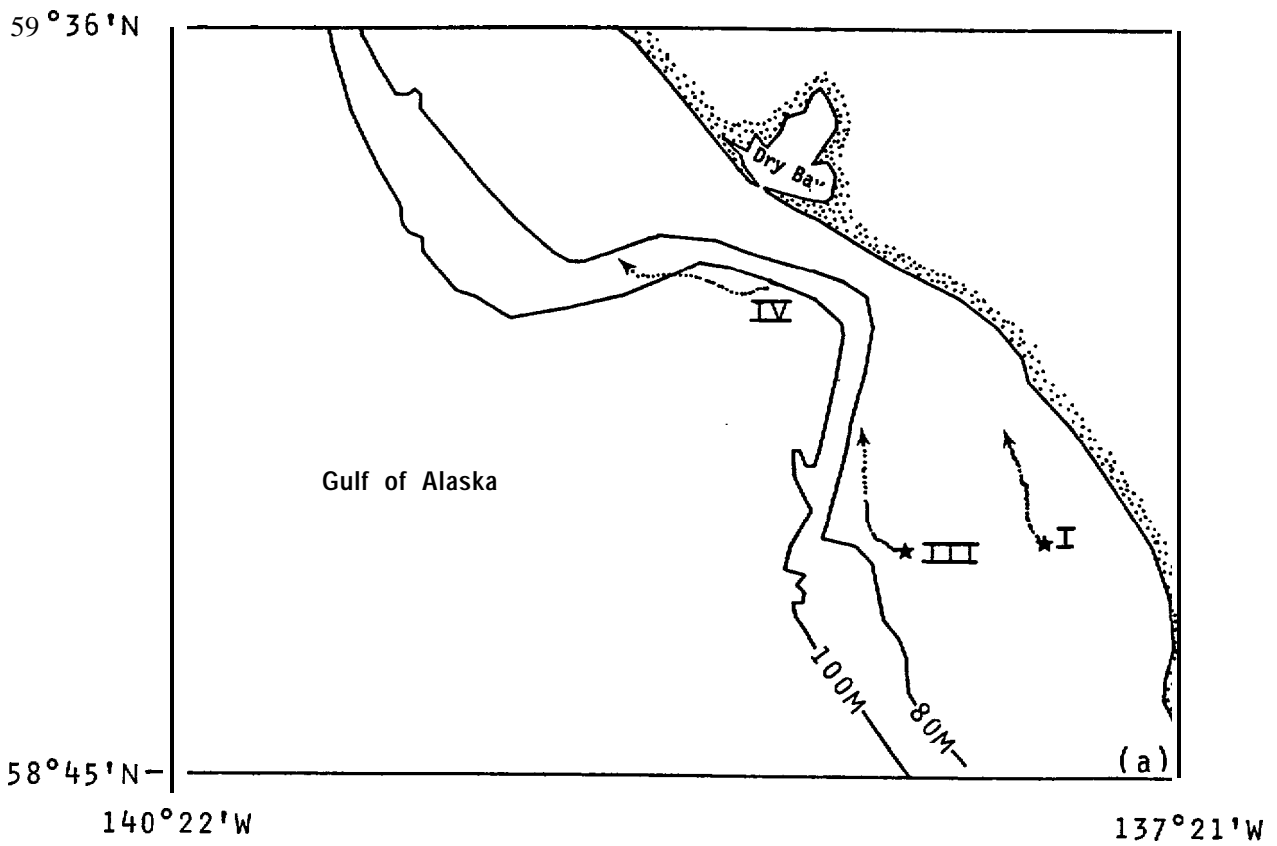


Figure 49. Drift tracks for drogues 4 (a), 5 (b) and 6 (c) during the second spring drogue experiment. Roman numerals (I-IV) refer to different phases of the experiment. Stars indicate deployment locations. See Table 5 for statistics.

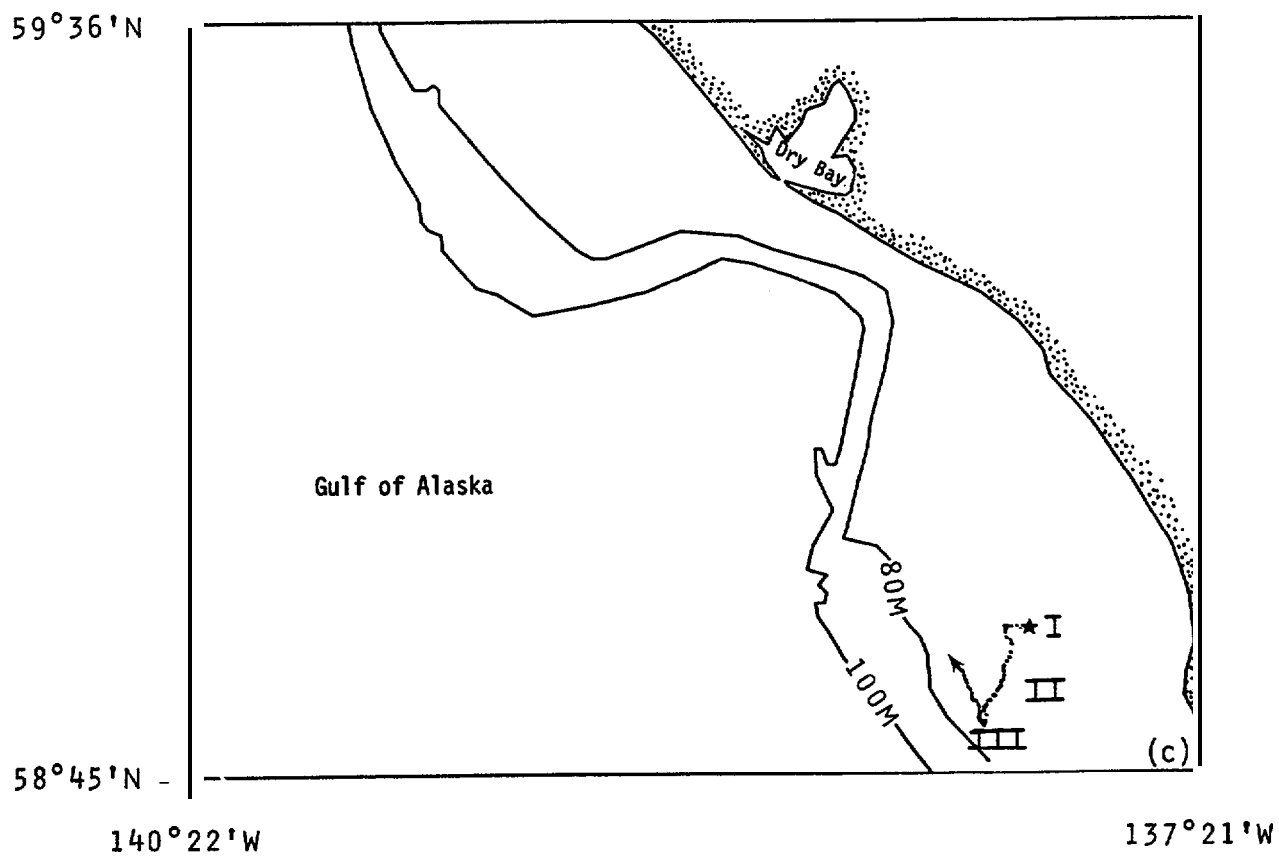


Figure 49 (continued).

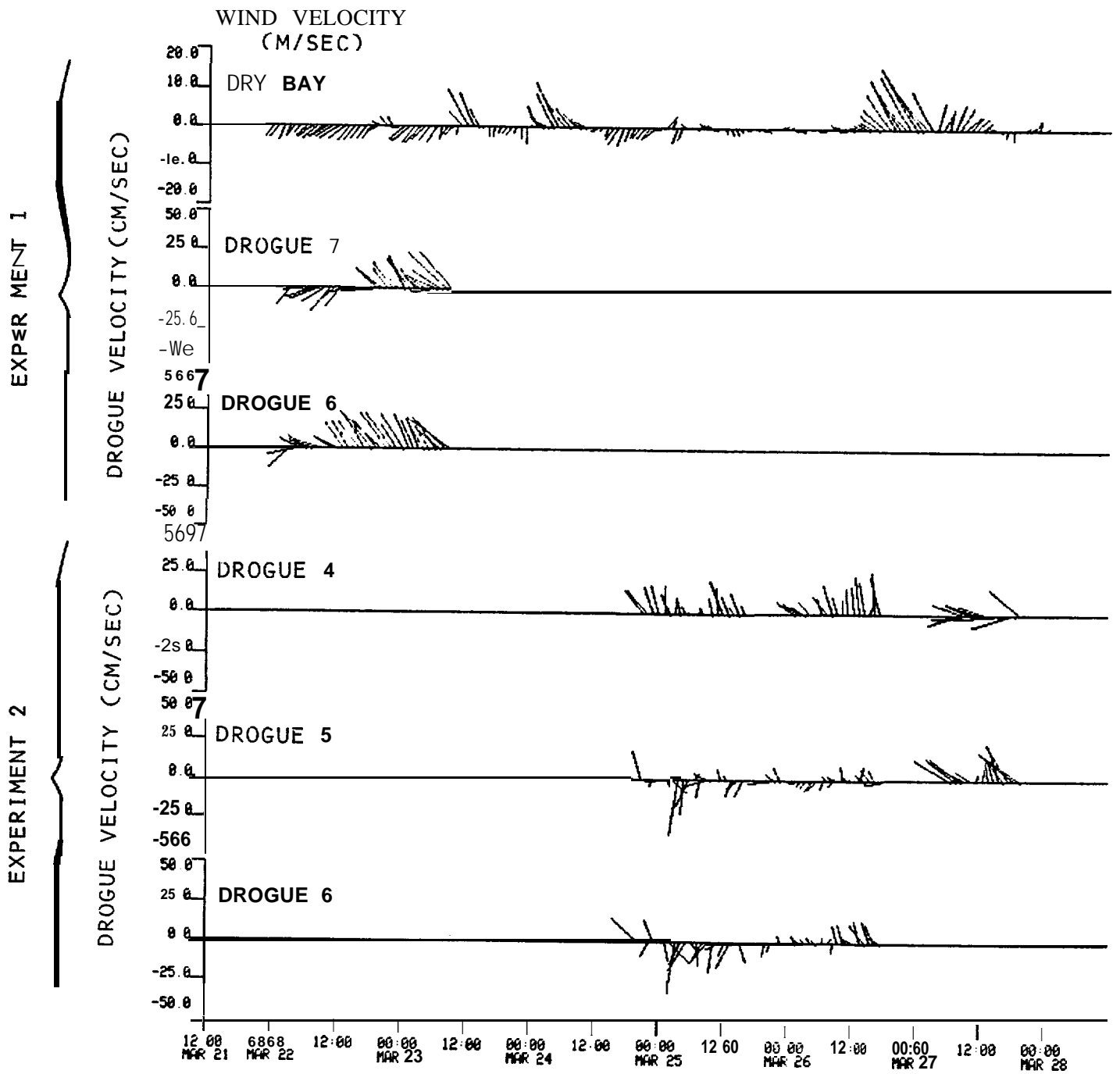


Figure 50. Plots of wind velocity as a function of time (uppermost plot), and drogue velocity derived from trajectories as a function of time. Both wind and drogue velocity vectors are oriented toward direction of movement. North is vertically upwards,

During Phase III all three buoys were redeployed. Buoy 4 was deployed in a region of northwestward flow, as evidenced by its significant mean and peak speeds (16 and 33 cm/sec, respectively). Buoys 5 and 6 changed direction towards the northwest and were entrained into the same strong flow (see Figure 48); this change, which can also be seen in Figure 50 along with the dramatic increase in speed for Buoy 6, happened simultaneously with the onset of a wind event (Figure 50). At this point Buoy 6 was retrieved.

During the final phase (IV) of the experiment, Buoys 4 and 5 moved in the northwesterly current with mean speeds of 20-26 **cm/sec** and peak speeds of 32-35 **cm/sec**. These two buoys moved along the coast and displayed the topographic steering effect that was evident during the same experiment of the autumn survey.

In summary, the spring survey showed consistent northwestward flow along the coast for the period of the drogue buoy study, in agreement with the moored current observations. There was some evidence that a storm event influenced the circulation. The topographic steering of the current seen in the autumn was observed at the head of the **Aisek** Canyon.

#### 4.2.3 Spring Littoral Currents

The **longshore** surface current speeds and seabed drifter recoveries showed much lower speeds in spring than in the previous autumn's survey, probably as a consequence of the lack of strong storm events during the spring measurement period.

As shown in Table 6, the wave-driven surface current was southeasterly at about 57 **cm/sec** the day of the launch, reversing to a strong northeasterly flow which subsided the next day and reversed direction again to southeasterly flow on the third day. The vector-averaged velocities (Table 6) show a pattern similar to that **seen** by the seabed drifters: the first day's average velocity values imply flow to the southeast while all three subsequent days show values which imply flow to the northwest. In a different **trend than** seen with the seabed drifters, the current speed decreased over **those three days, perhaps** as a result of uncertainties in estimating the wave parameters.

Table 6

SPRING SURFACE CURRENT VELOCITY  
ESTIMATED FROM WAVE PARAMETERS\*

	WAVE - ANGLE [ $^{\circ}$ ]	WAVE HEIGHT (m)	LONGSHORE SURFACE VELOCITY (cm/sec)	VECTOR- AVERAGED VELOCITY (cm/sec)
Launch	-10 ( $\pm 3$ )	<b>0.8 (<math>\pm 0.5</math>)</b>	- 57 ( $\pm 30$ )	- 57
Day 1	12 ( $\pm 3$ )	<b>1.5 (<math>\pm 0.5</math>)</b>	93 ( $\pm 37$ )	<b>62</b>
Day 2	1 ( $\pm 3$ )	2.2 ( $\pm 0.5$ )	<b>10 (<math>\pm 30</math>)</b>	41
Day 3	-10 ( $\pm 3$ )	0.8 ( $\pm 0.5$ )	- 57 ( $\pm 30$ )	13

\* Error estimates in velocity are those resulting from the uncertainties in angle and height of incident waves,

The seabed drifters were launched 21 March 1981, with strandings recovered over the following three-day period. Results from the in-shore group 1S (Figure 57a) show a slight southeast flow for the first-day recoveries, gradually changing to a moderate northwest flow. The drifters showed a range of speeds on the first day from -4 to 2.5 cm/sec, with a weighted mean of -2.5 cm/sec (negative values imply flow to the southeast). By the second day, the flow was to the northwest with a two-day average speed of 1 cm/sec and a range of 0-4 cm/sec. By the third day the northwestward flow was well-established, with one recovery reflecting a speed of 9 cm/sec.

The results from Group 2S (Figure 51b) also reflect this reversal of flow from southeast to the northwest. The first-day recoveries showed southeast flow with a weighted average of -2 cm/sec and a range from -3.5 to 1 cm/sec. On the second day the two-day average speed was 1 cm/sec, with a range from 0-5 cm/sec. The three-day average speeds ranged from 5-11 cm/sec with a mean of 8 cm/sec.

Group 1S and 2S thus showed similar patterns in the reversal from southeast to northwest flow. The third group 3S, which was farthest offshore, did not show this pattern, but its results are consistent with the other groups (Figure 51c). Since there were no recoveries of this group the first day, flow for that period was integrated into the two-day average values which showed a large number of recoveries centered around a mean of 4 cm/sec, slightly higher than the two-day mean values from the other groups. On the third day one drifter was recovered, reflecting a three-day average flow of 8 cm/sec; this is not significantly different from the two-day mean speed, considering the uncertainty in the measurements.

To summarize the spring data, the two in-shore groups of recovered drifters showed a reversal in current direction from southeast to northwest followed by a gradual increase in speed. While the offshore group did not show this reversal, its results are consistent with this pattern.

#### 4.2.4 Spring Wind Observations

Winds recorded at the beach locations near Dry Bay and Ocean Cape during the spring program (Figure 52) showed the same event-dominated wind pattern that had been observed during autumn 1981. Speeds at both locations were generally

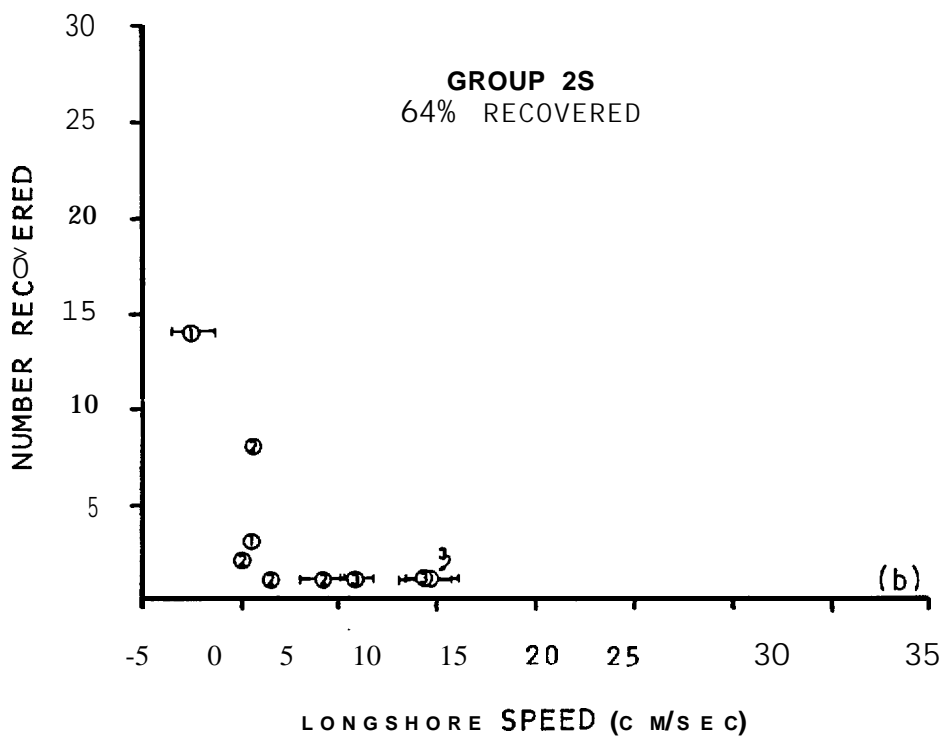
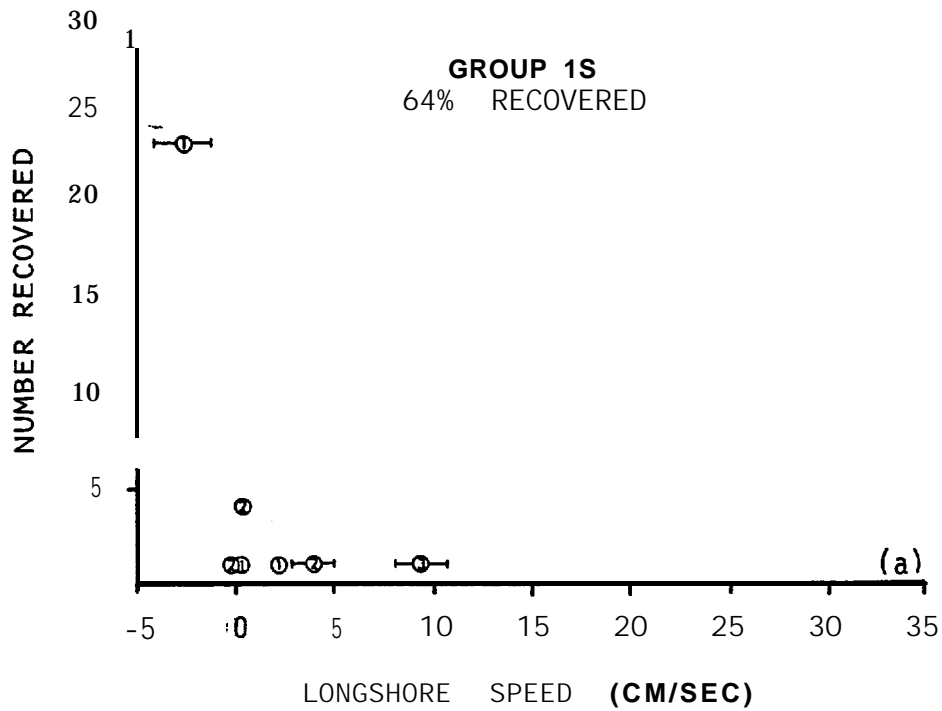


Figure 51. Histogram of alongshore speed for seabed drifters from groups 1 (a), 2 (b) and 3(c). Positive is northwestward.

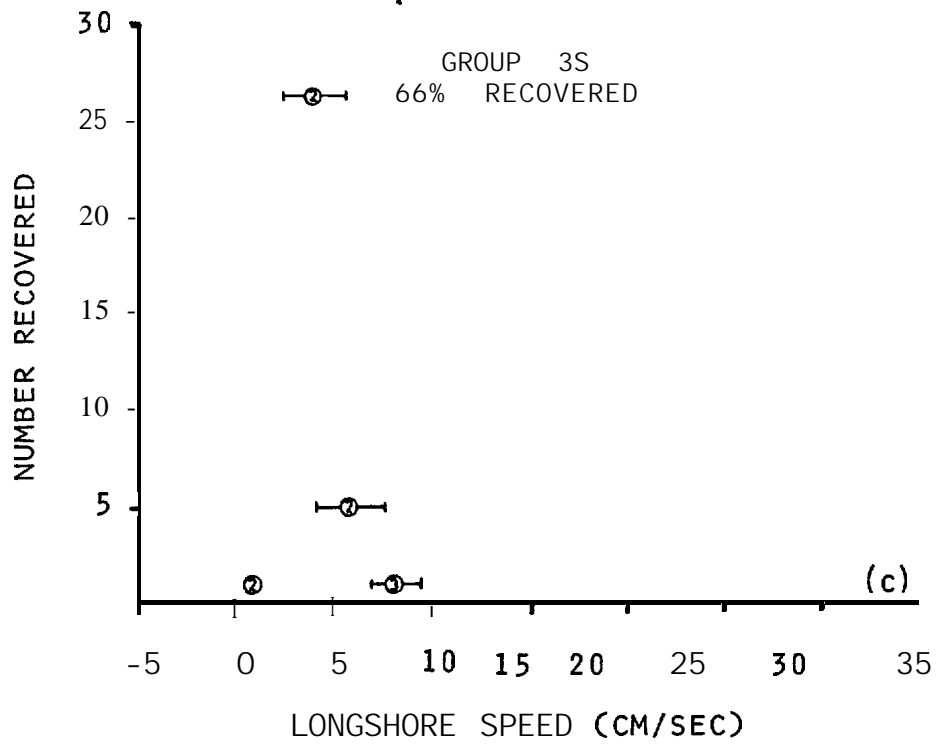


Figure 51 (continued).

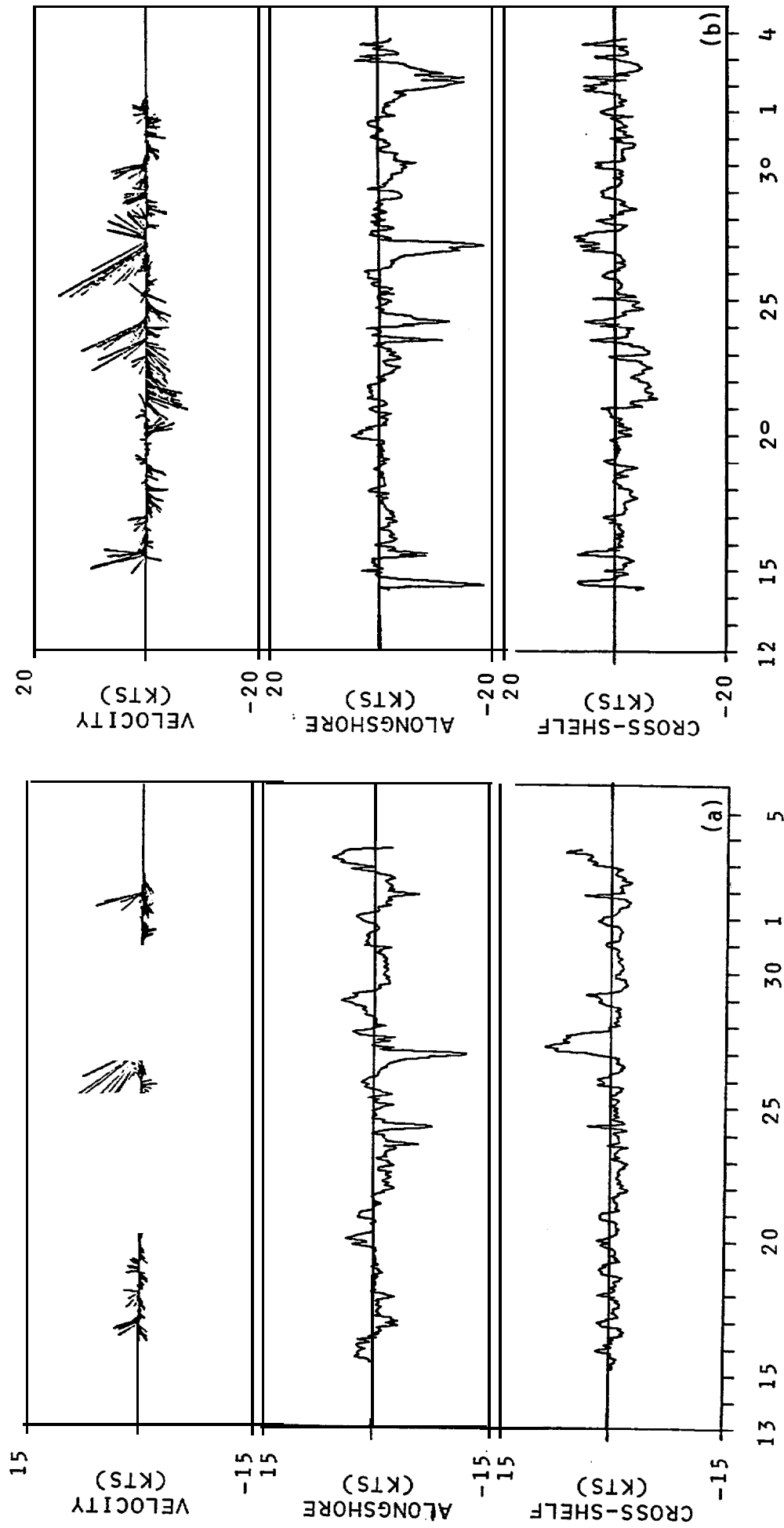


Figure 52. Time-series plots of 1-hour filtered wind velocity (north is vertically upward), alongshore and cross-shelf speed at Ocean Cape (a) and Dry Bay (b). Location of meteorological stations are indicated on Figure 2.

5 m/see **OR** less except when a storm event passed through the region. During periods **of low** wind speeds the winds were westerly. Discrete storm events, during which winds became easterly, were observed on 23-24 and 27 March; during these events, wind speeds attained values up to about 15-20 m/see, with the higher speeds being associated with the later storm event. The storm winds were **well** correlated between the Ocean Cape and Dry Bay recording stations and were also observed at the vessel which was carrying out the concurrent oceanographic observation program.

#### 4.3 Discussion of the Spring Experiment

The temperature and salinity fields observed in the study region during spring 1981 were characterized by generally lower temperatures, higher salinities, and smaller vertical and horizontal gradients than were observed in autumn 1980 (Section 3). There was, nevertheless, a level of spatial variability similar to that observed in the earlier experiment. Currents in spring exhibited a more consistent flow to the northwest than was present during autumn, **although** considerable speed variability was still present. The coastal current which had been observed in autumn was greatly diminished during spring. These observations are discussed below using temperature-salinity and time series analyses.

##### 4.3.1 Temperature-Salinity Analyses

A composite temperature-salinity (T-S) plot has been constructed for the shelf waters off the northeast Gulf of Alaska during spring 1981 (Figure 53). For comparison purposes, the water masses which were defined for the autumn 1980 data are indicated on this plot by dashed lines. It is immediately apparent that the only autumn water mass to retain its identity unchanged in spring was the "Deep Ocean" Water having temperatures below about 7.5 °C and salinities greater than 32.0 ‰. The Coastal Water, a major identifiable water mass during autumn, was represented in spring only by the scattered T-S points falling to the left (lower-salinity side) of the Deep Ocean Water. The Shelf Water had salinities between about 31.5 and 32.3 ‰, coincident with the highest salinities observed for this water mass in autumn, and temperatures **of 6-7.5** °C.

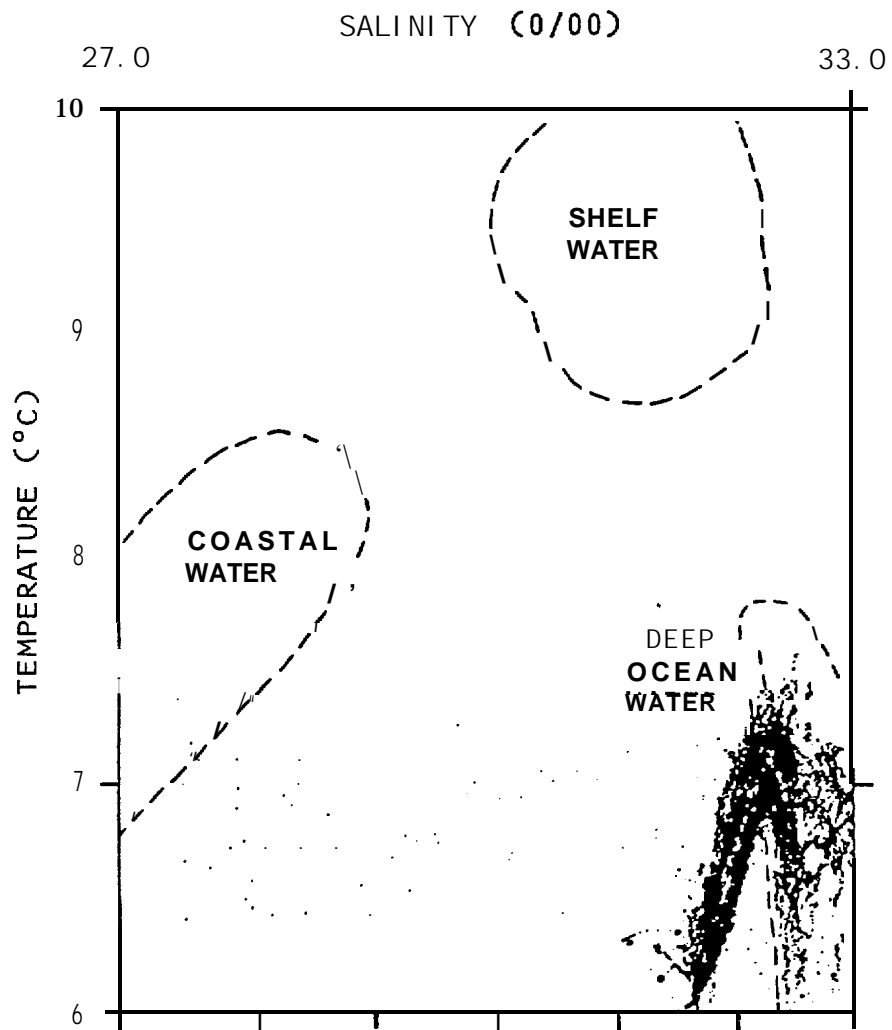


Figure 53. Composite temperature-salinity plot for the northeast Gulf of Alaska in spring 1981. Dashed lines define water masses which were identified during the autumn 1980 field experiment.

The altered (as compared to autumn) temperature-salinity characteristics of the water in spring can be explained qualitatively as due to the combined effects of winter cooling, wind-mixing, and near-cessation of coastal freshwater input to the coastal regions. The nearly complete absence of Coastal Water in spring was **due to the lack of coastal freshwater input which was in large part responsible for the presence of this water mass the preceding autumn.** The few scattered low-salinity points on Figure 53 were due to samples obtained within the few attenuated coastal river plumes along the coast and off Yakutat Bay. This input was not, however, sufficient to create a well defined low-salinity mass of Coastal Water.

Compression of the Shelf Water into a narrower range of salinities in spring than in autumn was also due in part to lack of freshwater admixture. Lateral mixing with the Coastal Water had been responsible, during autumn, for low-end salinities for the Shelf Water. Absence of the Coastal Water in spring therefore removed the source for low salinities in the Shelf Water, with the result that spring salinities were contained within a relatively narrow range of values.

Winter cooling prior to occupation of the spring CTD stations was responsible for the lower Shelf Water temperatures in spring than in autumn, with the lowest temperatures observed occurring in the near-surface near-coastal waters (see Figures 33-35) and higher temperatures occurring near the bottom at the shelfbreak. The Shelf Water temperature distribution in spring reflected, therefore, the **more intense cooling near the coast** due to lower air temperatures and shallower depths there, and the admixture of warmer Deep Ocean Water near the shelfbreak. The increase in temperature in the Deep Ocean **Water** between about 100 and 350 m between autumn and spring (see Section 4.1) was not due to local processes but rather an effect of circulation variations in flow off the shelfbreak. Vertical gradients associated with this feature were at times quite large; an example is shown in Figure 39, which shows a vertical profile from mid-shelf. The strength of the gradients suggests that the feature was being maintained by circulation because, in the absence of strong advection, vertical diffusive processes would have rapidly decreased the gradients.

Unlike the autumn case, spring temperature and salinity distributions were not characterized by well defined horizontal gradients or frontal zones which

separated the water masses (compare, for instance, Figures 10 and 35). This was due to combined cessation of the processes which acted during summer and autumn to maintain the gradients (i.e. warming and freshwater admixing) and an increase in the mixing processes which tend **to diminish** such gradients. Vertical mixing processes during winter would have been abetted in particular by **thermohaline** and wind mixing.

The appreciable accumulation of low-salinity near-coastal water at Section E (Figure 36d) suggests that freshwater was **still** being added to the head of Yakutat Bay through the winter. Since a significant portion of the freshwater addition to this Bay is thought to occur via subglacial streams (**Reeburgh et al.**, 1976), there is no way to verify this contention directly.

Much of the horizontal variability in temperature and salinity **at 100 m** (Figure 34) can be explained in terms of flow of Deep Ocean water onto the shelf. Such water was evident in **Aisek** Canyon as 7.3 °C water (Figure 34a) and had probably flowed shoreward **along** the canyon as was inferred from the autumn 1980 T-S distribution (Section 3). The parcels of relatively cold (6.1-6.7 °C) and saline (32.3-32.6 ‰) water **along** the shelfbreak south of Yakutat Bay and at the extreme southeastern corner of the study region (Figure 34b) were of the proper characteristics to be Deep **Ocean** water. The water in **Aisek** Canyon had originated from slightly greater depths than the water on the shallower portions of the shelf, which explains its higher temperature.

Some of the variability may **also** have been due to eddy-like structures originating off the shelfbreak. Royer and Muench (1977) have hypothesized the presence of such eddies in the region to the west using **satellite** data. Hayes (1979) hypothesized, using current data from the Icy Bay region, that current fluctuations near the shelfbreak were due to offshore eddies. **Lagerlof et al.** (1981) suggest that eddies may explain **low** frequency current **fl**uctuations observed on the shelf to the west of Dry Bay. **Cyclonic** "cold-core" eddies might explain presence of the **low** temperature areas observed off the shelfbreak, and are of the proper horizontal scale ( $\sim 50$  km) to be in qualitative agreement with previous work.

As in autumn, there was a general parallelism between the **isopleths** of temperature and salinity and the **isobaths**, upon which the above fluctuations were superposed. The parallelism supports the concept of a generally northwesterly flow along the coastline, as for the autumn case, and is in agreement with the dynamic principle that streamlines of flow should be expected to follow **isobaths** at these latitudes.

#### 4.3.2 Circulation Analyses

In this section, the circulation features observed during the spring deployments of Moorings 1-5 and the final segment of the overwinter deployment of Mooring 6 are considered. The comments provided at the beginning of Section 3.3.2 concerning record length apply also to this section.

In sharp contrast to the autumn records, the spring records from Moorings 1 and 4 nearest the coast indicate that flow was consistently toward the northwest in the along-shore direction (Figures 41 and 42). Large speed variations were present, superposed on this northwest flow. Inspection of the records reveals a good visual correlation between the identifiable current pulses at these moorings. Comparison with the wind records obtained over the same time period indicates that the current pulses on 22, 24, and 27 March were correlated with strong northwesterly wind events (cf. Figure 52), suggesting that these pulses were wind-driven in nature. Coherence between along-shore currents and winds is theoretically to be expected based upon shelf circulation theory (LeBlond and Mysak, 1979). A similar tendency was observed west of Yakutat by Hayes (1979), although his moorings were deployed only beyond about 10 km from the coastline. Hickey (1981) has recently shown a high correlation between coastal current events and local winds off the Pacific Northwest continental shelf.

The small cross-shelf (relative to along-shore) flow reveals a strong bathymetric control over the currents, which paralleled **isobaths**. While tidal currents were evident in the cross-shelf flow components, they were small (**< 10 cm/sec**) relative to an along-shore flow which at times approached instantaneous speeds of **70 cm/sec**. This small tidal flow near the coast is due to the continuity requirement that currents normal to the coastline go to zero at the coastline. A similar tidal current pattern was observed in the shelf region south of Kodiak Island (Muench and Schumacher, 1980).

**Mooring 5 exhibited flow which was northerly except for minor reversals on 21, 25, and 31 March.** The northerly orientation paralleled local **isobaths** which defined the shoreward end of **Alsek Canyon** (Figure 2). This was particularly pronounced at Mooring 5 because only the deeper of the two records was usable and proximity to the bottom made the tendency to parallel **isobaths** more pronounced.

Mooring 3, the farthest off the coast, exhibited a strong northward flow at both depths, with instantaneous speeds at 37 m depth of about 40 **cm/sec** and speeds at 120 m of about 20 **cm/sec** with one peak (on 12 April) approaching 40 **cm/sec**. The reason for this strong cross-shelf flow is uncertain, but it is probably related to interaction between the regional northwestward flow and local bathymetry.

The record from Mooring 6 was dominated by the tidal signal, which was considerably stronger than the weak mean flow (cf. Figure 46). This record was in sharp contrast to those from the other spring moorings, all of which had shown relatively consistent flows toward the north-northwest. Conversely, the long-term mean flow at Mooring 6 was easterly (see Section 5.1) and weak relative to the instantaneous current events. As for Mooring 3, the reason for this consistently "reversed" flow is uncertain; it probably is due to topographic effects, in particular the location of the mooring north of Fairweather Bank.

The overall circulation pattern observed in spring 1981 showed a consistent flow toward the north-northwest, with lower directional variability than in autumn 1980 except for Mooring 6. Results obtained from the moorings were in agreement with those derived from the drogued buoys (Figure 50) and, **unlike** the autumn case, showed less variation with depth. There was pronounced convergence of streamlines at the heads of the cross-shelf troughs, these being most evident at the head of Alsek Canyon both in currents obtained from the moorings and in the drifter results (Figure 49a). This convergence was responsible for the high currents at Moorings 1 and 4, relative to those observed at other moorings. Reasons for the strong cross-shelf flow component at Mooring 3 and for the small easterly mean flow at Mooring 6 are uncertain.

### 4.3.3 Littoral Currents

The seabed drifter program and accompanying analytical computations, as described in Section 4.2.3, revealed that the littoral currents were far weaker in spring 1981 than they had been the previous autumn (see Sections 3.2.3 and 3.3.3). This was because most wave activity was directed directly onshore in spring, and there was not therefore an appreciable **longshore** wave-induced transport. Some reversals to a southeasterly **longshore** flow in the littoral zone were also observed -- an indication that waves were actually coming from a westerly direction, in sharp contrast to the autumn picture.

Since the littoral currents are a response to waves impinging upon the beach, they reflect both the **swell** which has propagated **for** long distances across the North Pacific and the regionally-generated wind waves. Reference to Brewer et al. (1977) reveals that in the March-April period the wave field off Yakutat normally is undergoing a transition. Waves tend to come from the **east-southeast** or the west-southwest, with waves from the south occurring relatively infrequently. This directional **bimodality** appears to be a consequence of the wind direction field over the same period. By April, however, waves show a marked tendency to be from the west, with about 42 percent from the **west-southwest** (Brewer et al., 1977), and have a height preference from 1 to 3 m. This study's littoral current data, which are a direct reflection of the wave field, show this March-April transition toward eastward wave propagation. The lower littoral current speeds also are in part a reflection of smaller wave heights in March-April than in October-November. Based upon this comparison between the present results and those which **would** be inferred from the wave fields documented in Brewer et al. (1977), the autumn and spring observations made in this study appear to be representative for those times of year.

### 4.3.4 Summary

The results of the spring field experiment can be briefly summarized as follows:

1. The regional temperature and salinity distribution showed considerably less variability on the continental shelf **and** near shore in spring than during autumn. Of the three water masses defined on

the basis of their temperature-salinity characteristics in autumn, only the Deep Ocean Water remained relatively unaltered from autumn to spring. The Shelf Water had been cooled and mixed so that it occupied a far smaller temperature-salinity range than in autumn. The Coastal Water was nearly entirely absent, being represented only at a section off **Yakutat** Bay, and had *lower* temperatures than in autumn. The area which had been occupied in autumn by Coastal Water revealed presence only of Shelf Water in spring, except for the Yakutat Bay section. Deep Ocean Water occupied the region off the shelfbreak and extended shoreward along the bottom of **Alsek** Canyon, as it had during autumn. Temperature and salinity irregularities off the shelfbreak suggested the **presence thereof eddy-like structures associated with the shelfbreak flow.**

2. Circulation on the **shelf was** generally far less variable than during autumn and showed a consistent northwesterly **flow** upon which were superposed spatial variability due to interactions with the bottom topography and temporal variability due to local wind forcing. In particular, northwesterly flow pulses near shore coincided with strong southeasterly winds. Currents near the heads **of Alsek** and Yakutat canyons followed the bathymetry and showed accelerated speeds due to convergence of streamlines at the canyon heads. Only at Mooring 6, northeast of Fairweather Bank, was the observed current weak, variable, and tidally dominated, with a weak eastward component throughout the six-month record.
3. Littoral currents were smaller than in autumn and were **bimodal** in the along-shore direction, in response to the March-April shift in the wave field from southerly-easterly to **southeasterly-southwesterly**.

## 5. OVER-WINTER WINDS AND CURRENTS

As described above (Section 2), current mooring 6 was left deployed during the October 1980-April 1981 period in order to detect variations having longer time scales than would have been detectable with the 12-day autumn and spring Moorings 1-5. To supplement the data from Mooring 6, wind data taken at Yakutat Airport and computed **geostrophic** wind were obtained for the same **over-winter** period. This section briefly describes and discusses the results of these over-winter observational efforts.

### 5.1 Over-Winter Currents at Mooring 6

Two current meters were deployed on Mooring 6 (see Figure 2 for location). **The** shallower of the two malfunctioned early during the mooring period, and the usable portion of its record has been discussed above (Section 3). The current meter at the deeper **level** (102 m) provided a record nearly 5.5 months long, bracketing the over-winter period October 1980-April 1981; this record is shown in Figure 54. The along-shore and cross-shelf components have been one-hour filtered to remove high-frequency noise. Since, however, the sampling interval of the current meter was 30 minutes, the record is little altered from the raw data. The record is remarkably "clean" and shows no current speeds higher than about 50 **cm/sec**. Because of the compressed time scale, the tidal components appear as "**noise**" on the **lower frequency fluctuations** in Figure 54. The plot of velocity as a function of time (Figure 54, top) was derived from the one-hour filtered values by **subsampling** every eight hours. Although this probably removed some of the peak current speeds, it has preserved the essentially fluctuating nature of the record.

There were two prominent features of the 102-m deep current record from Mooring 6. The first, seen upon visual inspection of Figure 54, was the tendency for flow events to occur on a time scale of five to six days. These events were of similar magnitude **in** the along-shore and cross-shelf directions and consisted primarily of fluctuations between northeasterly and southeasterly **flow**, although reversals to westward flow did occur at infrequent intervals. The second was a net easterly flow which persisted throughout the record. Since the record was longer than 60 days, it satisfied the requirement derived by **Lagerloef** et al.

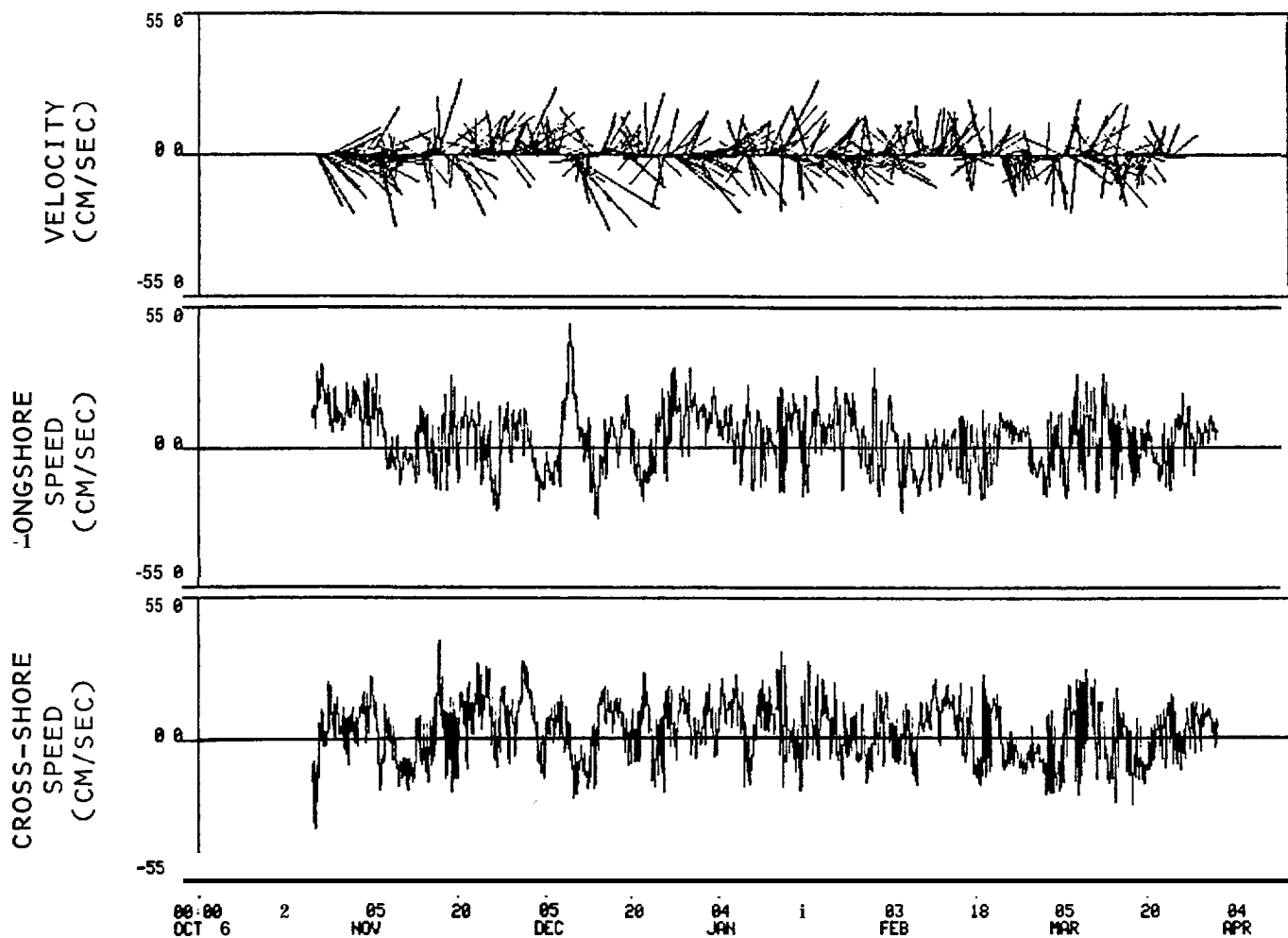


Figure 54. One-hour filtered currents at mooring 6 for the 102-m deep current meter plotted as a function of time.

(1981) for minimum record length needed to yield a mean current velocity valid at the 95 percent confidence level. The vector-averaged over-winter mean velocity at 102 m at Mooring 6 was 6.1 **cm/sec** at 82 °T.

The 5- to 6-day time scale for flow events was similar to that reported by Hayes (1979) for the continental shelf region off Icy Bay, about 100 km west of Yakutat. Hayes concluded that at the **100 m isobath**, a large part of the observed current variability in the 5- to 6-day band was due to local wind forcing. The observations that local winds during the mooring period were characterized by 4- to 6-day time scales (Section 5.2) is also consistent with this contention. However, lack of a long-term cross-shelf array of moorings containing both current meters and pressure gauges precludes a rigorous analysis of local wind/current interaction such as was carried out by Hayes. In addition, Hayes' analysis was carried out on data obtained **from a** relatively simple (compared to the region of the present field' program) shelf area, while the results reported here were subject to probable topographic influences not considered significant in Hayes' analyses.

The reason for the appreciable long-term net eastward flow at Mooring 6 is uncertain. It is probably related to location of the mooring north of Fairweather Bank, a shoal area, and may reflect an **anticyclonic** circulation around the Bank. A similar weak (5-10 cm/sec) **anticyclonic** flow over **Portlock** Bank in the **north-**west Gulf of Alaska off Kodiak Island was reported by **Muench** and Schumacher (1980), who speculate that flow over bottom topography in the region was controlled in large part by potential vorticity conservation constraints. A similar mechanism in the present study area would dictate **anticyclonic** flow about Fairweather Bank and a consequent southeasterly flow north of the Bank as observed at Mooring 6.

## 5.2 Over-Winter Local Winds

Winds used for the over-winter analysis were obtained from the National Weather Service office at Yakutat Airport in Yakutat (cf. Figure 1) and as computed geostrophic winds from FNWC in Monterey, California. The filtered time series obtained from these two sources are shown in Figures 55-57. The velocity time series (Figure 55) illustrate the overall directional trend of the winds. The easterly and northerly speed components illustrate the agreement

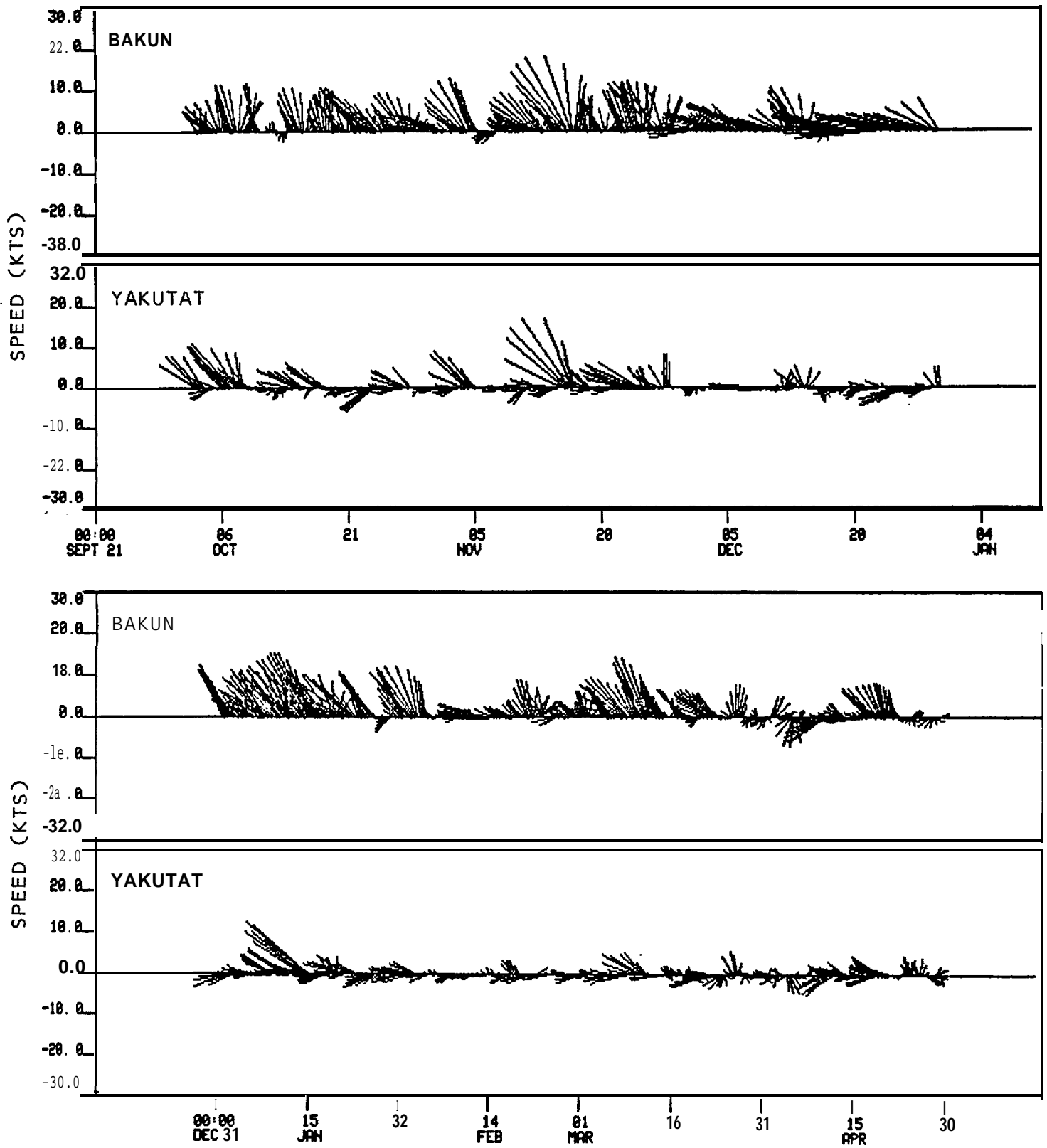


Figure 55. 30-hour filtered winds as observed at Yakutat airport and as computed **geostrophic** winds plotted as a function of time for September 1980- April 1981. Wind blowing toward north is up.

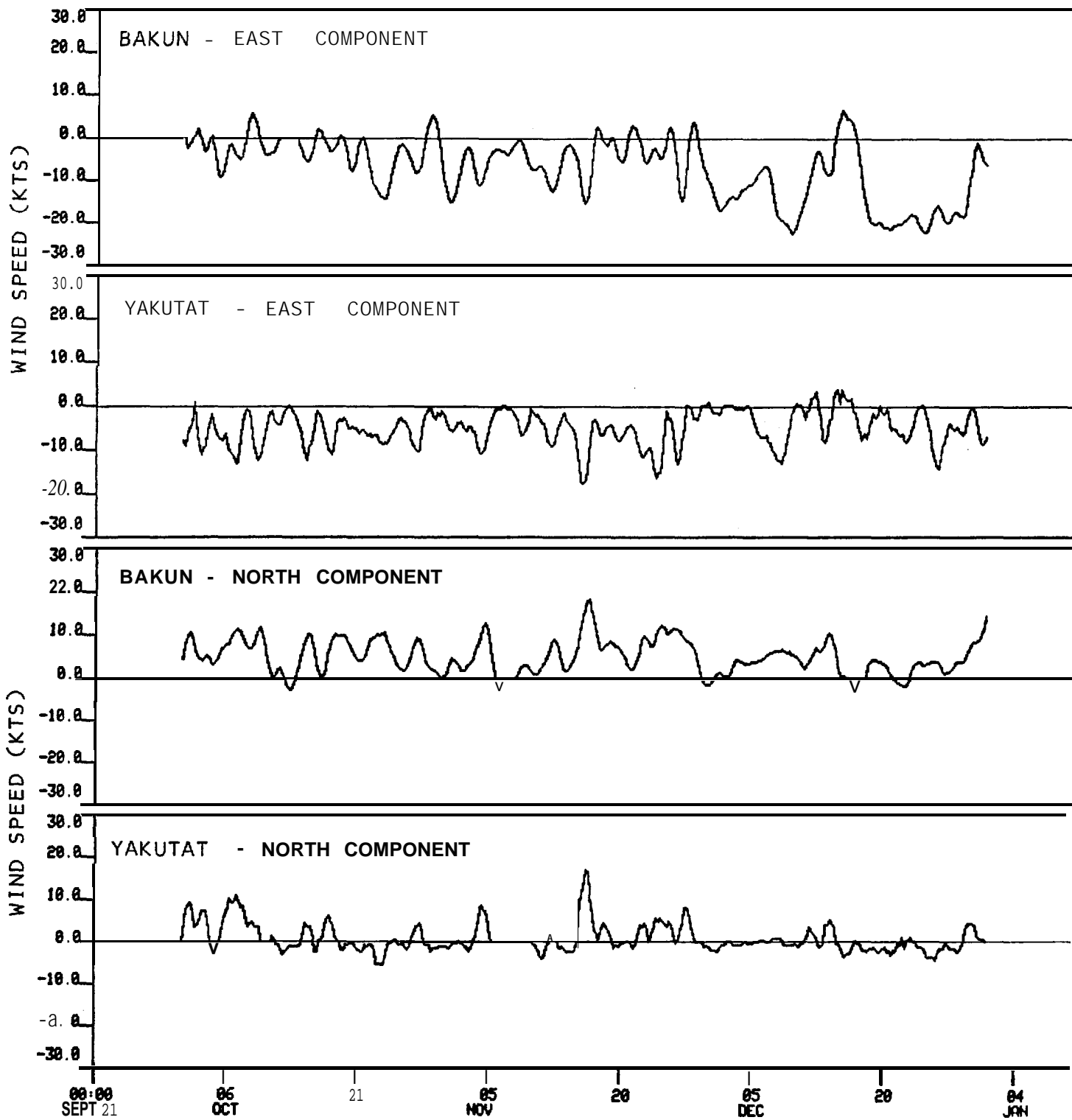


Figure 56. 30-hour filtered east and north wind speed components from Yakutat airport and as computed **geostrophic** winds plotted as a function of time for September-December 1980. Positive east (north) indicates wind was blowing toward the east (north).

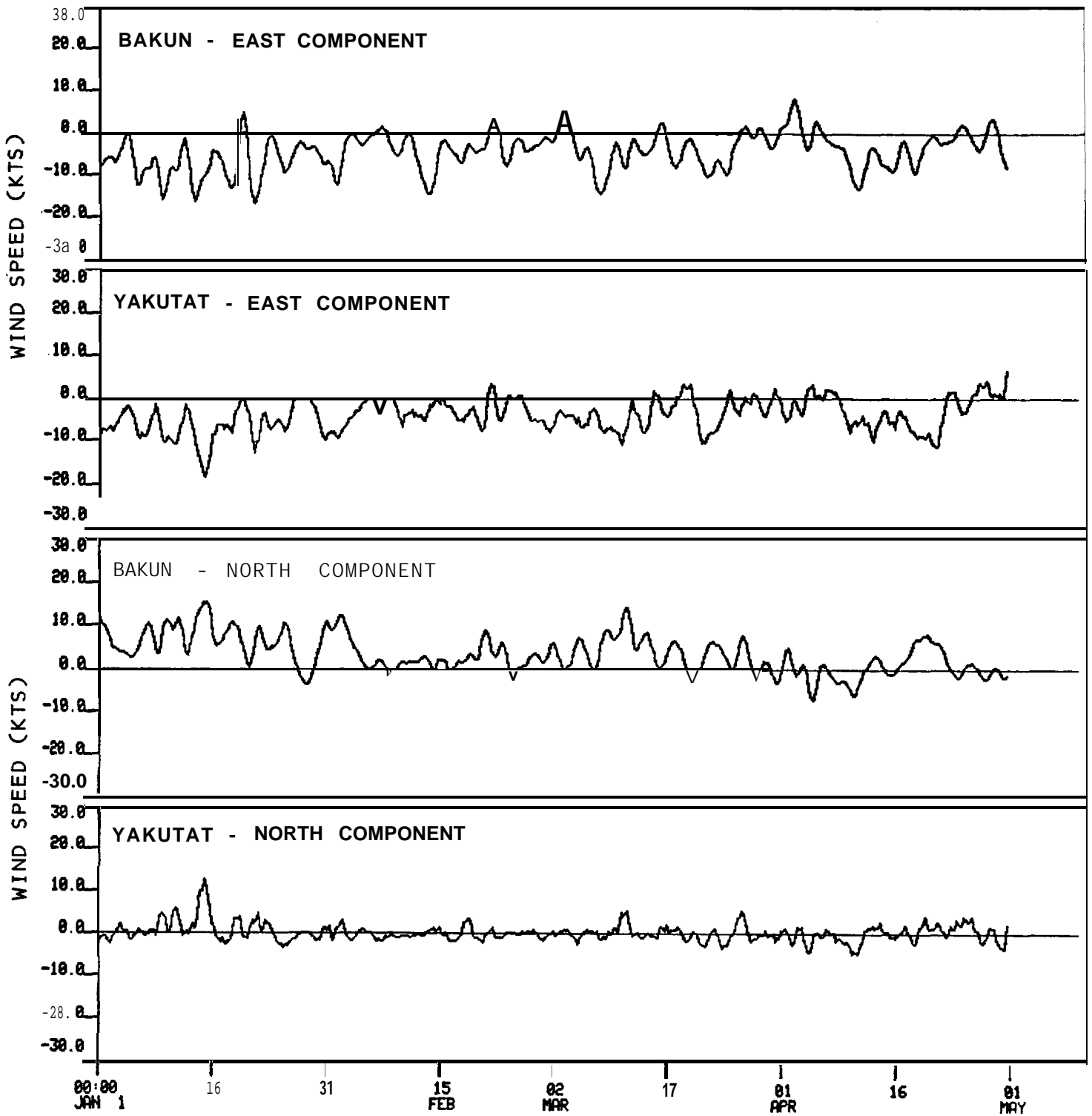


Figure 57. 30-hour filtered east and north wind speed components from Yakutat airport and as computed geostrophic winds plotted as a function of time for January-April 1981. Positive east (north) indicates wind was blowing toward the east (north).

between the Yakutat Airport and computed winds for individual events (Figures 56-57).

Both the wind series show two distinct features. First, the net wind direction through the winter was easterly-southeasterly, with the computed winds having a greater south component than the airport winds. **This net direction is because the winds fall along the northeastern portions** of cyclones which propagate into the region as part of the Aleutian low-pressure trough. **The directional difference between observed and computed winds is** due to isobaric blocking by the mountainous coastline which does not affect the computed winds but does, however, cause the observed winds to parallel the coastline. Thus, the computed winds may actually provide the better approximation to the true offshore wind field. Conversely, the observed winds may be more indicative of conditions over the 10-km wide coastal **oceanic region focused upon by this program.**

The second apparent feature of the winds is the domination by events having time scales of 4-6 days. This observation is in agreement with statistics computed from historical data by **Brewer et al.** (1977). The 4- to 6-day time scale is due to propagation of **cyclonic** low-pressure systems into the region along the Aleutian Low pressure trough. Visual comparison between the observed and computed winds shows that the majority of wind events were evident on both records. Because the storm systems propagate in a nonstationary fashion, i.e. they occur over time scales varying from about 4 to 6 days, spectral analyses applied to the entire record **yield** a broad flat energy peak over that range. Application of maximum energy method (**MEM**) analyses to monthly data sets through the winter yielded, however, more concise information on time scales. The **MEM** method is capable of resolving time scales (or periods, for periodic functions) given sample intervals which are short -- of order one period or even less. However, this method does not provide reliable estimates of the relative magnitude of energy peaks which are found at different frequencies. An example of a normalized MEM spectrum **for the computed geostrophic wind speeds** for the month of November 1980 is shown in Figure 58; the spectra for the other months were similar and will not be shown here. The peak at about four days shifted slightly from month to month but was consistent over most of the winter, and represents the most dominant frequency for propagation of high-wind-speed storm **events** into the area. These spectral estimates therefore are consistent with time scales derived from visual inspection and from the historical data as presented in Brewer et al. (1977).

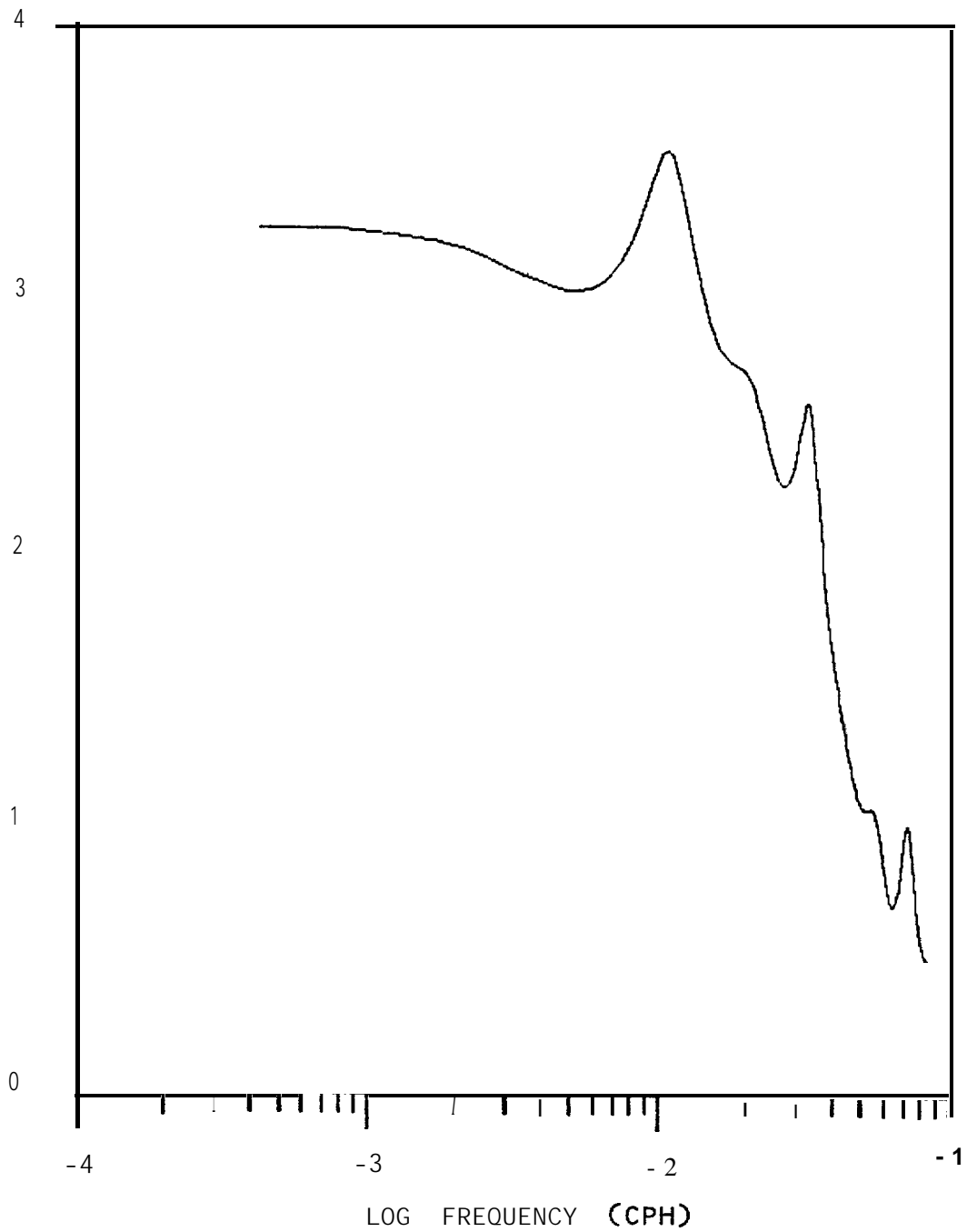


Figure 58. **Normalized spectral estimate** for computed geostrophic wind speeds during November 1980, computed using a Maximum Entropy Method (**MEM**) routine.

### 5.3 Summary

The results from the over-winter current observations from Mooring 6 and the over-winter wind observation program can be summarized as follows:

1. **Mean** flow at 102 m at Mooring 6 was about 6 cm/sec directed toward 82 °T for the entire October 1980-April 1981 period. Eastward flow at this location was probably due to interaction of a northwesterly regional flow with a rise in the bottom topography.
2. Mean winds for the region were southeasterly (toward the northwest) through the winter. This directional orientation reflects the origin of the winds from eastward-propagating **cyclonic** low-pressure systems, and is normal for the region.
3. Both currents and winds exhibited events which were large relative to the means and which had dominant time scales of 4-6 days. For the winds, the time scale was that associated with propagation of discrete **cyclonic** storm systems into the region. Conventional wisdom concerning continental shelf dynamics, coupled with the observed similarity in time scales, suggests that the current variations were a result of wind fluctuations, although complications introduced by a complex bottom topography precluded rigorous analyses of these interactions.

## 6. SUMMARY AND DISCUSSION

In this section the observational results presented in Sections 3-5 are summarized and discussed briefly within the context of possible effects on the fate of contaminants related to OCS petroleum development activities. Whereas each of the above sections dealt with a specific season, except for the **over-**winter time series, this section integrates results from the different seasons in order to present as general a depiction of regional transport processes as possible while at the same time retaining information pertinent to major seasonal variability. Finally, autumn and spring mean currents are summarily **com-**  
**pared** with the results of the Gait and **Watabayashi** (1980) diagnostic model.

The results of this investigation can be summarized:

1. A coastal band of water relatively low in temperature and low in salinity was present in autumn 1980 but was no longer in evidence in spring 1981. When present, this band was about 7 km wide and 20 m or **less thick. Its presence in autumn, but not in spring, was** due to admixture into the marine waters of the large autumn coastal freshwater input.
2. Currents within about 5 km from shore were almost entirely **along-**shore, with small on- and offshore components. In fall these currents were usually to the northwest at about 10 m depth, as shown by **drogue** studies. At 30 m **depth, however, the currents were bimodal** and flow was to the southeast and to the northwest for about equal percentages of the time. **In spring, flow** was consistently toward the northwest at all depths, and current speeds were 10-20 **cm/sec.**
3. At about 10 km offshore, outside the **immediate** coastal region, currents were variable with a net flow to the northwest and stronger on- and offshore components than were observed closer to shore. The currents were more consistently northwesterly in spring than during autumn, when reversals to southeasterly flow occurred.
4. The overall large-scale flow over the shelf was to the northwest except at the mooring just north of Fairweather Bank, where a net easterly and highly variable flow regime was observed. The **over-**  
**all** northwest flow was due to forcing by northwesterly currents along the shelfbreak and a net northwest-directed winter wind stress. The easterly flow north of Fairweather Bank was due to the influence of the shoal bottom **over** the banks, with resultant formation of an **anticyclonic gyral** flow around the Bank.

5. Currents responded to the topographic trough formed by Alsek Canyon by accelerating toward the head **of** the canyon. Both current meters and drogues revealed a shoreward flow along the southeast side of the canyon which fed an accelerated northwest coastal flow past the canyon head. There was some temperature and salinity evidence of deep shoreward flow in both **Alsek** and Yakutat canyons.
6. Currents within about 10 km of the coastline were **strongly** affected by passage of local storms. Strong northwest current **pulses** coincided with southeast wind events in this zone. Farther offshore, the wind events did not affect the currents as strongly. Long-term over-winter wind and current records revealed a common four- to five-day time scale for both, suggesting wind/current interaction.

The above general results are consistent with existing hypotheses concerning continental **shelf** circulation for a shelf regime characterized by a large seasonally varying coastal freshwater influx, frequent vigorous along-shore wind events, and a complex bottom topography. For purposes of estimating pollutant transport, the significant aspects are:

- The shelf-wide general net-northwesterly flow except for the location just north of Fairweather Bank where net flow was easterly;
- The **large** and primarily wind-induced variability superposed upon the net flow;
- Appreciable cross-shelf **transport resulting** from interaction of the net northwesterly flow with a complex bottom topography.

The first of these points suggests that a pollutant would be transported toward the northwest with the net flow. However, **the high wind-induced variability (particularly during autumn)** would limit the confidence to be placed in **such a prediction for time scales of two to three days. The observed correlation between upper-layer northwesterly flow, at least near the coast, and southeast winds** might be used to aid in predicting transports over time scales short relative to net flow. The infrequent occurrence of westerly flow north of Fairweather Bank suggests that pollutants entering the system there might be transported to the southeast. This raises the possibility that they might then circle the Bank in **anticyclonic** fashion within the suspected flow, increasing the chances of impact upon the Bank itself. The net eastward **flow of 6 cm/sec** north of the Bank suggests that between one and two weeks might be required for **a pollutant** to circle completely around the Bank. The probable occurrence of higher-speed flow events during this period could, however, **alter this time estimate considerably.**

The observed onshore transport along the southeast boundary of Alsek Canyon and at Mooring 3 to the northwest suggests that pollutants released in mid-shelf might find their way into the coastal region. Given the frequent occurrence of 20-30 **cm/sec** current pulses at virtually all of the moorings, such a cross-shelf transport might occur over a time scale of about two days. The radar-tracked **drogues** used in the coastal region did not indicate appreciable flow divergence in the along-shore direction. Therefore, it is probable that pollutants in the upper layer near the coast would tend to travel parallel to the coast with the current and would undergo little lateral spreading. Pollutants at the surface would, however, tend to follow the local winds rather than the current. A strong winter regional tendency toward coastal **downwelling** conditions would drive upper layer pollutants shoreward. As for all wind-driven processes in this region, however, downwelling is event-dominated and so can be predicted only insofar as local winds can be predicted.

Once introduced into the surf zone, it seems likely based upon the results of the seabed drifter studies that pollutants would become mixed into the bottom sediments by wave action and would make their way onto the beach in similar fashion to the drifters. In autumn, a northwesterly motion along the beach would be expected. Movement of pollutants along the beach due to littoral currents could be easily estimated in real time using empirical equations in conjunction with observed wave height and direction.

As elsewhere along the northern Gulf of Alaska coastline, the regime in the northeast Gulf is dominated by variability which has time scales of four to five days. Assuming a current of 30 **cm/sec** associated with this variability, a net displacement of a pollutant over a single event might be of order 60-70 km or approximately the **shelf** width. Except for the relatively strong net along-shore flow observed near the coast in spring, this event-driven transport will be greater than that due to the net flow over the same time period. Therefore, prediction of pollutant transport becomes a problem in predicting the local winds inasmuch as we can relate the current events to local wind events. In the absence of appreciable events, most likely to occur during spring, pollutants would tend to move shoreward across the shelf and become entrained in the northwestward along-shore coastal flow.

Results from Gait and **Watabayashi**'s (1980) diagnostic model of the study area compare favorably with our winter 1981 field results. The diagnostic model predicts surface currents using a **baroclinic** field computed from field observations in conjunction with an imposed, arbitrarily specified surface wind forcing. The model results shown (Figure 59) utilized March 1979 oceanographic data for **baroclinic** field computation and incorporate a moderate wind stress acting from the southeast. The **model** yields strong cross-shelf flow associated with Aisek Canyon, a strong northwestward alongshore coastal flow off Yakutat, and large, variable currents near the shelf break.

When comparing modeled and observed currents, it must be borne in mind that the observations were subsurface whereas the model computed surface currents. No attempt will therefore be made here to compare magnitudes. Rather, a qualitative comparison is sought.

Current observations in the northeast Gulf in March-April 1980 showed that, except for mooring 6, subsurface flow was generally along-shore and to the northwest (Figure 60). This northwestward flow was particularly vigorous, with mean speeds approaching 20 cm/see, nearest shore (moorings 1 and 4). Mooring 5 showed shoreward flow associated with **Aisek** Canyon, a feature which was also evident in the model output. Mooring 6 observed flow toward the east which was also evident at the same location (north of Fairweather Bank) in the model output. The strong flow at mooring 3 had a shoreward component and was also evident on the model output. Our observations did not extend sufficiently far offshore to allow comparison with the results of the model near the shelf break. Where available for comparison, the agreement between modeled and observed features suggests that the model adequately describes circulation on the inner portion of the shelf during late winter conditions.

The above comparison was between model results computed using late winter (1979) conditions of steady northwesterly wind stress and low runoff, and a set of current observations obtained under similar conditions two years later (1981). As a **final** comparison, **observed currents** during a period of high runoff and large, fluctuating northwestward wind stress (October-November 1980) are presented in Figure 61. While the current observations yielded no information seaward of about 10 km from the coastline, they indicate a northwesterly flow

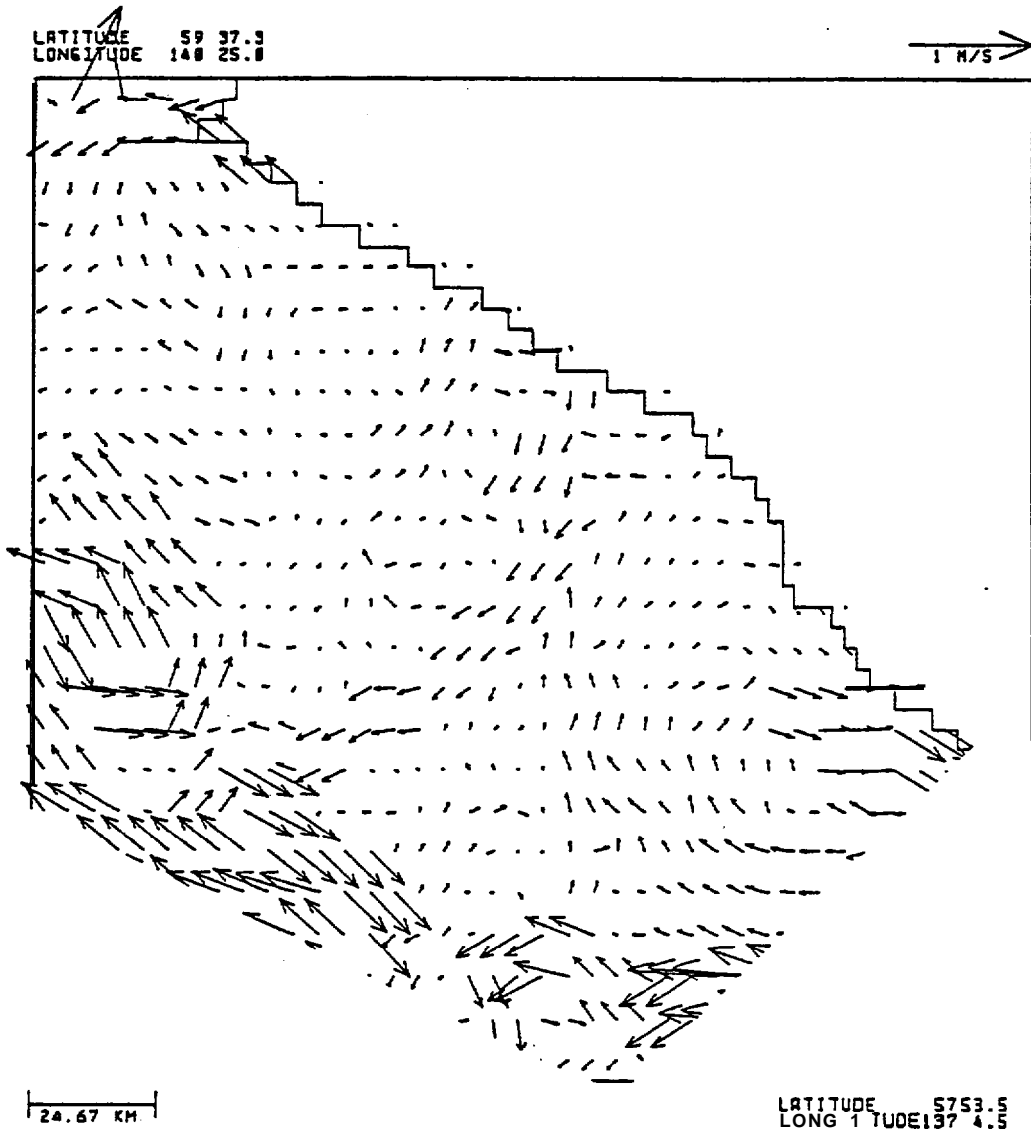


Figure 59. Surface current vectors constructed by application of a diagnostic model to March 1979 density data, assuming presence of a moderate southeasterly (towards the northwest) wind stress (from Gait and Watabayashi, 1980).

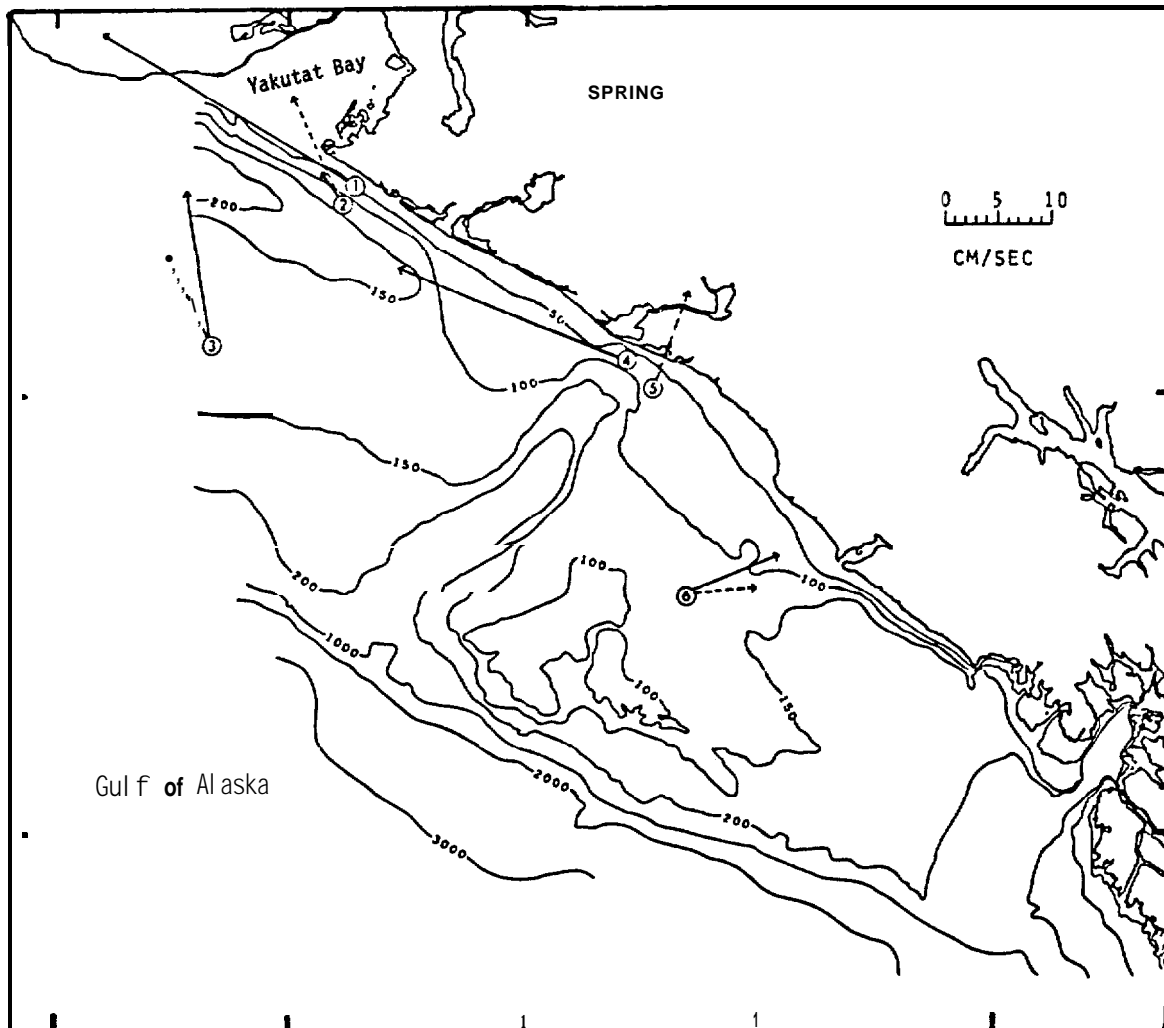


Figure 60. Vector-averaged currents from current meters deployed in March-April 1981 and for the October 1980-April 1981 record obtained at mooring 6. Dashed arrows depict the deeper, where available, of the two observations from a given mooring.

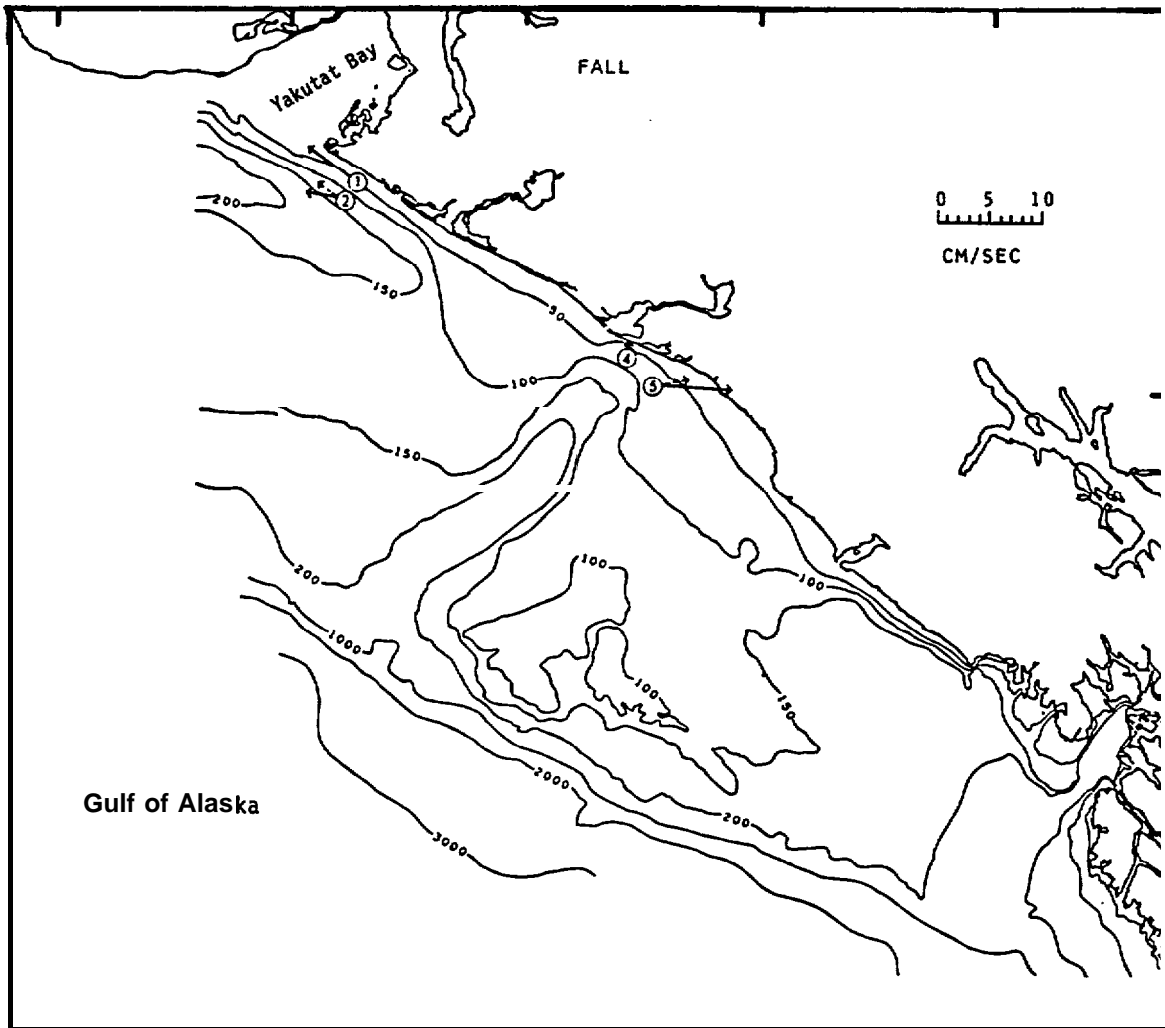


Figure 61. Vector-averaged currents from current meters deployed in October-November 1980. Dashed arrows depict the deeper, where available, of the two observations from a given mooring. These mean currents should be interpreted with caution because of extremely high speed and direction variability during the observation period.

tendency which was similar to that observed in late winter 1981. The "mean" currents in autumn 1981 should, however, be interpreted with considerable caution because the currents were highly variable throughout the observation period. The weak eastward mean flow observed at mooring 5 had superposed upon it a highly variable instantaneous flow. The coastal currents appeared to be dominated during autumn 1980 by wind-driven events as discussed above. Comparison between the observed autumn (Figure 61) and later winter (Figure 60) coastal currents suggests that the circulation became steadier and more consistently towards the northwest during the course of the winter. This seasonal trend may be due to a winter spinup of the entire coastal and offshore circulation by regional wind stress over the northern Gulf of Alaska, which reaches a maximum in mid-winter. The tendency for a mean northwesterly flow remains, however, a consistent regional circulation feature. While our **data** were inadequate to prove it, the effects of major topographic features such as the **Aisek** Canyon on the mean shelf circulation would be expected to persist throughout the year.

## 7. REFERENCES

- Bakun, A., 1975. Wind-driven convergence-divergence of surface waters in the Gulf of Alaska. *EOS*, **56**, 1008.
- Beardsley**, M. C., **W. Boicourt**, L. C. Huff and J. Scott, 1977. **CMICE 76**: A current meter intercomparison experiment conducted off Long Island in February-March 1976. Woods Hole **Oceanog. Inst. Tech. Rep. HOI 77-62**, 123 pp.
- Brower, W. A., Jr., **H.F. Diaz**, **A.S. Prectel**, **H.W. Searby** and **J.L. Wise**, 1977. Climatic atlas of the outer continental shelf waters and coastal regions of Alaska; Vol. I - Gulf of Alaska. AEIDC Pub. B-77, Anchorage, Alaska, 439 pp.
- Carrier, **G.F. and A.R. Robinson**, 1962. On the theory of the wind-driven ocean circulation. *J. Fluid Mech.*, **12**, 49-80.
- Csanady, G.T., 1974. **Barotropic** currents over the continental shelf. *J. Phys. Oceanog.*, **4**, 357-371.
- Csanady, G.T., 1975. Lateral momentum flux in boundary currents. *J. Phys. Oceanog.*, **5**, 705-717.
- Favorite, F., **A.J. Dodimead** and **K. Nasu**, 1976. Oceanography of the subarctic Pacific region, 1960-71. *Internatl. N. Pacific Fish. Comm. Bull.*, **33**, 187 pp.
- Gait, **J.A. and G. Watabayashi**, 1980. Modeling report to OCSEAP from RU 140, January 1980. 57 pp. Unpublished manuscript.
- Halpern**, D. and **R.D. Pillsbury**, 1976a. Influence of surface waves on subsurface current measurements in shallow water. *Limnol. and Oceanog.*, **21**, 611-616.
- Halpern** D. and **R.D. Pillsbury**, 1976b.. Near-surface moored current meter measurements. *MTS Journal*, **10**, 32-38.
- Hayes, S.P., 1978. Variability of current and bottom pressure across the continental shelf in the northeast Gulf of Alaska. *J. Phys. Oceanog.*, **9**, 88-103.
- Hayes, **S.P. and J.D. Schumacher**, 1976. Description of wind, current and bottom pressure variations on the continental shelf in the northeast Gulf of Alaska from February to May 1975. *J. Geophys. Res.*, **81**, 6411-6419.
- Hickey, B.M., 1981. Alongshore coherence on the Pacific Northwest continental shelf (January-April, 1975). *J. Phys. Oceanog.*, **11**, 822-835.
- Holbrook**, **J.R.** and **D. Halpern**, 1977. A compilation of wind, current, **bottom-pressure** and **STD/CTD** measurements in the northeast Gulf of Alaska, February-May 1975. NOAA Tech. Memo. **ERL/PMEL-10**, 11 pp.
- Hsueh, Y., 1980. On the theory of deep flow in the Hudson Shelf Valley. *J. Geophys. Res.*, **85**, 4913-4918.
- Ingraham**, **W.J., Jr.**, **A. Bakun** and **F. Favorite**, 1976. Physical oceanography of the Gulf of Alaska. Northwest Fish. Center Processed Rep., **July 1976**, 132 pp.
- Komar**, P. D., 1976. Beach Processes and Sedimentation. Prentice-Hall, Englewood Cliffs., N.J., 429 pp.

- Lagerloef, G. S., **R.D. Muench** and **J.D. Schumacher**, 1981. Low-frequency variations in currents near the shelf break: northeast Gulf of Alaska. *J. Phys. Oceanog.*, **11**, 627-638.
- Lavelle, J.W., G.F. Keller and T.L. Clarke, 1975. Possible bottom current response to surface winds in the Hudson shelf channel, *J. Geophys. Res.*, **80**, 1953-1956.
- LeBlond, P.H. and L.A. Mysak, 1978. Waves in the Ocean. Elsevier, N.Y., N.Y., 602 pp.
- Lee, T.N., 1975. Florida Current spin-off eddies. *Deep-Sea Res.*, **22**, 753-765.
- Mayer, D.C., D.V. Hansen and D.A. Ortman, 1979. Long-term current and temperature observations on the middle Atlantic shelf. *J. Geophys. Res.*, **84**, 1776-1792.
- McEwen, G.F., T.G. Thompson and R. Van **Cleve**, 1930. Hydrographic sections and calculated currents in the Gulf of Alaska, 1927-1928. *Rep. Int. Fish. Comm.*, **4**, 36 pp.
- Muench, R.D.** and **J.D. Schumacher**, 1979. Some observations of physical oceanographic conditions on the northeast Gulf of Alaska continental shelf. NOAA Tech. Memo., ERL **PMEL-17**, 84 pp.
- Muench, R.D.** and **J.D. Schumacher**, 1980. Physical oceanographic and meteorological conditions in the northwest Gulf of Alaska. NOAA Tech. Memo., **ERL-PMEL-22**, 147 pp.
- Munk, W.H.**, 1950. On the wind-driven ocean circulation. *J. Met.*, **7**, 79-93.
- Mysak, L.A., 1980. Topographically trapped waves. *Ann. Rev. Fluid Mech.*, **12**, 45-76.
- Nelsen, T.A., P.E. Gadd and T.L. Clarke, 1978. Wind-induced current flow in the upper Hudson shelf valley. *J. Geophys. Res.*, **83**, 6073-6082.
- Pearson, C.A., **J.D. Schumacher** and **R.D. Muench**, 1981. Non-effects of wave-induced mooring noise on tidal and low-frequency current observations. *Deep-Sea Res.*, **28**, in press.
- Reeburgh, W.S.**, **R.D. Muench** and **R.T. Cooney**, 1976. Oceanographic conditions during 1973 in Russell Fjord, Alaska. *Estuarine and Coastal Mar. Sci.*, **4**, 129-145.
- Reed, R.K., 1980. Direct measurement of recirculation in the Alaska Stream. *J. Phys. Oceanog.*, **10**, 976-978.
- Reed, R.K., **R.D. Muench** and **J.D. Schumacher**, 1980. On **baroclinic** transport of the Alaskan Stream near Kodiak Island. *Deep-Sea Res.*, **27**, 509-523.
- Reed, **R.K.** and **J.D. Schumacher**, 1981. Sea level variations in relation to coastal flow around the Gulf of Alaska. *J. Geophys. Res.*, **86**, 6543-6546.
- Reid, **J.L.** and **A.W. Mantyla**, 1976. The effect of the **geostrophic** flow upon coastal flow sea elevations in the northern North Pacific Ocean. *J. Geophys. Res.*, **81**, 3100-3110.

- Royer, T.C., 1975. Seasonal variation of waters in the northern Gulf of Alaska. *Deep-Sea Res.*, 22, 403-416.
- Royer, T.C., 1979. On the effect of precipitation and runoff on coastal circulation in the Gulf of Alaska. *J. Phys. Oceanog.*, 9, 555-563.
- Royer, T.C., 1981a. Baroclinic transport** in the Gulf of Alaska, Part I. Seasonal variations in the Alaska Current. *J. Mar. Res.*, 39, 239-250.
- Royer, T.C., 1981b. **Baroclinic** transport in the Gulf of Alaska, Part 11. A freshwater driven coastal current. *J. Mar. Res.*, 39, 251-266.
- Royer, T.C., 1981c. Coastal freshwater discharge in the northeast Pacific. *J. Phys. Oceanog.*, in press.
- Royer, T.C. and R.D. Muench**, 1977. On the ocean temperature distribution in the northern Gulf of Alaska, 1974-1975. *J. Phys. Oceanog.*, 7, 92-99.
- Royer, T.C., **D.V. Hansen** and **D.J. Pashinski**, 1979. Coastal flow in the northern Gulf of Alaska as observed by dynamic topography and satellite-tracked **drogued** drift buoys. *J. Phys. Oceanog.*, 9, 785-801.
- Thomson, R. D., 1972. On the Alaskan Stream. *J. Phys. Oceanog.*, 2, 363-371.